

Design, Synthesis, and Evaluation of Bicyclic Peptides as Ammonium Ionophores

By

Cheryl L. Nowak

A Thesis submitted to the Faculty of the

WORCESTER POLYTECHNIC INSTITUTE

In partial fulfillment of the requirements for the

Degree of Master of Science

In

Chemistry

April 30, 2003

Approved:

Dr. W. Grant McGimpsey, Major Advisor

Dr. James P. Dittami, Department Head

Abstract

A series of bicyclic peptides have been designed and synthesized to provide ammonium ion complexation sites via hydrogen bonding in a tetrahedral geometry. Molecular modeling dynamics and electrostatics studies indicate that target compounds **1d-6d** may provide better selectivity for ammonium ions over potassium ions than the ammonium ionophore currently used for blood analysis applications, nonactin. Attempts to synthesize **1d**, cyclo(L-Glu¹—D-Val²—L-Ala³—D-Lys⁴—D-Val⁵—L-Val⁶)-cyclo-(1 γ -4 ϵ), were unsuccessful due to poor solubility of the synthetic intermediates. This led to the design of **2d-6d** in which specific amino acid residues were chosen to provide higher solubility. Compound **2d**, cyclo(L-Glu¹—D-Ala²—D-Ala³—L-Lys⁴—D-Ala⁵—L-Ala⁶)-cyclo-(1 γ -4 ϵ), was successfully synthesized, but was also too insoluble for characterization or testing in an ion selective electrode (ISE) sensor format. Compound **6d**, cyclo(L-Glu¹—D-Leu²—Aib³—L-Lys⁴—D-Leu⁵—D-Ala⁶)-cyclo-(1 γ -4 ϵ), was successfully synthesized and characterized. When **6d** was incorporated into an ISE sensor and tested as an ammonium ionophore, results indicated that the bicyclic peptide lacked solubility in the ISE membrane. A ¹³C-NMR study has been initiated in order to evaluate selectivity of **6d** for ammonium over potassium and sodium cations in solution. Preliminary results with the potassium ionophore valinomycin as a control have been completed.

Acknowledgements

For his guidance and support, I would like to express my sincere gratitude to my advisor, Dr. W.G. McGimpsey. It has been a pleasure to know you and work under your leadership.

For his expert advice in the design and synthesis of these compounds, I would like to gratefully acknowledge Dr. S.J. Weininger. In addition, I have thoroughly enjoyed his classroom instruction.

I would like to thank my friends and colleagues Dr. John Benco, Dr. Hubert Nienaber, Ernesto Soto, Chris Cooper, Kathy Dennen, Nantanit Wanichacheva, Selman Yavuz, and Man Phewluangdee for their ideas and advice and for making my time at WPI so enjoyable. In particular, Dr. John Benco has been the driving force behind this research, which would not have been possible without his patient counsel and untiring enthusiasm.

I would like to thank my family and friends for their love and support.

In addition, I would like to acknowledge Bayer Corporation for the financial support that made this research possible.

Table of Contents

Abstract.....	ii
Acknowledgements	iii
Table of Contents	iv
List of Figures.....	v
List of Schemes and Tables	vii
1 Introduction.....	1
2 Experimental	13
2.1 <i>General Methods and Materials</i>	<i>13</i>
2.2 <i>Molecular Modeling Calculations</i>	<i>13</i>
2.3 <i>Synthesis.....</i>	<i>14</i>
2.4 <i>ISE Membrane and Electrode Preparation</i>	<i>34</i>
2.5 <i>ISE Testing.....</i>	<i>35</i>
2.6 <i>¹³C-NMR Study of Valinomycin binding Potassium Cations.....</i>	<i>36</i>
3 Results and Discussion.....	38
3.1 <i>Selection of Synthetic Methods</i>	<i>38</i>
3.2 <i>Design and Synthesis</i>	<i>40</i>
3.3 <i>Sensor Fabrication and Testing.....</i>	<i>52</i>
3.4 <i>¹³C-NMR Study of Valinomycin binding Potassium Cations.....</i>	<i>56</i>
4 Conclusions.....	62
References.....	63
Additional References.....	66
Appendix: ¹H, ¹³C, and DEPT135 NMR spectra and ESI MS.....	69

List of Figures

Figure 1: Nonactin, the current industry standard ammonium ionophore.....	8
Figure 2: Lehn's macrotricyclic cryptand.....	10
Figure 3: 1,3,5-tris(3,5-dimethylpyrazol-1-ylmethyl)-2,4,6-triethyl benzene ammonium ionophore.....	11
Figure 4: 19-crown-6 ether with decalino subunits.....	12
Figure 5: Dibenzo-18-crown-6 ether with thiazole subunits.....	13
Figure 6: Two benzene rings held together by three benzocrown ether units.....	14
Figure 7: (a) Valinomycin (b) new depsipeptide ammonium ionophore.....	15
Figure 8: (a) cyclo(1,5- ϵ -succinoyl) (Lys-Gly-Gly-Gly) ₂ (b) cyclo(Glu ¹ -X ² -Pro ³ - Gly ⁴ -Lys ⁵ -X ⁶ -Pro ⁷ -Gly ⁸)-cyclo-(1 γ \rightarrow 5 ϵ) Gly ⁹ , where X = Ala or Leu.....	16
Figure 9: Target bicyclic peptide ammonium ionophores.....	17
Figure 10: General synthetic scheme for target compound 1d	18
Figure 11: Mechanism of Fmoc deprotection.....	44
Figure 12: Mechanism of PyBOP/HOBT-mediated coupling reaction.....	45
Figure 13: Depsipeptide ammonium ionophore (left) and target compound 1d (right).....	47
Figure 14: Complexation of 1d with ammonium (left) and potassium (right) cations....	48
Figure 15: The two possible atropoisomers of (a) target compound 1d (b) target compound 2d	51
Figure 16: Potentiometric responses of planar ISEs to NH ₄ ⁺ (10 ⁻⁴ – 10 ⁻¹ M) for membranes 1-3 based on 6d	59

Figure 17: Potentiometric responses of planar ISEs to NH_4^+ ($10^{-4} - 10^{-1}$ M) for membranes 4-6 based on **6d**.....60

Figure 18: ^{13}C -NMR carbonyl signals of valinomycin as a function of $[\text{KSCN}]$65

Figure 19: Valinomycin-potassium complex as a function of potassium concentration.67

List of Schemes and Tables

Scheme 1: Synthesis of 1d	23
Scheme 2: Synthesis of 4a and 4b	33
Table 1: ¹³ C-NMR experiments of valinomycin with increasing amounts of KSCN.....	44
Table 2: Selectivity of 6d for Ammonium over Other Cations.....	67

1 Introduction

The levels of urea and creatinine in blood are important diagnostic indicators of renal, thyroid, and muscle function.¹ Significant effort has been expended in developing reliable sensors for the detection of these analytes. At the present time, urea and creatinine levels are measured indirectly following enzyme-catalyzed hydrolysis to produce ammonium ions. Typically, measurement of ammonium ion concentrations is achieved by carrier-based ion selective electrodes (ISEs) containing the natural antibiotic nonactin as an ionophore.² In ISEs, a highly viscous liquid membrane (such as plasticized PVC) lies between the aqueous sample containing the ion and an internal electrolyte solution. The membrane is doped with a selective ion carrier (nonactin in the case of ammonium) and a lipophilic salt that acts as an ion exchanger. The potential that develops at the membrane/sample interface is proportional to the activity (concentration) of ammonium ions in the aqueous sample.³

The two key properties of any ion sensor are sensitivity to the desired ion in the required concentration range and selectivity for one specific ion over all other interfering ions, properties that are primarily imparted by the ionophore. As an ammonium ionophore, nonactin, shown in **Figure 1**, forms four hydrogen bonds from its ethereal oxygens to the ammonium ion.⁴ Nonactin-based ISEs show reasonable selectivity for ammonium over sodium ions ($\log K_{NH_4^+,Na^+} = -2.4$)⁴, but only modest selectivity over potassium ions ($\log K_{NH_4^+,K^+} = -1.0$)⁴. For this reason, much effort has focused on the development of new

ammonium ionophores, particularly with increased selectivity over potassium ions to improve accuracy of ammonium ion determinations in the presence of potassium ions.⁴

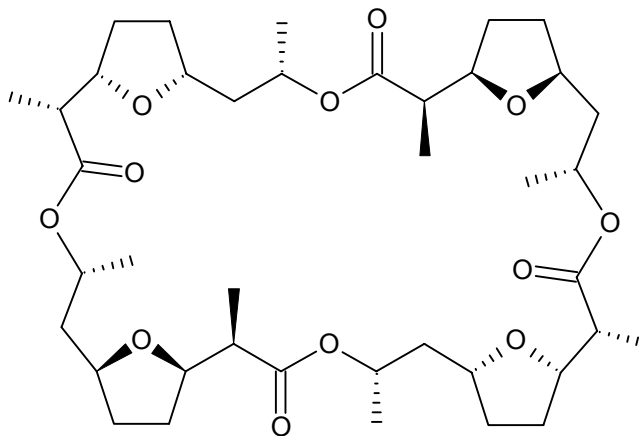


Figure 1: Nonactin, the current industry standard ammonium ionophore

In designing ammonium ionophores, there are three main factors to consider. The first is size-fit requirements. A rigid framework with a cavity appropriately sized for ammonium ion (ionic radius 1.43 \AA)⁵ is necessary to impart high selectivity over interfering cations of other sizes.^{6,7} If the substrate is too flexible, it can change conformations to allow coordination with larger and smaller cations besides the desired ion. In addition, complexation is thermodynamically more favorable when the ionophore is conformationally preorganized into the correct binding geometry in order to minimize the entropic cost of cation binding.³ Secondly, the ammonium ionophore should exhibit a spatial distribution of lone-pair electrons for effective hydrogen bonding with the tetrahedral ammonium ion.⁶ Interfering potassium ions are of similar size (1.33 \AA)⁵ to ammonium ions, but have spherical symmetry and therefore prefer ionic bonds with coordination numbers of six or higher.² For this reason, the coordination geometry is responsible for imparting selectivity for ammonium over potassium ions. Lastly, the

ionophore should be highly lipophilic⁶ in order to be compatible with the nonpolar membrane environment⁸ of ion selective electrodes and to prevent extraction of the ionophore from the sensor during testing.³

One of the earliest ammonium ionophores exhibiting some of these design elements was the spherical macrotricyclic cryptand reported by Lehn et al.⁵ (shown in **Figure 2**). This compound exhibited extremely high ammonium over potassium ion selectivity (250 times higher than nonactin) as determined by NMR studies and formed highly stable ammonium complexes (10^5 times higher than nonactin) as calculated by pH metric titration to determine stability constants in aqueous solution. The high selectivity over potassium ion has been attributed to the tetrahedral binding site geometry that favors complexation of the tetrahedral ammonium ion over that of the spherically symmetrical potassium ion. In addition, the macrocyclic nature of the cryptand provides the rigidity necessary to prevent complexation of larger and smaller interfering cations. However, the cryptand is too basic (it exists in its conjugate acid form near neutral blood pH) and hydrophilic (it would leach from the membrane into the aqueous phase during sensor operation) for use as an ionophore in an ISE sensor format.² In addition, this system exhibits a very low dissociation constant indicating very slow cation exchange. For this reason, the cryptand is effectively an ammonium ion sink, whereas an ISE sensor application requires reversible ion binding.⁸

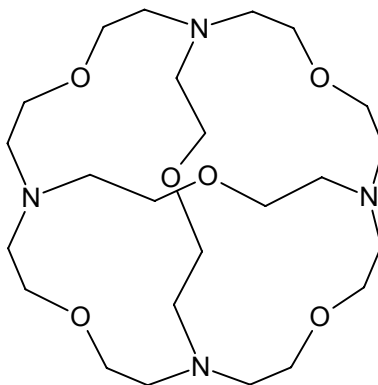


Figure 2: Lehn's macrotricyclic cryptand

Chin et al. reported a rationally designed ammonium receptor, 1,3,5-tris(3,5-dimethylpyrazol-1-ylmethyl)-2,4,6-triethyl benzene (shown in **Figure 3**).² This ionophore was designed to have the lone pair electrons on the imine nitrogens preorganized into the correct geometry for binding ammonium ions through hydrogen bonds. The ethyl and methyl groups provide steric interactions to force the receptor into the desired geometry and to block the ligands from binding potassium ions. This ionophore was highly selective ($\log K_{NH_4^+,K^+} = -2.6$ (nonactin -1.0)⁴, $\log K_{NH_4^+,Na^+} = -2.8$ (nonactin -2.6)⁴) in an ISE sensor format. However, the ammonium detection limit was 10^{-4} M (100 times higher than nonactin) and therefore the sensor was not sufficiently sensitive.⁹ A sensor for blood analysis applications must exhibit sufficient sensitivity to detect lower limits of normal urea and creatinine blood concentrations, which are 1×10^{-3} M and 5×10^{-5} M respectively.¹⁰

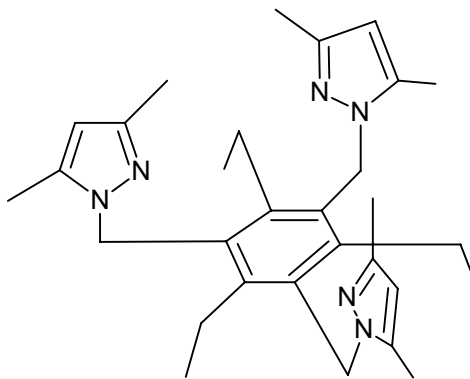


Figure 3: 1,3,5-tris(3,5-dimethylpyrazol-1-ylmethyl)-2,4,6-triethyl benzene ammonium ionophore

Suzuki et al. have synthesized an ammonium ionophore based on a 19-membered crown ether containing three decalino subunits (shown in **Figure 4**).⁶ The decalino subunits add rigidity to prevent folding of the receptor to coordinate smaller cations, add bulkiness to block larger interfering cations from entering the cavity, and also increase the lipophilicity of the ionophore. In an ISE sensor format, this ionophore exhibited similar ammonium over potassium ion selectivity ($\log K_{NH_4^+,K^+} = -1.00$ (nonactin -1.0)⁴) and increased ammonium over sodium ion selectivity ($\log K_{NH_4^+,Na^+} = -3.52$ (nonactin -2.6)⁴) compared to nonactin and a nearly Nernstian response (58.1 mV/decade) in the activity range $5 \times 10^{-6} - 10^{-1}$ M ammonium ion. The observation of Nernstian behavior is particularly important. The relation between the potential difference across the sensor membrane and the activity of ammonium ion should follow the well-known Nernst equation (**Equation 1**):

$$E = E^\circ - (2.303RT/nF) \log a \quad (1)$$

Here, E is the electromotive force (emf) of the cell in volts, E° is the emf cell constant, F is the Faraday constant, a is the activity of the analyte, n is the charge of the measured species, R is the gas constant, and T is the temperature. This equation is in the form of $y = mx + b$ and therefore a plot of E versus $\log a$ will give a straight line with a slope of $2.303RT/nF$. For the measurement of monovalent cations at 25°C , $n = 1$ and the slope becomes 59.16 mV/dec . Thus an ISE that measures ammonium ion and operates according to the Nernst equation should exhibit a slope of 59.16 mV/dec .

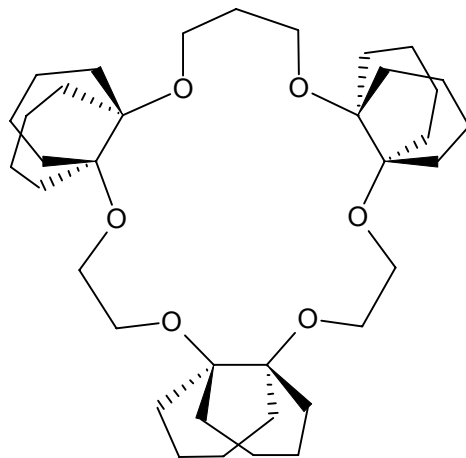


Figure 4: 19-crown-6 ether with decalino subunits

Nam et al. have reported a thiazole containing dibenzo-18-crown-6 derivative (shown in **Figure 5**) as an ammonium ionophore in an ISE sensor format.⁹ This design is primarily based on size-fit factors. The aromatic units increase rigidity and the thiazoles provide hydrogen bonding sites. This ionophore exhibited high selectivity ($\log K_{NH_4^+,K^+} = -1.3$ (nonactin -1.0)⁴, $\log K_{NH_4^+,Na^+} = -3.9$ (nonactin -2.6)⁴) and a similar detection limit of $\sim 3 \times 10^{-6} \text{ M}$ compared to nonactin (10^{-6} M)⁶ in an ISE sensor format.

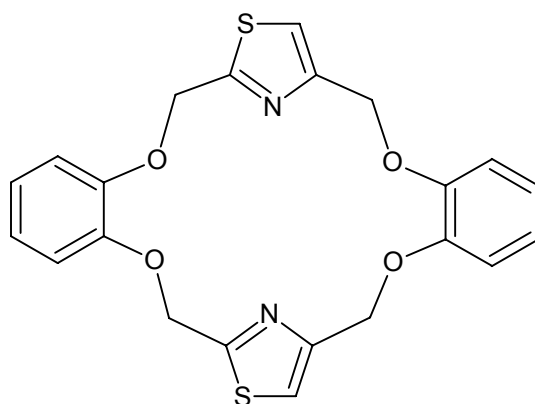


Figure 5: Dibenzo-18-crown-6 ether with thiazole subunits

Kim et al. designed and synthesized an ammonium receptor based on both hydrogen bonding and cation- π interactions, consisting of two benzene rings held rigidly together by three benzocrown ether units as shown in **Figure 6**.⁶ This ionophore design involves a rigid cavity of the appropriate size containing a spatial distribution of ether lone pair electrons for tetrahedral coordination to ammonium along with cation- π interactions provided by the top and bottom benzene rings. Compared to nonactin-based sensors, ISEs doped with this ionophore exhibited similar selectivity ($\log K_{NH_4^+,K^+} = -0.97$ (nonactin -1.0)⁴, $\log K_{NH_4^+,Na^+} = -3.00$ (nonactin -2.6)⁴) and a similar detection limit of 3.2×10^{-6} M (nonactin (10^{-6} M)⁶).

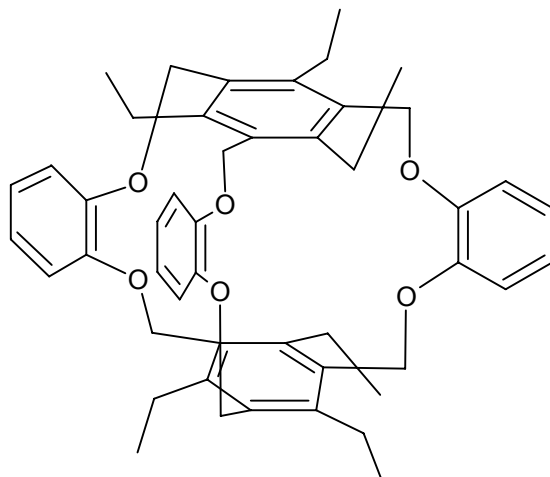


Figure 6: Two benzene rings held together by three benzocrown ether units

McGimpsey et al. have designed and synthesized an ammonium ionophore for an ISE based on a cyclic depsipeptide structure.⁸ The design of this ionophore was inspired by valinomycin, the naturally occurring antibiotic having a high selectivity for potassium ions. Valinomycin, a cyclic depsipeptide consisting of alternating amide and ester linkages (12 total) (shown in **Figure 7a**), preorganizes through hydrogen bonding of its amide carbonyl groups to form a pocket with its six ester carbonyl oxygens available for electrostatic stabilization of potassium ions through octahedral-type complexation.¹¹ The new ionophore (shown in **Figure 7b**) consists of alternating amide and ester units (6 total), which is effectively half of a valinomycin molecule. Unlike valinomycin, this depsipeptide is too rigid to fold upon itself and therefore provides a cavity appropriately sized for ammonium ions, which provides the tetrahedral complexation geometry required for ammonium ion binding, but not the octahedral binding geometry required by potassium ions. ISE sensors incorporating this ionophore exhibited similar selectivity for ammonium over potassium and sodium ions compared to nonactin-based sensors (log

$K_{NH_4^+,K^+} = -0.6$ (nonactin -1.0)⁴, $\log K_{NH_4^+,Na^+} = -2.1$ (nonactin -2.4)⁴) and a nearly Nernstian response (60.1 mV/decade at 37°C).

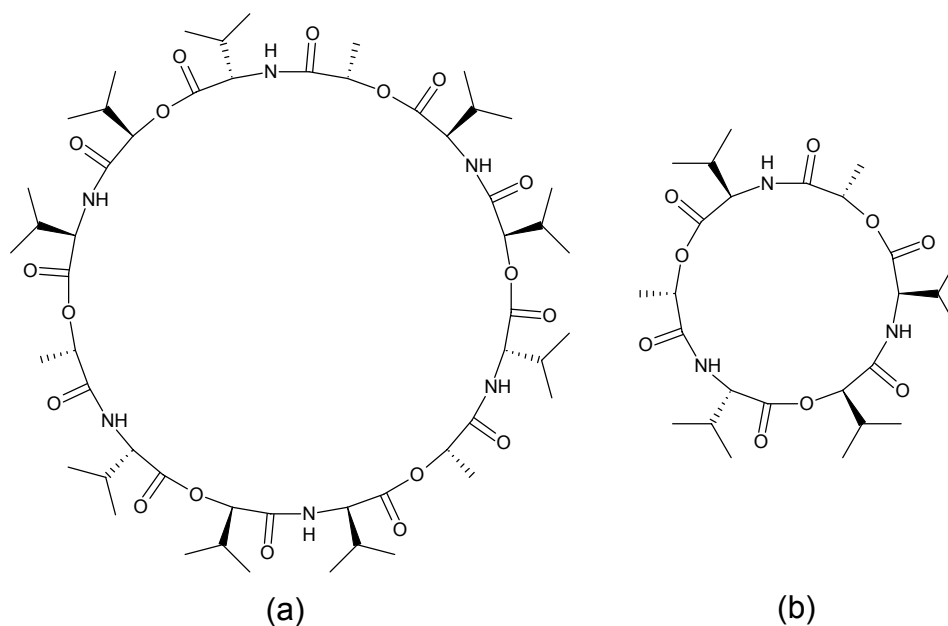


Figure 7: (a) Valinomycin (b) new depsipeptide ammonium ionophore

Cyclic peptides are known to bind and transport metal cations in biological systems.¹² Their ease of synthesis and potential for flexible sequence modification make them good candidates for new ionophores.¹³ However, ordinary cyclic peptides are too flexible to bind substrates in a well-defined cavity¹⁴, leading to low selectivity as sensor components. The addition of a second ring in bicyclic peptides should increase cation binding selectivity by increasing rigidity. Andreu et al. have synthesized cyclo(1,5- ϵ -succinoyl) (Lys-Gly-Gly-Gly)₂ (shown in **Figure 8a**) which exhibits a slight preference for binding Sr²⁺ over other cations.¹³ Zanotti et al. have reported synthesis, conformation, and calcium-binding studies for the bicyclic nonapeptides cyclo(Glu¹-X²-

Pro³-Gly⁴-Lys⁵-X⁶-Pro⁷-Gly⁸)-cyclo-(1 γ \rightarrow 5 ϵ) Gly⁹, where X = Ala or Leu (shown in **Figure 8b**).^{15,16}

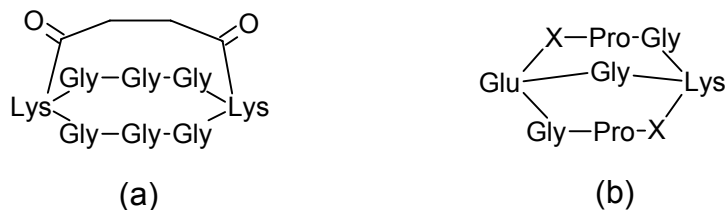


Figure 8: (a) cyclo(1,5- ϵ -succinoyl) (Lys-Gly-Gly-Gly)₂ (b) cyclo(Glu¹-X²-Pro³-Gly⁴-Lys⁵-X⁶-Pro⁷-Gly⁸)-cyclo-(1 γ \rightarrow 5 ϵ) Gly⁹, where X = Ala or Leu

Our research has been directed toward the synthesis and evaluation of new bicyclic peptide ammonium ionophores with predicted ammonium over potassium ion selectivity greater than the industry standard nonactin in an ISE sensor format in order to improve the accuracy of ammonium ion determinations in the presence of potassium ions for clinical evaluation of urea and creatinine levels. The ease of synthesis and demonstrated cation-binding ability make bicyclic peptides promising candidates. Molecular modeling suggests the target compounds **1d**, **2d**, **3d**, **4d**, **5d**, and **6d** shown in **Figure 9** should exhibit tetrahedral coordination geometry in a cavity appropriately sized for ammonium ions.

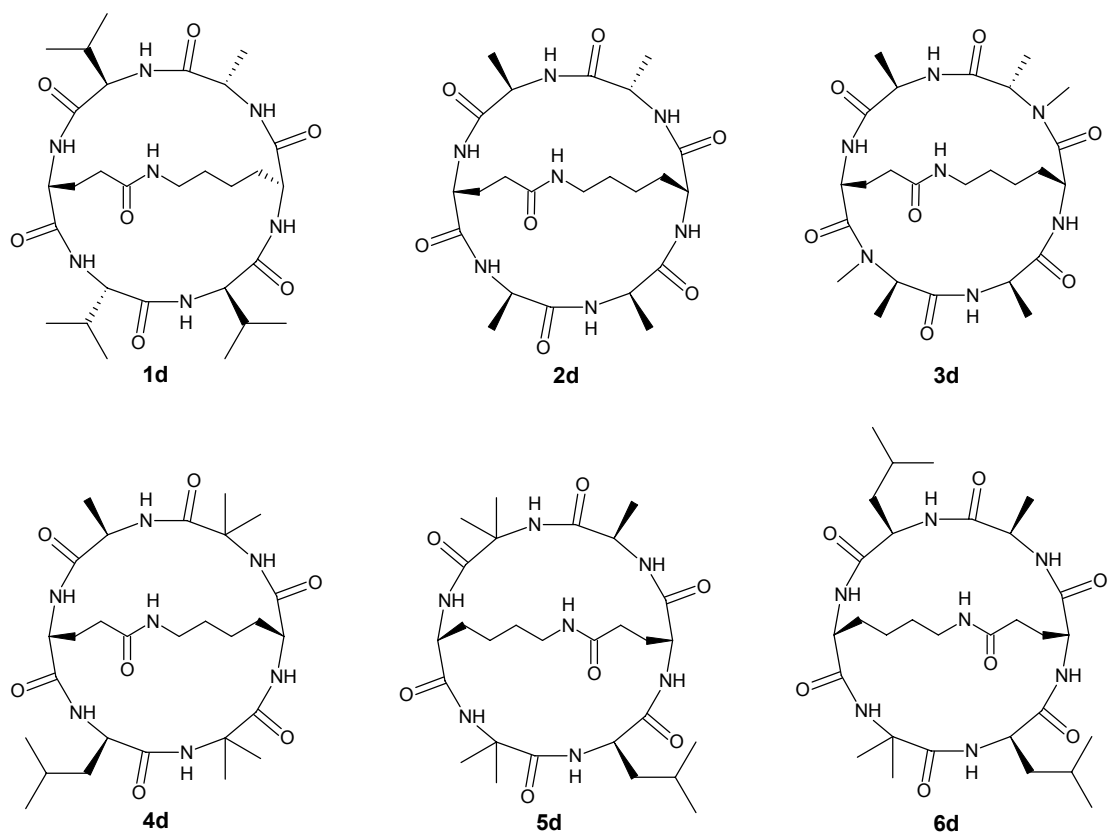


Figure 9: Target bicyclic peptide ammonium ionophores

The naming system for these compounds is based on their preparation from three important synthetic precursors, as shown in **Figure 10** for target **1d** (applicable to all target compounds).

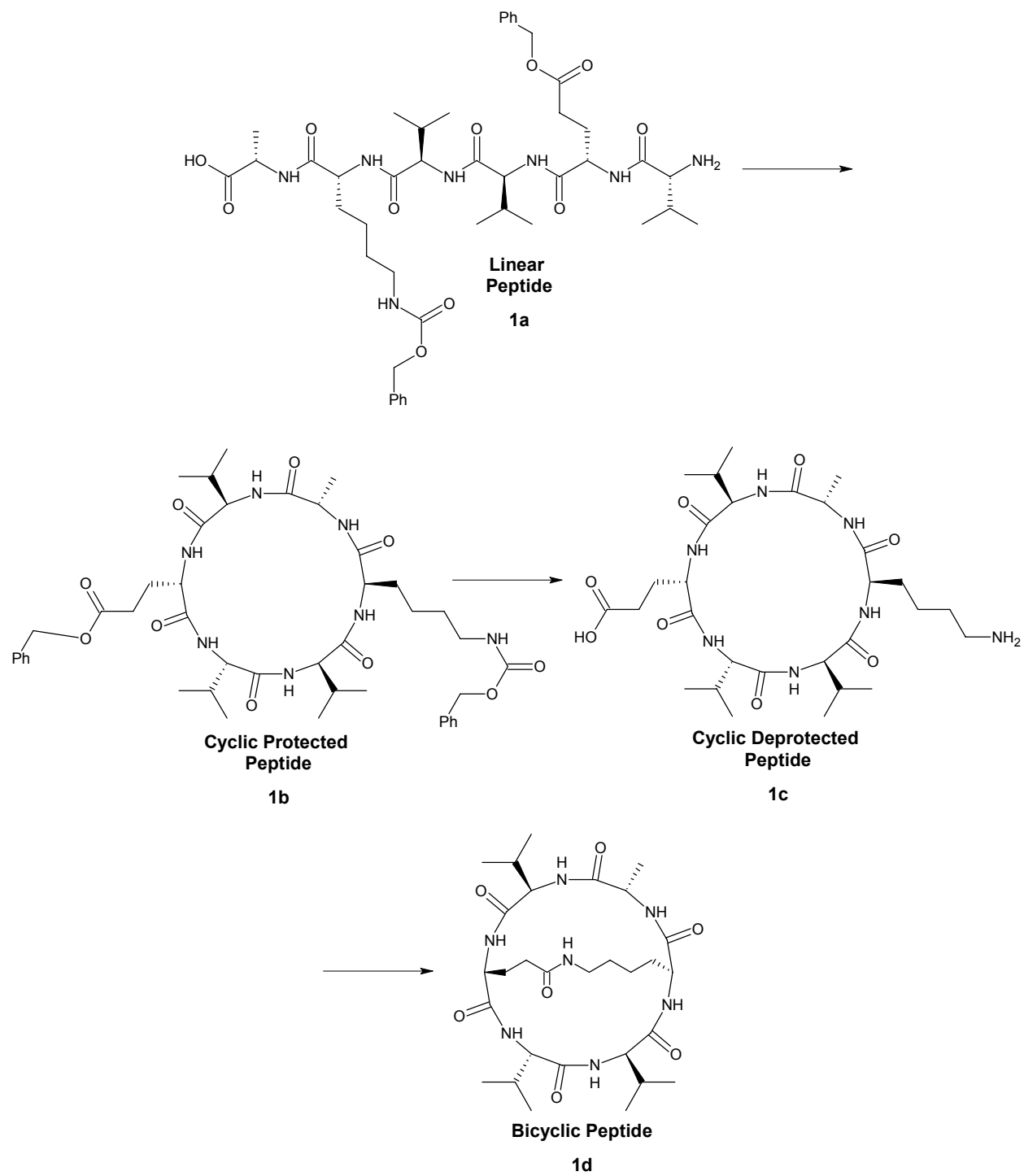


Figure 10: General synthetic scheme for target compound **1d**

2 Experimental

2.1 *General Methods and Materials*

Mass spectra were performed by Synpep Corp. (Dublin, CA) and Bayer Diagnostics Analytical Department (Medfield, MA). ^1H and ^{13}C -NMR were recorded on a Bruker Avance 400. All Fmoc-protected amino acids, all Wang resins, benzotriazole-1-yl-oxy-tris-pyrrolidino-phosphonium hexafluorophosphate (PyBOP), and 1-hydroxybenzotriazole hydrate (HOBT) were purchased from Calbiochem-Novabiochem Corp. All solvents and reagents were analytical reagent grade, purchased from local suppliers, and used as received without further purification. Buffers were prepared with deionized water (18 M Ω :cm).

2.2 *Molecular Modeling Calculations*

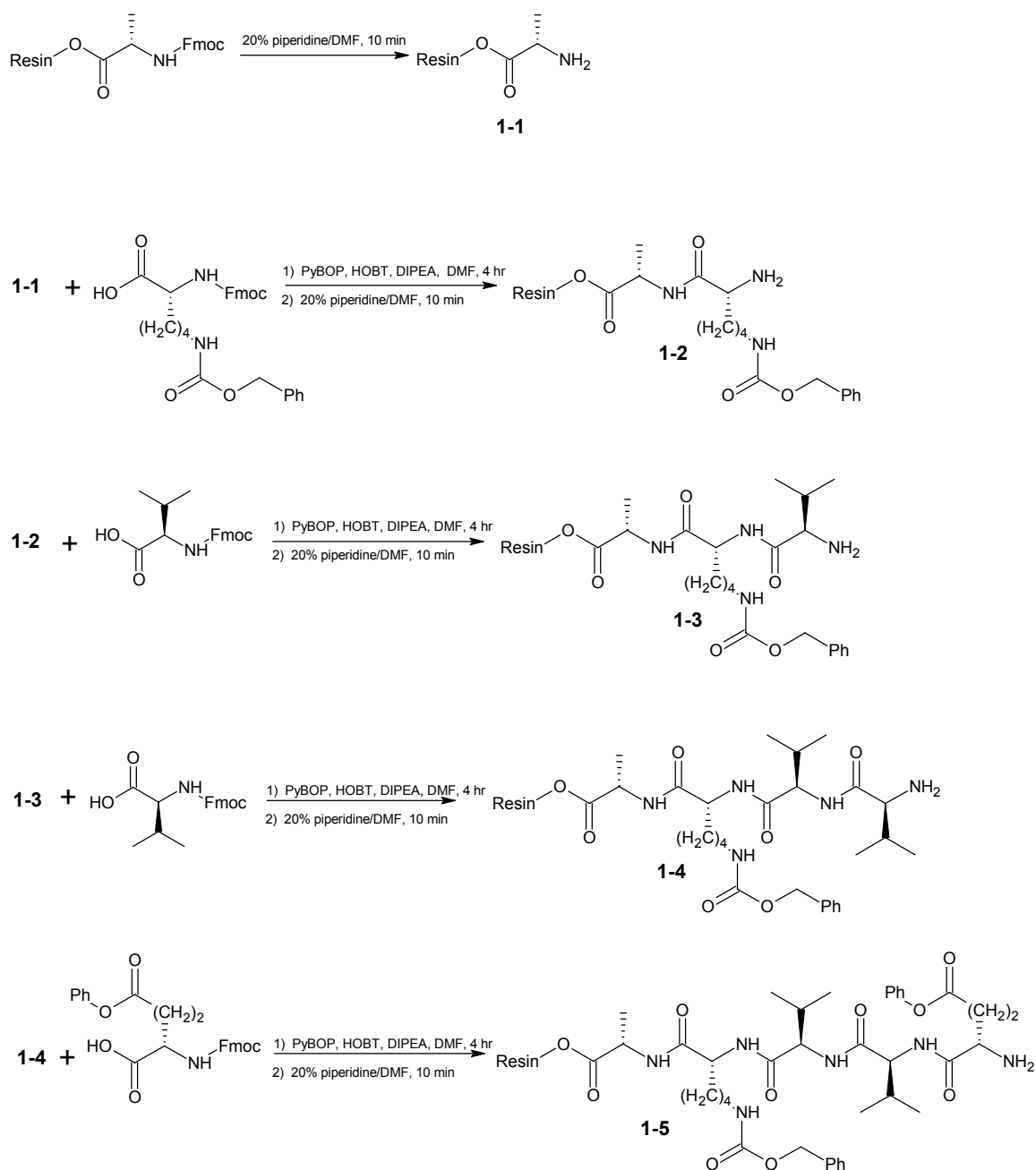
Molecular modeling was performed on an SGI 320 running Windows NT, as previously reported.⁸ Calculations were carried out using the Molecular Operating Environment version 2000.02 computing package (Chemical Computing Group Inc., Montreal, PQ, Canada). Structures were minimized first using the AMBER94 potential control under a solvent dielectric of 5. PEF95SAC was used to calculate partial charges. Minimized structures were then subjected to a 30-ps molecular dynamics simulation employing the NVT statistical ensemble. The structures were heated to 400 K, equilibrated at 310 K, and cooled to 290 K in the dynamics thermal cycle at a rate of 10 K/ps. The lowest energy structures obtained from these dynamics calculations were then minimized again.

Using the minimized structures, docking energies of the ammonium and the potassium cations were calculated by employing the default parameters supplied with the program.

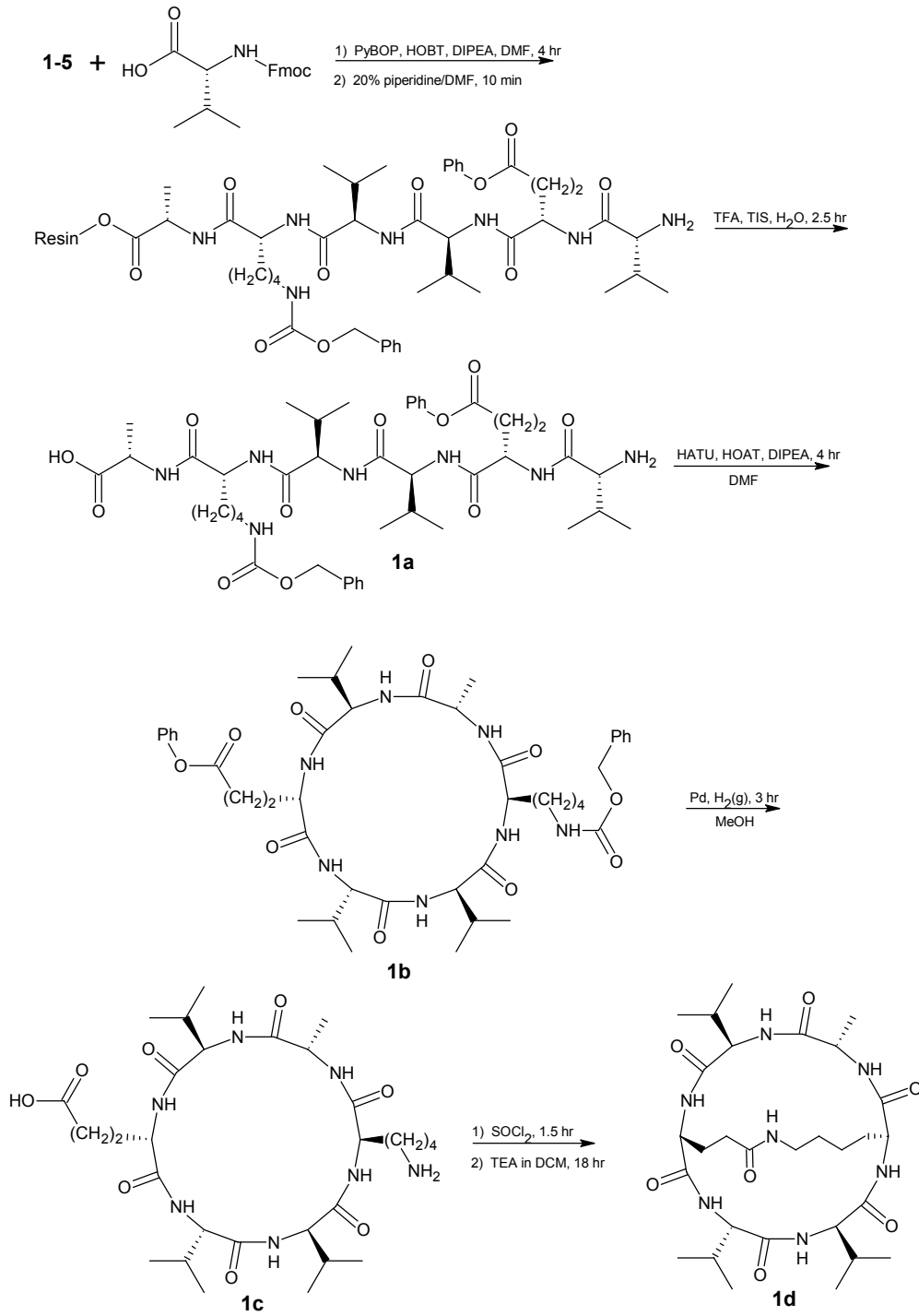
2.3 *Synthesis*

The synthetic scheme for target compound **1d** is shown in **Scheme 1**.

Scheme 1: Synthesis of **1d**



Scheme 1: continued



2.3.1 Synthesis of 1a

Solid phase peptide synthesis was carried out on 5 g of Fmoc-Ala-Wang resin (0.41 mmol/g loading). The resin was swelled by adding 30 mL DMF and mixing with N₂ for 30 min., at which point the DMF was removed by aspiration. The resin-bound N-Fmoc protected alanine was deprotected with 20% piperidine in DMF (30 mL, 10 min.). The solution was removed by aspiration and the resin was washed 3x with 30 mL DMF, 3x with 30 mL MeOH, 1x with 30 mL EtOH, and vacuum dried. A Kaiser test was performed by adding 2 drops of each of three solutions to a few resin beads and heating in the oven for 3-4 min. The solutions were prepared by dissolving 5 g of ninhydrin in 100 mL EtOH, dissolving 80 g of phenol in 20 mL EtOH, and adding 2 mL of a 0.001 M aqueous solution of potassium cyanide to 98 mL pyridine.¹⁷ A positive Kaiser test for free amine, as indicated by blue beads, confirmed successful deprotection. The resin was reswelled in 30 mL of DMF mixed with N₂ for 10 min. 2.60 g (2.5 eq) Fmoc-D-Lys(Z), 2.67 g (2.5 eq) PyBOP, 0.69 g (2.5 eq) HOBT, and 1.8 mL (5 eq) diisopropylethylamine (DIPEA) were dissolved in 5 mL DMF and added to the prepared resin. The total volume was increased to 30 mL and mixed with N₂ for 4 hr. at which time the solution was removed by aspiration and the resin was rinsed 3x with DMF, 3x with MeOH, 1x with EtOH, and vacuum dried. A negative Kaiser test confirmed complete coupling. This [deprotection - rinses - Kaiser test - coupling reaction - rinses - Kaiser test] cycle was repeated for the remaining four amino acid residues to give (Resin)—(L-Ala)—(D-Lys(Z))—(D-Val)—(L-Val)—(L-Glu(OBzl))—(D-Val-Fmoc). In the event of incomplete coupling, as indicated by a positive Kaiser test, the coupling reaction was repeated. The terminal valine residue was deprotected and a Kaiser test was performed to

confirm successful deprotection. The resin was rinsed 3x with DMF, 3x with MeOH, 2x with DMF, 2x with MeOH, and vacuum dried.

The linear peptide was cleaved from the resin with 30 mL of TFA/H₂O/triisopropylsilane (TIS) 95/2.5/2.5 over 2.5 hr. by mixing with N₂. The peptide solution was removed by aspiration and concentrated down to a few mL's. Cold ether precipitated the linear peptide as a white solid, which was collected by filtration. The peptide was dissolved in MeOH and reprecipitated twice to obtain 1.2 g (67% yield) of a white powder. ¹H and ¹³C-NMR and ESI MS of this and subsequent compounds may be found in **Appendix A**. ¹H-NMR (400 MHz, DMSO), δ 0.64-1.02 (m, 18H), 1.13-1.68 (m, 9H), 1.75-2.15 (m, 5H), 2.28-2.51 (m, 2H), 2.88-3.02 (m, 2H), 4.10-4.56 (m, 7H), 5.00 (s, 2H), 5.08 (s, 2H), 7.17-7.51 (m, 12H), 7.65-8.18 (m, 7H), 8.42 (d, *J* = 7.8 Hz, 1H); ¹³C-NMR (100 MHz, DMSO), δ 17.7, 17.9, 18.2, 18.2, 18.7, 18.9, 19.7 (CH₃), 22.9, 28.1, 29.4 (CH₂), 30.3 (CH), 30.4 (CH₂), 30.8, 31.1 (CH), 32.2, 40.5 (CH₂), 47.8, 52.2, 52.7, 57.7, 57.7, 58.2 (CH), 65.5, 65.9 (CH₂), 128.1, 128.3, 128.4, 128.7, 128.8 (CH, Ar), 136.5, 137.6 (C, Ar), 156.4, 168.5, 170.9, 171.0, 171.1, 171.4, 172.3, 174.3 (C=O). ESI MS *m/z* (%) calcd. for C₄₄H₆₆N₇O₁₁ (M+H⁺) 868.5 found 868.2 (100).

2.3.2 Synthesis of **1b**

The 1.20 g (1.38 mmol) of linear peptide **1a** was dissolved in approximately 450 mL DMF and 50 mL benzene. 0.682 g (1.3 eq) O-(7-Azabenzotriazole-1-yl)-N,N,N',N'-tetramethyluronium hexafluorophosphate (HATU), 0.244 g (1.3 eq) 1-Hydroxy-7-

azabenzotriazole (HOAT), and 2.4 mL (10 eq) DIPEA dissolved in 5 mL of DMF was added and the solution was stirred for 24 hr. at room temperature. At this point, the DMF was removed in vacuo, 55-60 °C. The residue was dissolved in DCM and extracted 3x with 100 mL of saturated NaHCO₃, 3x with 100 mL of 10% citric acid, and dried over Na₂SO₄. The organic solution was concentrated completely, and then dissolved in MeOH. The peptide was precipitated with ether/hexanes at -4 °C and collected by filtration to give 170 mg (14% yield) of crude monocyclused peptide. Characterization by ¹H and ¹³C-NMR and ESI MS was inconclusive.

2.3.3 Synthesis of **1c**

The 170 mg (0.200 mmol) of **1b** was combined with 30 mg from a previous synthesis and dissolved in 100 mL of MeOH. The benzyl protecting groups on the glutamic acid and lysine side chains were removed by using 0.2 g of Pd activated carbon (10 wt%), and H₂ at atmospheric pressure while stirring the solution for 3 hr. The spent catalyst was removed by filtration and the solution was concentrated totally in vacuo, 40 °C. ¹H and ¹³C-NMR spectra in DMSO confirmed loss of benzyl groups. The 120 mg (96% yield) of peptide was used without further purification or characterization.

2.3.4 Synthesis of **1d**

The 120 mg (0.192 mmol) of **1c** was stirred in 15 mL thionyl chloride for 1.5 hr. at which point the thionyl chloride was removed in vacuo. The residue was dissolved in benzene,

and then concentrated completely to remove residual thionyl chloride. The peptide acid chloride was dissolved in 30 mL DCM, to which 0.27 mL (10 eq) triethylamine (TEA) was added and the solution was stirred for 18 hr. at which point, the solution was concentrated completely, then redissolved in 5% MeOH/DCM. The addition of cold ether precipitated 20 mg of a brown solid which was collected by filtration. Characterization by ESI MS was inconclusive.

2.3.5 Synthesis of 2a

Solid phase synthesis was carried out on 5.035 g of Fmoc-Ala-Wang resin (0.41 mmol/g loading) for the amino acid sequence (L-Ala)—(L-Lys(Z))—(D-Ala)—(D-Ala)—(L-Glu(OBzl))—(D-Ala) using the same general solid phase methods described for compound **1a**.

The linear peptide was cleaved from the resin with 30 mL of TFA/H₂O/TIS 95/2.5/2.5 mixed with N₂ for 2.5 hr. The peptide solution was removed by aspiration and concentrated down to a few mL's. Cold ether precipitated the linear peptide as a white solid, which was collected by filtration. The peptide was dissolved in MeOH, precipitated with cold ether, and filtered to obtain 1.24 g (77% yield) of a white powder. R_f (RP) .35 (1.9:1 H₂O/MeCN); ¹H-NMR (400 MHz, DMSO), δ 0.90-1.33 (m, 21H), 1.35-1.49 (m, 1H), 1.53-1.77 (m, 2H), 2.05-2.31 (m, 4H), 2.62-2.77 (m, 2H), 3.10-3.26 (m, 1H), 3.53-3.66 (m, 1H), 3.75-4.14 (m, 7H), 4.76 (s, 2H), 4.85 (s, 2H), 7.00 (t, J = 5.6 Hz, 1H), 7.03-7.22 (m, 10H, Ar), 7.67 (d, J = 8.8 Hz, 1H), 7.75 (d, J = 7.1 Hz, 1H), 7.83

(d, $J = 7.1$ Hz, 1H), 8.19 (d, $J = 7.3$ Hz, 1H), 8.59 (d, $J = 8.1$ Hz, 1H); ^{13}C -NMR (100 MHz, DMSO), δ 17.9, 17.9, 18.4, 18.4 (CH_3), 22.8, 27.7, 29.4, 30.2, 32.0, 40.5 (CH_2), 48.4, 48.6, 48.6, 48.8, 52.1, 52.4 (CH), 65.5, 66.0 (CH_2), 128.1, 128.3, 128.4, 128.7, 128.8 (CH, Ar), 136.4, 137.6 (C, Ar), 156.4, 170.4, 170.8, 171.6, 172.1, 172.3, 172.3, 174.7 (C=O). ESI MS m/z (%) calcd. for $\text{C}_{38}\text{H}_{54}\text{N}_7\text{O}_{11}$ ($\text{M}+\text{H}^+$) 784.4 found 784.0 (100).

2.3.6 Synthesis of 2b

1.26 g (1.61 mmol) of **2a** was dissolved in 600 mL of DMF and stirred at 0 °C. 0.791 g (1.3 eq) HATU, 0.283 g (1.3 eq) HOAT, and 2.8 mL (10 eq) DIPEA dissolved in 5 mL of DMF was added and the reaction mixture was stirred for 4 hr., at which point the DMF was removed in vacuo, 55-60 °C. The residue was dissolved in MeOH and cold ether was added to precipitate a white solid, which was collected by filtration and redissolved in MeOH. A white solid that precipitated out of the MeOH solution was removed by filtration. The solution was concentrated completely and purified by reverse phase (C18) column chromatography (1.2:1 $\text{H}_2\text{O}:\text{MeCN}$) to obtain 250 mg (20% yield) of a white solid. $R_f(\text{RP})$.31 (1.2:1 $\text{H}_2\text{O}:\text{MeCN}$); ^1H -NMR (400 MHz, MeOD), δ 1.50-1.82 (m, 18H), 1.91-2.14 (m, 2H), 2.17-2.37 (m, 2H), 2.64-2.79 (m, 2H), 3.31-3.44 (m, 2H), 4.28-4.33 (m, 1H), 4.38-4.44 (m, 1H), 4.51-4.61 (m, 2H), 4.68-4.80 (m, 2H), 5.31 (s, 2H), 5.37 (s, 2H), 7.47-7.71 (m, 10H, Ar); ^{13}C -NMR (100 MHz, MeOD), δ 17.4, 17.9, 18.1, 19.2 (CH_3), 24.4, 27.6, 30.9, 31.5, 32.2, 41.6 (CH_2), 50.0, 50.7, 51.0, 52.0, 55.0, 56.7 (CH), 67.8, 67.9 (CH_2), 129.2, 129.4, 129.6, 129.7, 129.9, 130.0 (CH, Ar), 137.9, 138.8 (C, Ar),

159.4, 174.3, 174.6, 174.6, 174.8, 174.8, 174.9, 175.9 (C=O). ESI MS m/z (%) calcd. for $C_{38}H_{52}N_7O_{10}$ (M+H⁺) 766.4 found 766.3 (6), calcd. M+Na⁺ 788.4 found 788.3 (100).

2.3.7 Synthesis of 2c

250 mg of **2b** was combined with 120 mg from a previous synthesis for a total of 370 mg (0.483 mmol) and dissolved in 50 mL of MeOH. The benzyl protecting groups on the glutamic acid and lysine side chains were removed by using 0.2 g of Pd activated carbon (10 wt%), and H₂ at atmospheric pressure while stirring the solution for 3.5 hr. The spent catalyst was removed by filtration and the solution was concentrated completely. Analytical TLC with ninhydrin tests showed a product mixture and therefore the hydrogenation reaction was repeated for 3.5 hr. The product was 160 mg (61% yield) of a white solid. Essentially complete loss of benzyl protecting groups was confirmed by ¹H and ¹³C-NMR. The peptide was used without further purification or characterization.

2.3.8 Synthesis of 2d

160 mg (0.295 mmol) of **2c** was dissolved in 125 mL of DMF and stirred at 0 °C. 0.146 (1.3 eq) HATU, 0.052 g (1.3 eq) HOAT, and 0.52 mL (10 eq) DIPEA dissolved in 5 mL of DMF was added and the reaction mixture was stirred for 4 hr., at which point the DMF was removed in vacuo, 45°C. The residue was dissolved in MeOH and a white suspension was removed by centrifugation. The solution was concentrated completely and extracted 3x with DCM/H₂O. The aqueous portion was vacuum evaporated and

dissolved in 1:1:3 MeOH:EtOAc:DCM. The insoluble portion was removed by filtration. Again, the solution was concentrated completely, dissolved in MeOH, reprecipitated with cold ether, and collected by centrifugation 4x to obtain 45 mg (29% yield) of a yellow solid. This was redissolved in 50 mL of MeOH, cooled to 5 °C for 4 hr., and centrifuged to collect 10 mg of an insoluble white precipitate. ESI MS m/z (%) calcd. for $C_{23}H_{37}N_7O_7Na$ ($M+Na^+$) 546.3 found 546.3 (25) in the partially purified product (prior to the final precipitation from MeOH).

2.3.9 Synthesis of 3a

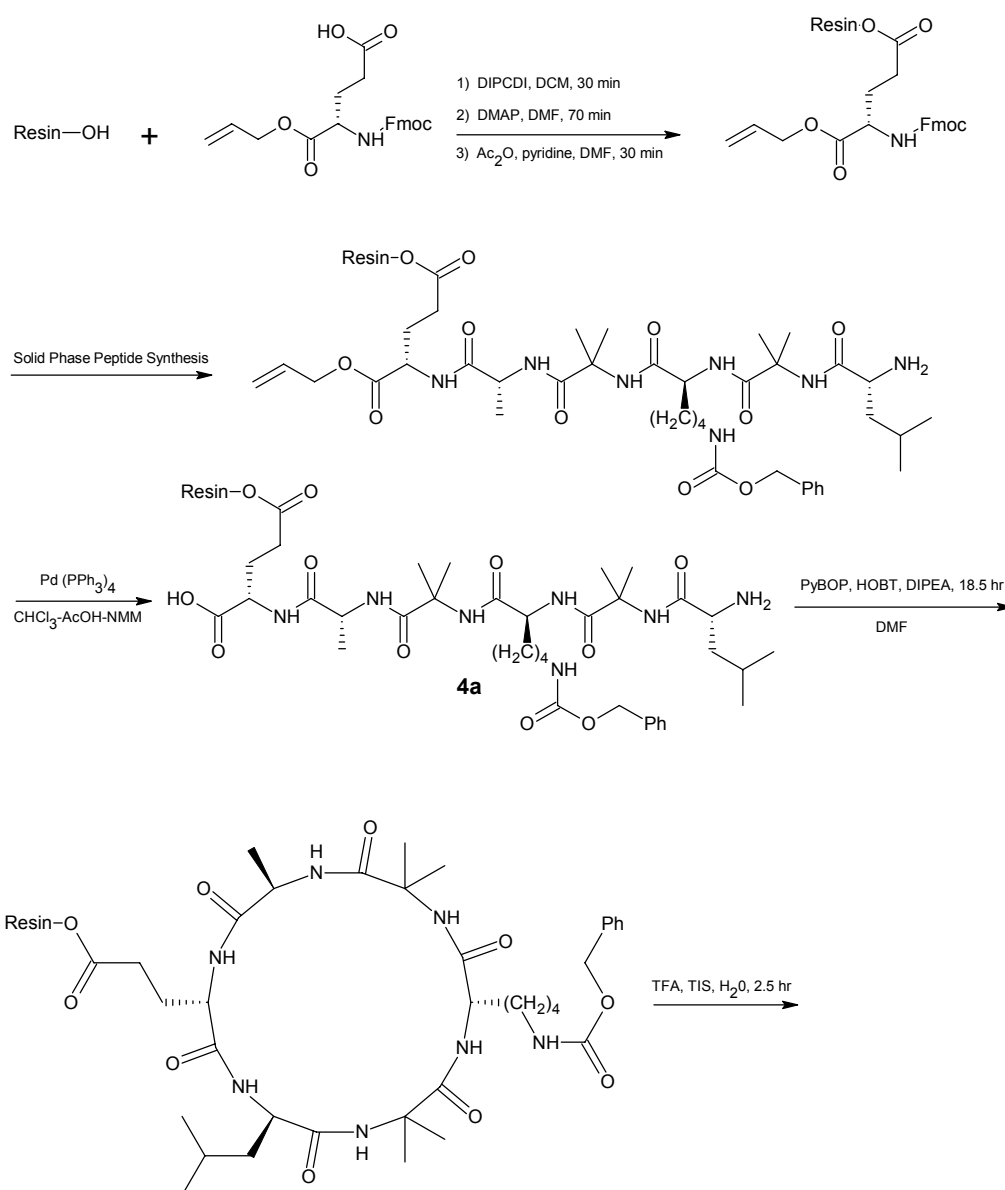
Solid phase synthesis was carried out on Wang resin (1.1 mmol/g loading) for the amino acid sequence (L-MeAla)—(L-Lys(Z))—(D-Ala)—(D-MeAla)—(L-Glu(OBzl))—(D-Ala). 2.803 g Wang resin was swelled in 30 mL DMF mixed with N_2 for 30 min. at which point the DMF was removed by aspiration. 3.006 g (3 eq) of Fmoc-MeAla was dissolved in 50 mL of dry DCM and stirred at 0 °C. 1.45 mL diisopropylcarbodiimide (DIPCDI) in 5 mL of DMF was added and the reaction mixture was stirred for 30 min. At this point, the solution was concentrated completely, dissolved in 5 mL DMF, and added to the resin. 0.038 g (0.1 eq) dimethylaminopyridine (DMAP) in DMF was added to the resin and the total volume was increased to 40 mL. The solution was mixed with N_2 for 1.5 hr. covered at room temperature. Loading of the first amino acid to the resin was evaluated by cleaving the Fmoc protection group from a known mass of resin (20 mg) in a 100 mL solution of 20% piperidine in DMF and monitoring the UV absorption at 290 nm. Using a molar extinction coefficient of 4950 a loading of 72% was obtained.

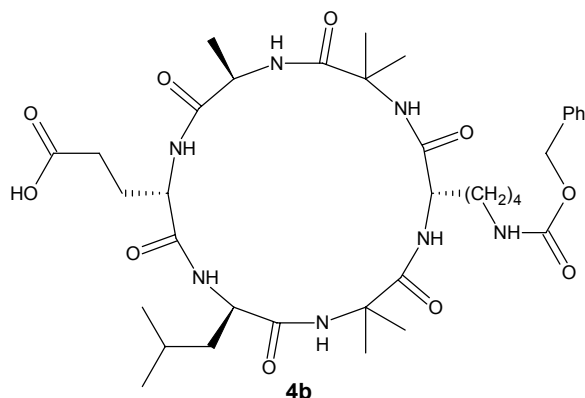
Stepwise addition of the next 5 amino acids was carried out according to the standard solid phase method described for compound **1a**. The Kaiser test was inconclusive for secondary amines, so completeness of reaction was monitored by UV absorption of Fmoc when coupling to resin-bound terminal MeAla residues. In addition, deprotection reactions were allowed longer reaction time (15-20 min.) and repeated.

The linear peptide was cleaved from the resin with 30 mL of TFA/H₂O/TIS 95/2.5/2.5 over 2.5 hr. by mixing with N₂. The peptide solution was removed by aspiration and concentrated completely to yield an oil. ESI MS indicated that none of the desired product was formed.

The general scheme for synthesis of the intermediates **4a** and **4b** of target compound **4d** is shown in **Scheme 2**.

Scheme 2: Synthesis of 4a and 4b





2.3.10 Synthesis of 4a

Solid phase synthesis was carried out on Wang resin (1.0 mmol/g loading) for the amino acid sequence (L-Glu-OAll)—(D-Ala)—(Aib)—(L-Lys(Z))—(Aib)—(D-Leu). 2.013 g Wang resin was swelled in 30 mL DMF mixed with N₂ for 30 min. at which point the DMF was removed by aspiration. 2.059 g (2.5 eq) of Fmoc-Glu-OAll was dissolved in 50 mL of dry DCM and stirred at 0 °C. 0.79 mL DIPCDI in 5 mL of DMF was added and the reaction mixture was stirred for 30 min., at which point the solution was concentrated completely, dissolved in 5 mL DMF, and added to the resin. 0.025 g (0.1 eq) DMAP in DMF was added to the resin and the total volume was increased to 40 mL. The solution was mixed with N₂ for 70 min. at room temperature. Loading of the first amino acid to the resin was evaluated by cleaving the Fmoc protecting group from a known mass of resin (20 mg) in a 100 mL solution of 20% piperidine in DMF and monitoring the UV absorption at 290 nm. Using a molar extinction coefficient of 4950 a loading of 59% was obtained. The resin was capped with 0.22 mL (2 eq to resin-glutamic acid) acetic anhydride and 0.19 mL (2 eq to resin-glutamic acid) pyridine in 30

mL of DMF for 30 min. mixing with N₂. Stepwise addition of the next 5 amino acids was carried out according to the solid phase method described for compound **1a**. The Kaiser test was inconclusive for aminoisobutyric acid free amine, so coupling reactions were repeated twice for 10 hr. for resin-bound terminal Aib residues.

The glutamic acid O-Allyl protecting group was removed according to a modified procedure.¹⁷ A solution of 5.398 g (3 eq) of tetrakis(triphenylphosphine)palladium(0) dissolved in 67.5 mL (15 mL/g of resin) 37:2:1 chloroform/acetic acid/N-methylmorpholine (NMM) was added to the resin and mixed with N₂ for 2 hr. At this point, the solution was filtered off and the resin was subjected to a series of rinses: 30 mL 0.5% DIPEA in DMF, 3x 2 min.; 30 mL 0.5% sodium diethyldithiocarbamate in DMF, 3x 10 min.; 30 mL DMF, 1x 2 hr.; 30 mL DMF, 1x 10 min.; 30 mL 0.5% HOBT in DMF, 3x 5 min.; 30 mL DMF, 3x 1 min.; 30 mL MeOH, 3x 1 min.; 30 mL EtOH, 1x 1 min. The deprotection reaction was repeated and the resin was subjected to similar rinses.

2.3.11 Synthesis of 4b

The resin was swelled in 30 mL DMF mixing with N₂ for 30 min. to prepare for on-resin cyclization. 2.024 g (2.5 eq) PyBOP, 0.526 g (2.5 eq) HOBT, and 1.4 mL (5 eq) DIPEA dissolved in 5 mL DMF was added to the resin. The volume was increased to 50 mL and mixed with N₂ for 18.5 hr. The resin was subjected to the normal solid phase rinses and vacuum dried. The Kaiser test was weakly positive, indicating incomplete cyclization, so

the cyclization reaction was repeated for 23 hr. Again, the Kaiser test was weakly positive, so the reaction was repeated a third time for 6 hr. The resin was then rinsed and vacuum dried.

The peptide was cleaved from the resin with 30 mL of TFA/H₂O/TIS 95/2.5/2.5 over 2.5 hr. by mixing with N₂. The peptide solution was removed by aspiration and concentrated down to a few mL's. A white solid precipitated out with the addition of cold ether and was collected by centrifugation. The solid was dissolved in 1 mL MeOH. Added H₂O precipitated a white solid and the yellow solution was decanted off to give 60 mg (5% yield) of a white solid. ESI MS m/z (%) calcd. for C₃₆H₅₆N₇O₁₀ (M+H⁺) 746.4 found 746.2 (4), calcd. M-(Z)+H⁺ 612.4 found 611.9 (100).

2.3.12 Synthesis of 5a

Solid phase synthesis was carried out on 5.228 g D-Ala-Wang resin (0.72 mmol/g loading) for the amino acid sequence (D-Ala)—(L-Glu(OBzl))—(D-Leu)—(Aib)—(L-Lys(Z))—(Aib) as described for compound **1a**. The Kaiser test was inconclusive for aminoisobutyric acid free amine so the coupling reaction of the resin-bound terminal Aib residue with Fmoc-Lys(Z) was repeated twice for 20 hr. each time.

The peptide was cleaved from the resin with 30 mL of TFA/H₂O/TIS 95/2.5/2.5 over 1.5 hr. by mixing with N₂. The peptide solution was removed by aspiration and concentrated down to a few mL's. The residue was purified by flash column chromatography (19:1

DCM:MeOH then 6.1:1 DCM:MeOH) to give 650 mg of a white solid. Column chromatography (2.6:1 DCM:MeOH) was used to purify additional fractions recovered from the second flash column to give an additional 330 mg for a total of 980 mg (31% yield) of linear peptide. R_f .30 (3:1 DCM/MeOH); $^1\text{H-NMR}$ (400 MHz, MeOD), δ 0.58-1.66 (m, 37H), 1.81-1.95 (m, 2H), 2.16-2.30 (m, 1H), 2.36-2.45 (m, 1H), 2.82-2.94 (m, 2H), 3.12 (s, 2H), 3.80-4.06 (m, 4H), 4.75-4.89 (m, 4H), 6.99-7.16 (m, 10H, Ar); $^{13}\text{C-NMR}$ (100 MHz, MeOD), δ 19.3, 21.8, 23.9, 23.9, 24.1 (CH_3), 24.4 (CH_2), 26.0 (CH_3), 26.9 (CH), 27.8 (CH_3), 28.0, 31.1, 32.2, 32.3, 40.7, 41.8 (CH_2), 52.2, 54.6, 55.1, 56.4 (CH), 58.3, 58.4 (C), 67.6, 67.8 (CH_2), 129.2, 129.4, 129.5, 129.9 (CH, Ar), 138.0, 138.8 (C, Ar), 159.4, 173.4, 174.6, 174.7, 174.8, 176.3, 177.6, 180.2 (C=O). ESI MS m/z (%) calcd. for $\text{C}_{43}\text{H}_{63}\text{N}_7\text{O}_{11}$ ($\text{M}+\text{H}^+$) 854.5 found 854.3 (100), calcd. $\text{M}+\text{Na}^+$ 876.5 found 876.3 (33), calcd. $\text{M}+\text{K}^+$ 892.5 found 892.3 (23).

2.3.13 Synthesis of 5b

800 mg (0.937 mmol) of linear peptide **5a** was dissolved in 400 mL DMF and stirred at 0 °C. 0.464 g (1.3 eq) HATU, 0.166 g (1.3 eq) HOAT, and 2.4 mL (10 eq) DIPEA in 5 mL of DMF was added and the solution was stirred for 4 hr. at which point the DMF was removed in vacuo, 45 °C. The residue was taken up in EtOAc and the insoluble white precipitate was removed by filtration. The organic solution was extracted 3x with 30 mL 10% citric acid, 3x with 30 mL saturated NaHCO_3 , and dried over Na_2SO_4 . The solution was purified by flash column chromatography (EtOAc) to give 450 mg (57% yield) of a white solid. R_f .47 (EtOAc); $^1\text{H-NMR}$ (400 MHz, CDCl_3), δ 0.79-0.98 (m, 6H), 1.09-

2.49 (m, 29H), 2.93-3.36 (m, 2H), 3.73 (t, $J = 6.7$ Hz, 1H), 4.03-4.21 (m, 1H), 4.41-4.58 (m, 1H), 4.79-4.94 (m, 1H), 4.98-5.18 (m, 4H), 5.62 (t, $J = 5.6$ Hz, 1H), 6.17 (s, 1H), 6.35-6.57 (m, 1H), 6.97-7.20 (m, 2H), 7.21-7.44 (m, 10H, Ar), 7.61 (s, 1H); ^{13}C -NMR (100 MHz, CDCl_3), δ 16.5, 21.4, 21.4 (CH_3), 21.8, 22.5 (CH_2), 22.9, 23.4, 23.8 (CH_3), 24.8 (CH), 26.0, 27.9 (CH_2), 27.9 (CH_3), 30.3, 38.8, 39.5 (CH_2), 50.4, 51.4, 51.5, 53.2 (CH), 56.9, 57.4 (C), 66.4, 66.7 (CH_2), 128.5, 128.6, 128.8, 128.9, 129.1 (CH, Ar), 136.2, 136.9 (C, Ar), 156.8, 172.2, 172.9, 173.5, 174.0, 174.6, 175.9, 176.5 (C=O). ESI MS m/z (%) calcd. for $\text{C}_{43}\text{H}_{62}\text{N}_7\text{O}_{10}$ ($\text{M}+\text{H}^+$) 836.4 found 836.2 (6), calcd. $\text{M}+\text{Na}^+$ 858.4 found 858.2 (100).

2.3.14 Synthesis of **5c**

400 mg (0.478 mmol) of **5b** was dissolved in 100 mL of 1:1 DCM:MeOH. The benzyl protecting groups on the glutamic acid and lysine side chains were removed by using 0.2 g of Pd activated carbon (10 wt%) and H_2 at atmospheric pressure while stirring the solution for 1.5 hr. The spent catalyst was removed by filtration and the solution was concentrated completely in vacuo, 40 °C, to give 305 mg (105% yield) of a white solid. ^1H and ^{13}C -NMR spectra in MeOD confirmed complete loss of benzyl protecting groups. The peptide was used without further purification or characterization.

2.3.15 Synthesis of 5d

305 mg (0.498 mmol) of **5c** was dissolved in 150 mL of DMF and stirred at 0 °C. 0.246 g (1.3 eq) HATU, 0.088 g (1.3 eq) HOAT, and 0.87 mL (10 eq) DIPEA dissolved in 5 mL of DMF was added to the peptide solution for 4 hr. at which point the DMF was removed in vacuo, 45 °C. The residue was taken up in EtOAc and the insoluble white precipitate was removed by centrifugation. The organic solution was extracted 3x with 30 mL of 10% citric acid and 3x with 30 mL of saturated NaHCO₃ and dried with Na₂SO₄. The solution was concentrated completely and dried in vacuo to give 5 mg of a white solid. Characterization by ESI MS was inconclusive.

2.3.16 Synthesis of 6a

Solid phase synthesis was carried out on 5.642 g D-Ala-Wang resin (0.72 mmol/g loading) for the amino acid sequence (D-Ala)—(L-Glu(OBzl))—(D-Leu)—(Aib)—(L-Lys(Z))—(D-Leu) as described for compound **5a**.

The peptide was cleaved from the resin in two consecutive reactions of 30 mL of TFA/H₂O/TIS 95/2.5/2.5 mixed with N₂ for 30 min. each. The peptide solutions were removed by aspiration, combined, and concentrated to a few mL's. The residue was purified by column chromatography (4.6:1 DCM:MeOH) and then flash column chromatography (19:1 DCM:MeOH) to give 1.40 g (39% yield) of a light yellow solid. R_f .30 (4.6:1 DCM/MeOH); ¹H-NMR (400 MHz, MeOD), δ 0.61-0.79 (m, 14H), 1.01-1.35 (m, 16H), 1.37-1.63 (m, 9H), 1.82-1.99 (m, 2H), 2.17-2.30 (m, 1H), 2.32-2.43 (m,

1H), 2.89 (t, $J = 6.7$ Hz, 2H), 3.36-3.48 (m, 2H), 3.67-3.75 (m, 1H), 3.82-3.91 (m, 2H), 4.01-4.11 (m, 2H), 4.80-4.91 (m, 4H), 7.03-7.16 (m, 10H, Ar); ^{13}C -NMR (100 MHz, MeOD), δ 18.9, 21.7, 22.8, 23.5, 24.0, 24.1 (CH₃), 24.5 (CH₂), 26.0, 26.9 (CH), 27.7 (CH₃), 28.4, 31.0, 32.0, 32.6, 40.6, 41.8, 41.8 (CH₂), 52.5, 53.3, 54.4, 54.7, 56.1 (CH), 58.3 (C), 67.6, 67.8 (CH₂), 129.2, 129.4, 129.5, 129.9 (CH, Ar), 138.0, 138.8 (C, Ar), 159.4, 173.7, 174.9, 174.9, 175.1, 175.9, 177.5, 180.6 (C=O). ESI MS m/z (%) calcd. for C₄₅H₆₇N₇O₁₁ (M+H⁺) 882.5 found 882.6 (15), calcd. M+Na⁺ 904.5 found 904.6 (30), calcd. M+K⁺ 920.5 found 920.6 (18).

2.3.17 Synthesis of 6b

1.361 g (1.544 mmol) of linear peptide **6a** was dissolved in 680 mL DMF and stirred at 0 °C. 0.764 g (1.3 eq) HATU, 0.274 g (1.3 eq) HOAT, and 2.7 mL (10 eq) DIPEA dissolved in 5 mL of DMF was added and the solution was stirred for 4 hr. at which point the DMF was removed in vacuo, 45 °C. The residue was taken up in EtOAc and the insoluble white precipitate was removed by filtration. The organic solution was extracted 3x with 30 mL 10% citric acid, 3x with 30 mL saturated NaHCO₃, and dried over Na₂SO₄. The solution was purified by flash column chromatography (EtOAc) to give 600 mg (45% yield) of a white solid. R_f .40 (EtOAc); ^1H -NMR (400 MHz, CDCl₃), δ 0.80-0.99 (m, 12H), 1.19-1.91 (m, 21H), 2.01-2.24 (m, 3H), 2.39-2.48 (m, 2H), 3.10-3.26 (m, 2H), 3.98-4.15 (m, 2H), 4.18-4.28 (m, 1H), 4.28-4.40 (m, 1H), 4.48-4.58 (m, 1H), 5.02-5.12 (m, 4H, Ar), 5.44 (t, $J = 5.9$ Hz, 1H), 6.58 (d, $J = 7.8$ Hz, 1H), 6.64 (d, $J = 8.6$ Hz, 1H), 6.94 (d, $J = 5.06$ Hz, 1H), 7.06 (s, 1H), 7.28-7.36 (m, 10H, Ar), 7.41-7.46 (m,

1H), 7.56 (d, $J = 7.1$ Hz, 1H); ^{13}C -NMR (100 MHz, CDCl_3), δ 17.3, 21.9, 22.1 (CH_3), 22.5 (CH_2), 23.6, 23.6 (CH_3), 23.7 (CH_3), 24.4 (CH_2), 25.4, 25.4 (CH), 28.0 (CH_3), 28.1, 29.2, 30.5, 39.7, 40.3, 40.4 (CH_2), 51.5, 51.7, 52.4, 52.6, 54.1 (CH), 57.0 (C), 66.9, 67.0 (CH_2), 128.2, 128.3, 128.4, 128.7, 128.7 (CH , Ar), 135.9, 136.8 (C , Ar), 156.8, 172.0, 172.9, 173.0, 173.0, 173.3, 174.1, 174.7 ($\text{C}=\text{O}$). ESI MS m/z (%) calcd. for $\text{C}_{45}\text{H}_{65}\text{N}_7\text{O}_{10}\text{Na}$ ($\text{M}+\text{Na}^+$) 886.5 found 886.6 (100).

2.3.18 Synthesis of 6c

571 mg (0.661 mmol) of **6b** was dissolved in 150 mL of 1:1 DCM:MeOH. The benzyl protecting groups on the glutamic acid and lysine side chains were removed by using 0.2 g of Pd activated carbon (10 wt%) and H_2 at atmospheric pressure while stirring the solution for 1.5 hr. The spent catalyst was removed by filtration and the solution was concentrated completely in vacuo, 40 °C, to give 400 mg (94% yield) of a white solid. ^1H and ^{13}C -NMR spectra in MeOD confirmed complete loss of benzyl groups. The peptide was used without further purification or characterization.

2.3.19 Synthesis of 6d

202 mg (0.316 mmol) of **6c** was dissolved in 100 mL DMF and stirred at 0 °C. 0.156 g (1.3 eq) HATU, 0.056 g (1.3 eq) HOAT, and 0.55 mL (10 eq) DIPEA dissolved in 5 mL DMF was added to the peptide solution and stirred for 4 hr. at which point the DMF was removed in vacuo, 45 °C. The residue was taken up in EtOAc and the insoluble white

precipitate was removed by filtration. The organic solution was extracted 3x with 30 mL 10% citric acid, 3x with 30 mL saturated NaHCO₃, dried over Na₂SO₄, and concentrated completely to give 26 mg of a whitish yellow solid.

The cyclization reaction and workup described above were repeated on the remaining 190 mg of **6c** to give an additional 33 mg for a total of 60 mg (16% yield) of whitish yellow solid. ¹H-NMR (400 MHz, MeOD), δ 0.84-1.00 (m, 12H), 1.25-1.89 (m, 24H), 1.99-2.21 (m, 4H), 4.09-4.42 (m, 5H); ¹³C-NMR (100 MHz, MeOD), δ 17.4, 22.0, 22.7, 23.8, 23.9 (CH₃), 24.4 (CH₂), 24.8, 26.4 (CH₃), 26.6, 26.6 (CH), 27.7, 29.0, 31.7, 31.9, 40.2, 41.7, 41.8 (CH₂), 54.3, 54.3, 54.0, 54.0, 52.8 (CH), 58.2 (C), 174.2, 174.5, 174.9, 175.3, 175.4, 175.6, 176.9 (C=O). ESI MS m/z (%) calcd. for C₃₀H₅₂N₇O₇ (M+H⁺) 622.4 found 622.3 (100).

2.4 ISE Membrane and Electrode Preparation

This work was performed by Dr. John Benco. Six membrane cocktails were prepared to test **6d**. The specific formulations are as follows: M1, 69/30/1 wt % of nitrophenyl octyl ether (NPOE)/PVC/**6d**; M2, same as M1 with 10 mol % of potassium tetrakis (4-chlorophenyl)borate (KtpCIPB) to **6d**; M3, same as M1 with 50 mol % of KtpCIPB to **6d**; M4, 69/30/1 wt % of dioctyl phthalate (DOP)/PVC/**6d**; M5, same as M4 with 10 mol % of KtpCIPB to **6d**; M6, same as M4 with 50 mol % of KtpCIPB to **6d**. Membrane cocktails were prepared as 10 wt % solutions in THF. The base electrodes were constructed in a thick-film planar format using a polymeric internal electrolyte layer as

previously reported.⁸ Two wafers composed of 100 individual electrode elements each were used for the sensor construction. The polymer, methacrylamidopropylmethylammonium chloride (MAPTAC), for the internal electrolyte was prepared as a 10 wt % solution in EtOH, spun on to the planar wafers at 750 rpm for 30 s, and allowed to dry for 1 h before membrane deposition. Internal electrolyte thickness was $\sim 3.5 \mu\text{m}$. The wafers were then quartered, giving wafers of 25 sensors each. Membrane cocktails were deposited (0.9 mL) onto the wafers and allowed to cure for 24 h before use, giving a membrane thickness of $\sim 105 \mu\text{m}$. The planar wafers were singulated by hand, giving 25 sensors for each formulation.

2.5 ISE Testing

This work was carried out by Dr. John Benco. The sensors were housed in the proprietary flow-through cell used with the Bayer Diagnostics Rapidpoint 400 critical care system as previously reported.⁸ This system uses a saturated Ag/AgCl reference cell. Two flow cells were constructed, which contained 1-2 sensors of each formulation for a total of 14 tested sensors. Each cell was tested individually on the Rapidpoint system that maintains a 37°C temperature for the cell. The sensors were tested using solutions containing NH_4Cl (0.5-100 mM), 100 mM Tris buffer (pH 7.2), and 0.05 g/L Brij 700. Selectivity testing was based on the separate solution method (SSM)¹⁸, where $i = j = 0.1 \text{ M}$.

2.6 ^{13}C -NMR Study of Valinomycin binding Potassium Cations

This study was based on a modified procedure.¹⁹ A solution was made by dissolving 20 mg of commercially available valinomycin in 0.50 mL of 1:1 (v:v) MeOD:CDCl₃. A ^{13}C -NMR spectrum was recorded after each 10 μL addition of stock solutions of potassium thiocyanate in 1:1 (v:v) MeOH:CHCl₃. **Table 1** shows the KSCN concentrations for each experiment. ^{13}C -NMR spectra were recorded by locking on MeOD with 512—9000 scans and the spectra were calibrated with respect to MeOD.

Table 1: ^{13}C -NMR experiments of valinomycin with increasing amounts of KSCN

Spectrum	KSCN (mmol)	Total Volume (mL)	[KSCN] (mM)
1	0.0	0.50	0.0
2	0.2	0.51	0.4
3	0.4	0.52	0.8
4	0.6	0.53	1.1
5	0.8	0.54	1.5
6	1.2	0.55	2.2
7	1.6	0.56	2.9
8	2.0	0.57	3.5
9	2.4	0.58	4.1
10	2.8	0.59	4.7
11	3.2	0.60	5.3
12	3.6	0.61	5.9
13	4.5	0.62	7.3
14	5.4	0.63	8.6
15	6.3	0.64	9.8
16	7.2	0.65	11.1
17	8.1	0.66	12.3
18	9.0	0.67	13.4
19	9.9	0.68	14.6
20	10.8	0.69	15.7
21	11.7	0.70	16.7
22	12.6	0.71	17.7
23	13.5	0.72	18.8
24	14.4	0.73	19.7
25	15.3	0.74	20.7
26	16.2	0.75	21.6
27	17.1	0.76	22.5

3 Results and Discussion

3.1 Selection of Synthetic Methods

The decision to utilize a solid phase Fmoc-protection strategy on a Wang resin was based on the demonstrated success of that strategy in our working group as well as by others.^{17,20-23} These methods are well understood and give good yields. The mechanisms of Fmoc deprotection and PyBOP/HOBT-mediated amino acid coupling are shown below in **Figures 11** and **12**. The benzyl protecting groups on the glutamic acid and lysine side chains were chosen because the protected residues are available commercially and because they are known to be stable to Fmoc deprotection conditions (basic) and resin cleavage conditions (acidic). These groups are easily removed by hydrogenation.

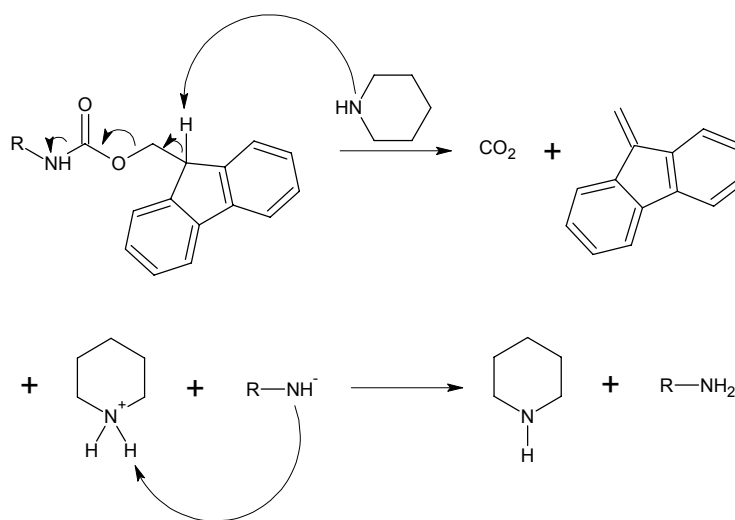


Figure 11: Mechanism of Fmoc deprotection

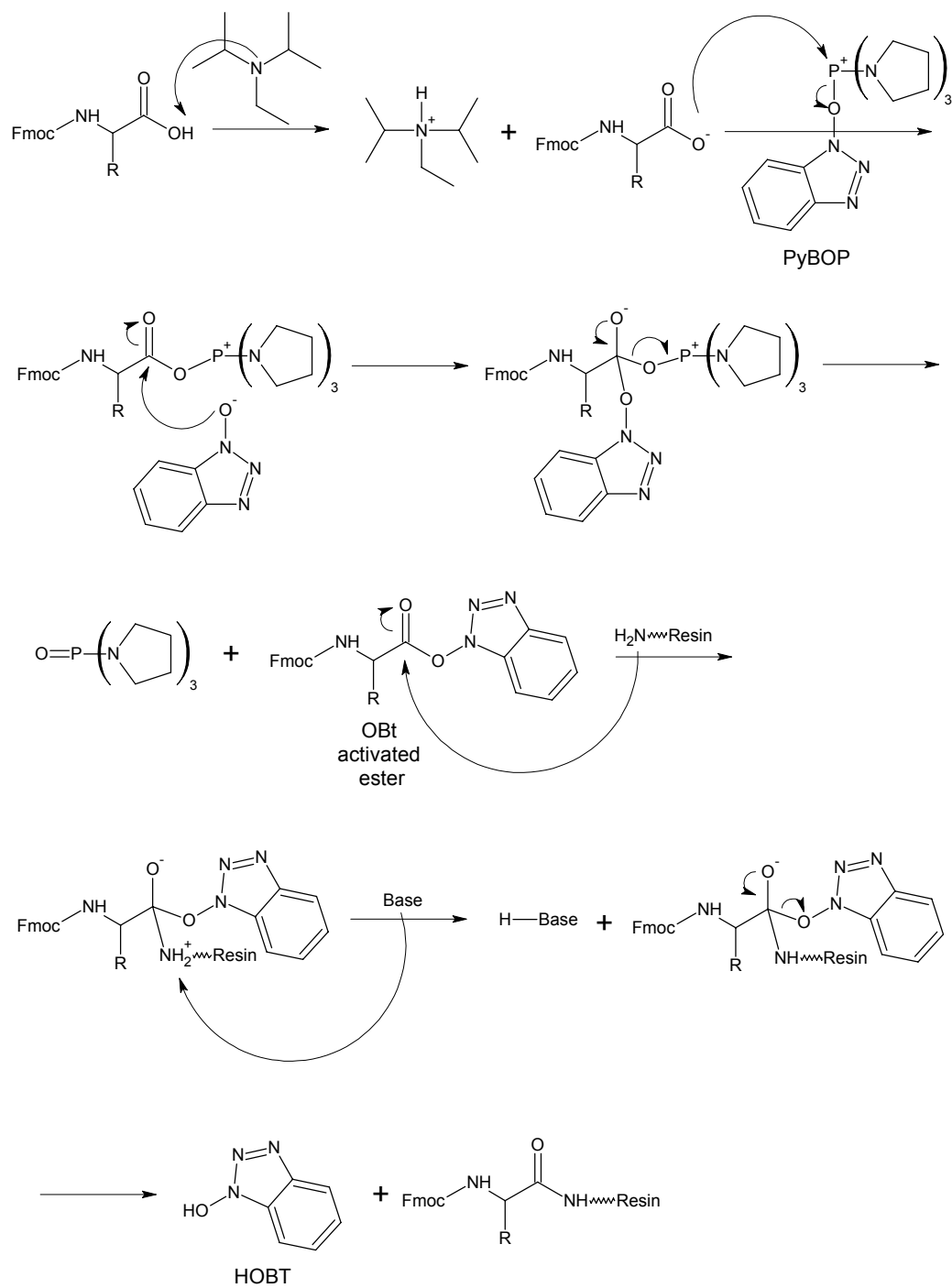


Figure 12: Mechanism of PyBOP/HOBT-mediated coupling reaction

The use of the activating agents HATU and HOAT in cyclization of the linear peptide was based on the experience of both Ghadiri's working group²⁴ as well as that of our own. The reaction is carried out in DMF under dilute (2 mg/ mL) conditions in order to favor intramolecular cyclization over intermolecular coupling. The mechanism of HATU/HOAT-mediated coupling is very similar to that shown for PyBOP in **Figure 12**. Thionyl chloride was employed for the second cyclization step, based on the success our group has had with the reagent in the cyclization of a depsipeptide ammonium ionophore.⁸

3.2 Design and Synthesis

3.2.1.1 Design of **1d**

The design of bicyclic peptide target compound **1d** has elements that are similar to the cyclic depsipeptide ammonium ionophore⁸ reported recently by our group (shown in **Figure 7b**). Target **1d** is the bicyclic and all-amide equivalent of this depsipeptide, both of which are shown in **Figure 13**. The stereochemical pattern, L—D—D—L—L—D, of both is based on the potassium ionophore valinomycin (L—D—D—L)₃ and was expected, based on modeling, to prevent formation of helices that would hinder cyclization.

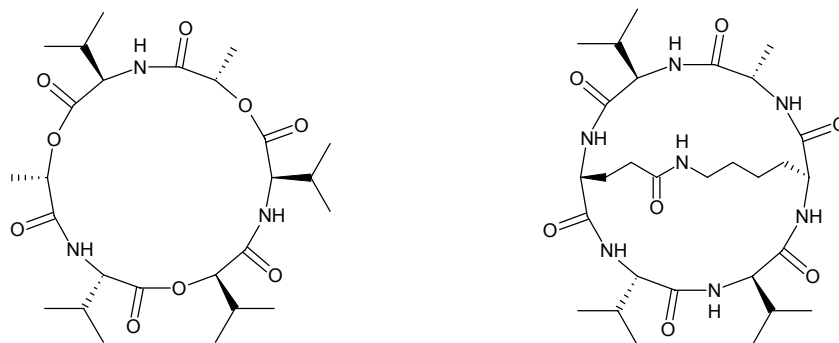


Figure 13: Depsipeptide ammonium ionophore (left) and target compound **1d** (right)

Molecular modeling of **1d** indicated that it may offer enhanced ammonium over potassium selectivity compared to nonactin, the industry standard ammonium ionophore. Whereas nonactin has a flexible crown-ether backbone that allows wrapping-type complexes with both ammonium and potassium ions, bicyclic peptide **1d** has a more rigid structure that provides the tetrahedral coordination required for complexation of ammonium ions, but cannot effectively exhibit the octahedral coordination required for complexation of potassium ions. **Figure 14** shows minimized structures of **1d** with both ammonium and potassium ions. Ammonium ion sits deeply within the cavity and forms at least four hydrogen bonds to **1d**. On the other hand, potassium does not sit as deeply within the pocket, indicating less favorable complexation.

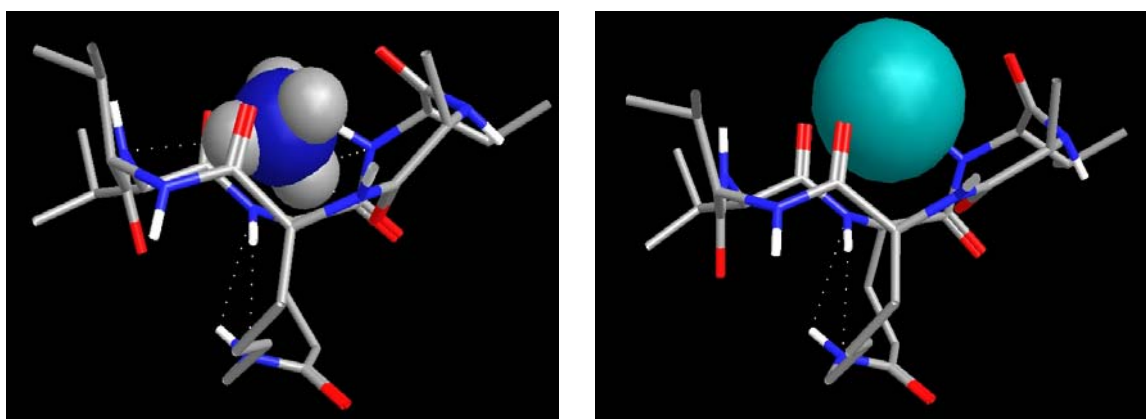


Figure 14: Complexation of **1d** with ammonium (left) and potassium (right) cations

To estimate the selectivity of **1d** for binding ammonium over potassium ions compared to nonactin, docking energies were obtained for the ion/ionophore complex in each case, as previously reported.⁸ The difference in docking energies between ammonium and potassium ion for **1d** was 12 kcal/mol more negative than that calculated for nonactin. While these calculations give relative values only, they indicate qualitatively that **1d** may show increased ammonium over potassium selectivity compared to nonactin.

3.2.1.2 Attempted Synthesis of **1d**

The linear peptide **1a** was synthesized and characterized in good (67%) yield. However, **1a** exhibited poor solubility and was very difficult to dissolve in a variety of solvents, including DMSO and DMF. After the first cyclization reaction to give **1b**, the solvent extraction process created an emulsion between the DCM and aqueous layers, probably due to the limited solubility of the peptide in either phase. Based on the low yield of **1b**

(14 %), the decision was made to start a new synthesis of **1a** in order to scale up the amount of the intermediate **1b**. In an attempt to increase the yield during the cyclization of the second batch of **1a**, the reaction was carried out in 500 mL of DMF at 0 °C for 4 hr in order to favor intramolecular cyclization over intermolecular coupling by decreasing the rate of collisions by lowering the temperature. The product of the second synthesis was purified by multiple precipitations from MeOH/ether only, since **1b** did not exhibit sufficient solubility to purify by column chromatography and we believed much of the desired product of the first synthetic attempt was lost during the solvent extraction in the emulsion that formed. Intermediate **1b** was never unambiguously characterized due to the large amount of impurities present, ultimately caused by the poor solubility that prevented the use of effective purification techniques. The ¹H and ¹³C-NMR spectra showed the expected signals for peptide **1b**, but clearly contained considerable impurities. The MS showed no **1b**, but this can potentially be explained by the poor solubility of **1b** (Synpep Corp., the contractor who provided the MS analysis, used only acetonitrile as a matrix). The final cyclization with thionyl chloride appeared completely unsuccessful, resulting in a brown solid that contained no **1d** by MS. In fact, activation of the carboxyl group by acid chloride formation is rarely done by peptide practitioners due to its reputation of being “overactivated” and therefore prone to numerous side reactions.²⁵

3.2.2.1 Design of 2d

The attempted synthesis of target compound **1d** highlighted the importance of solubility in the synthesis of peptides. Target compound **2d** was designed in an attempt to increase solubility of intermediate and final compounds by decreasing aggregation through the replacement of bulky valine residues by smaller alanine residues. Additionally, it was realized that the incorporation of D-lysine and L-glutamic acid in target compound **1d** would result in two different atropoisomers depending on which side of the cyclic peptide the second ring is formed. As shown in **Figure 15**, one isomer has the bridgehead hydrogen on glutamic acid pointing outside the cavity and the bridgehead hydrogen on lysine pointing in towards the cavity and the other has the bridgehead hydrogen on glutamic acid pointing in towards the cavity and the bridgehead hydrogen on lysine pointing outside the cavity. In an attempt to favor the formation of just one atropoisomer, the stereochemistry of the bridgehead residues were both designed as L. As shown in **Figure 15**, the two possible atropoisomers of **2d** can have both of the bridgehead hydrogens pointing in toward the central cavity or both pointing out away from the central cavity. Based on the work of Paolillo et al.¹⁶, the isomer with both hydrogens pointing out away from the central cavity should be favored by steric interactions during formation of the second ring. The stereochemistry assignment, L—L—D—D—L—D, was designed to give the two most expensive amino acids, the benzyl protected lysine and glutamic acid residues, the naturally occurring L configuration in order to minimize overall cost of the synthesis while still retaining the stereochemical pattern seen in valinomycin and the previous bicyclic target compound **1d**. Molecular modeling calculations to estimate the selectivity of target compound **2d** with ammonium and

potassium ions gave a difference in docking energies similar to that calculated for target compound **1d**, indicating that the change in amino acid residues and stereochemistry should not significantly affect complexation behavior.

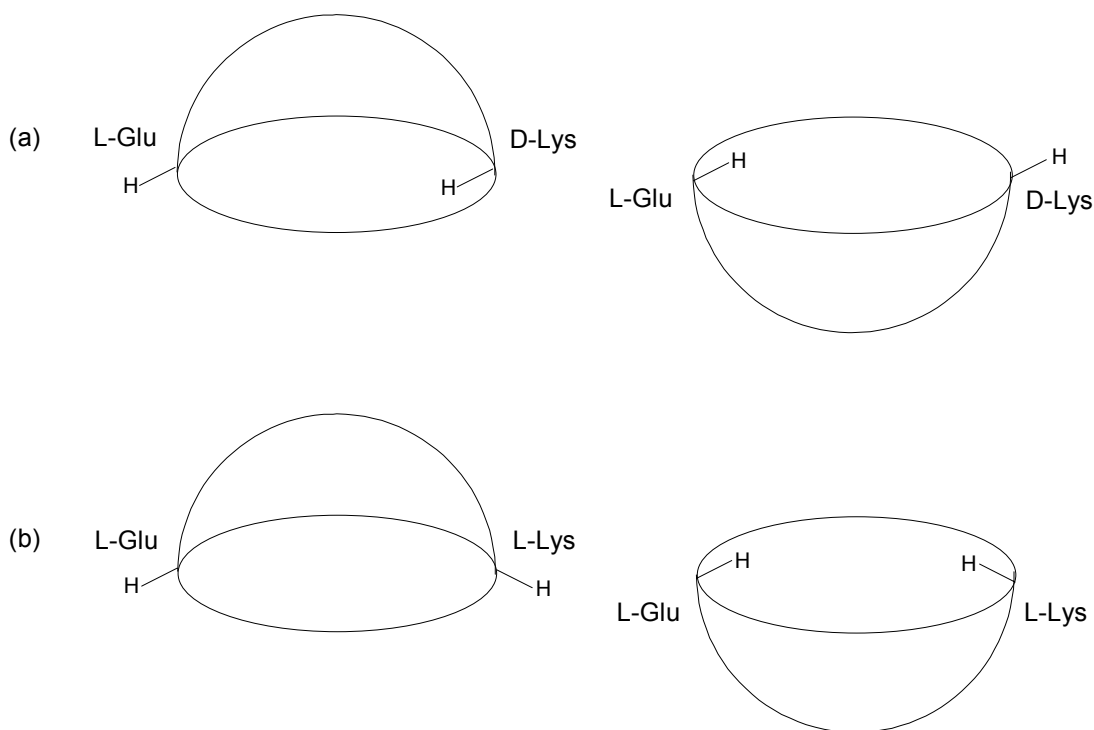


Figure 15: The two possible atropoisomers of (a) target compound **1d** (b) target compound **2d**

3.2.2.2 Synthesis of **2d**

In order to evaluate the most effective cyclization conditions, the preliminary synthesis product **2a** was divided. One portion was subjected to cyclization using HATU/HOAT activation and the other portion was activated with thionyl chloride. The product of the HATU/HOAT cyclization **2b** was characterized by MS and ^1H and ^{13}C -NMR, but no **2b** was visible in the MS of the product of the thionyl chloride reaction. Acid chlorides of benzyloxycarbonyl-protected peptides such as **2a** are known to undergo the serious side

reaction of spontaneous decomposition to the corresponding Leuchs anhydride with loss of benzyl chloride.²⁵ Both the linear peptide **2a** and the monocyclized intermediate **2b** showed limited solubility. However, solubility was sufficiently high in acetonitrile/water solvent systems to successfully purify **2b** through reverse phase column chromatography. The success of the HATU/HOAT method in the first cyclization led to the decision to employ this method for the final cyclization. Compound **2d** was characterized by MS in the crude product mixture and was subsequently purified by a series of precipitations from MeOH/ether in which a marked decrease in solubility was observed. The final precipitated **2d** was essentially insoluble and therefore it was impossible to characterize by MS or NMR or to test its utility as an ammonium ionophore in an ISE sensor format.

3.2.3.1 Design of **3d**

Target compound **3d** was designed to exhibit increased solubility by preventing the intermolecular hydrogen bonding that is generally believed to be responsible for the poor solubility of peptides²⁶ such as **2a-2d**. We predicted, based on investigations by Narita²⁶, that the replacement of two of the alanine residues in **2d** with N-methyl alanine residues in **3d** would increase solubility by disrupting hydrogen bonding between molecules. The amino acid sequence was designed to prevent cyclization at a hindered N-methylated amine. The stereochemistry was unchanged from bicyclic peptide **2d** to bicyclic peptide target **3d**.

3.2.3.2 Attempted Synthesis of **3d**

Solid phase synthesis of **3a** was complicated by the incorporation of the two N-methylated residues because the Kaiser test used to monitor deprotection and coupling reactions is inconclusive for secondary amines. The Novabiochem catalog contains a method for detecting the free secondary amine of proline residues called a chloranil test.¹⁷ However, this technique was inconclusive, usually giving orange or brown resin beads, when a blue color is indicative of a positive test, in both the presence and absence of secondary amine. For this reason, the extent of coupling was instead estimated by cleaving the Fmoc protecting group from a known mass of resin (20 mg) in a 100 mL solution of 20% piperidine in DMF and monitoring the UV absorption at 290 nm. Since the extinction coefficient of the Fmoc group is known at this wavelength to be 4950 M⁻¹cm⁻¹, the UV absorption of the free Fmoc moiety can be used to calculate the concentration of the Fmoc group in solution, which can be related to the amount of peptide on the known mass of resin. However, this technique has limited sensitivity. The MS of the crude mixture after the resin cleavage reaction showed that the linear peptide **3a** was not present, but various deletion peptides were present. This was strong evidence that N-terminal coupling reactions of the N-methylated residues were not effective.

3.2.4.1 Design of **4d**

Like target compound **3d**, **4d** was designed to have increased solubility by preventing intermolecular hydrogen bonding. However, due to the limited success of coupling reactions involving N-methylated residues in the synthesis of **3d**, the decision was made

to incorporate two aminoisobutyric acid residues, which are also known to increase solubility by disrupting β -sheet formation²⁶, instead of the N-methylated alanine residues. Additionally, we replaced one alanine residue with a leucine residue in an attempt to increase the solubility of the peptides by increasing their lipophilicity.

The synthetic strategy for target **4d** was developed after a literature search of on-resin cyclization methods.²⁷⁻³⁷ On-resin cyclization methods are desirable because, in theory, intermolecular reactions to form polymers are impossible and therefore yields of the intramolecular reaction should be increased dramatically compared to solution-phase cyclization reactions. In addition, this strategy would eliminate one step from the synthesis. The method involves anchoring the side chain of glutamic acid to the resin and building the linear peptide using standard solid phase techniques using an allyl protecting group on the carboxy terminus during chain elongation. This is followed by solution-phase deprotection of the allyl protecting group prior to on-resin head-to-tail peptide cyclization.³⁷ The allyl-protecting group strategy was chosen over other on-resin cyclization methods because it required the smallest overall change in strategy. This synthetic scheme still allowed the use of Fmoc protecting groups on the Wang resin and benzyl protection for the lysine residue.

3.2.4.2 Attempted synthesis of 4d

The allyl-protecting group on-resin cyclization method gave only 5% yield of crude peptide **4b** based on an estimated resin loading of 59%. This is too low for a practical

synthesis of **4d**. In addition, MS showed that ~97% of the crude peptide **4b** had been deprotected (benzyloxycarbonyl protecting group) at the lysine residue leading to the conclusion that the benzyl group was removed during the allyl deprotection reaction. Since deprotection occurred prior to the cyclization reaction, the deprotected and monocyclused peptide formed was most likely a mixture of head-to-tail cyclized and head-to-side chain cyclized products since both the N-terminus and the lysine side chain amine were available for participation in the cyclization reaction.

3.2.5.1 Design of 5d

Based on the low yield (5% to resin loading) obtained by this on-resin cyclization method, the decision was made to return to our previous synthetic strategy of solid phase synthesis to produce the linear peptide followed by two solution-phase cyclization reactions. Target compound **5d** is the analogue of **4d** produced by this synthetic strategy. The amino acid sequence was reversed in order to make the solid phase synthesis easier by starting with an alanine residue, which is commercially available preloaded on the resin.

3.2.5.2 Attempted synthesis of 5d

The first attempt to make **5a** via solid phase synthesis resulted in a low yield of an oil. This oil was found to contain primarily **5a** that had been deprotected (the benzyloxycarbonyl protecting group had been lost from the lysine side chain according to

the MS). We suspected that the benzyloxycarbonyl protecting group was lost during the 6 hr. cleavage reaction. The work of Erickson et al. confirmed that benzyloxycarbonyl protecting groups are approximately 40 to 60 times less stable than benzyl ester protecting groups, and that they are removed under the acidic conditions (95% TFA) of the cleavage reaction.³⁸ They observed 0.5% deprotection of Lys(Z) after 20 min. exposure to 50% TFA in CH₂Cl₂. In the second solid phase synthesis of **5a**, the cleavage reaction time was shortened to 1.5 hr. and repeated twice in order to test which reaction time produced optimum yields of the linear peptide. MS of the two cleavage fractions showed a good yield of **5a** in the first fraction, but essentially none in the second cleavage fraction. This supported the conclusion that longer cleavage times lowered the yield of linear peptide **5a** through loss of the benzyloxycarbonyl protecting group.

Both the linear peptide **5a** and the monocyclized intermediate **5b** exhibited dramatically increased solubility in organic solvents compared to intermediates **1a**, **2a**, **1b**, and **2b**. The linear peptide **5a** was completely soluble in pure DCM, despite the free acid and free amine functions that may be expected to prevent solubility in such a nonpolar solvent. The great solubility of the intermediates **5a** and **5b** made purification by column chromatography highly successful.

The final cyclization reaction and subsequent work-up were performed exactly the same as the first cyclization reaction, but gave only 5 mg of a white solid after the solvent extraction. Characterization by MS was inconclusive, since only very low intensity signals of the correct mass were observed.

3.2.6.1 Design of **6d**

After study structures generated by molecular modeling and physical models of target peptide **5d**, we concluded that the bulky aminoisobutyric acid residues were causing the ring to be too rigid to allow for the second cyclization to occur. Specifically, we hypothesized that the methyl groups on the aminoisobutyric acid residue between the alanine and lysine residues were initiating an unfavorable steric interaction with the alanine carbonyl group as the lysine and glutamic acid side chains began to come together to form the second ring.

Target bicyclic peptide **6d** was designed on the basis of this hypothesis. The interfering aminoisobutyric acid residue was replaced by a lipophilic leucine residue for the purpose of decreasing steric hindrance while attempting to retain the good solubility observed in the intermediates of **5d**. Both computer and physical models led us to believe that a D configuration for the alanine and leucine residues would be most favorable for promoting the second cyclization reaction through steric interactions forcing the L-glutamic acid and L-lysine side chains onto the same side of the ring.

3.2.6.2 Synthesis of **6d**

Intermediates **6a** and **6b** were synthesized and purified using the same methods that proved successful for the second synthesis of **5a** and **5b**. Both intermediates also exhibited the good solubility seen in **5a** and **5b**. In this case, the second cyclization reaction was successful in producing bicyclic peptide **6d** in 16% yield, lending support to

our hypothesis of harmful steric interactions caused by the aminoisobutyric acid residue preventing cyclization of **5c**.

Multiple precipitations were performed on **6d** from THF/ether, DCM/hexane, and MeOH/ether/hexane solvent systems in attempts to purify the bicyclic peptide (purification by chromatography was not possible because **6d** was not visible on TLC plates by UV absorption, iodine, or p-anisaldehyde visualization methods). Unfortunately, none of these precipitations purified the bicyclic peptide based on ^1H and ^{13}C -NMR (**6d** seemed partially soluble in all of the tried solvent systems).

3.3 Sensor Fabrication and Testing

Bicyclic peptide **6d** was incorporated into a planar ISE structure employing a polymeric solid contact material and tested in a commercially available point-of-care clinical diagnostic system, as previously reported.⁸ Six membrane formulations were tested in order to determine which environment would yield the best potentiometric response. Each sensor membrane consisted of plasticized PVC. Formulations differed as to the type of plasticizer used (NPOE or DOP) and the amount of the lipophilic salt KtpCIPB present (0, 10, or 50 mol% to **6d**).

Figures 16 and **17** show the potentiometric responses of the six membrane formulations to increasing concentrations of aqueous NH_4Cl . The membrane containing the plasticizer NPOE with 50 mol% KtpCIPB to **6d** exhibited the largest potential increases with

increasing ammonium concentration (highest slope (60.7 mV/dec), closest to the ideal Nernstian response (see **Table 2**)). The membranes containing the plasticizer NPOE in the absence of KtpCIPB and all formulations containing the plasticizer DOP exhibited sub Nernstian behavior.

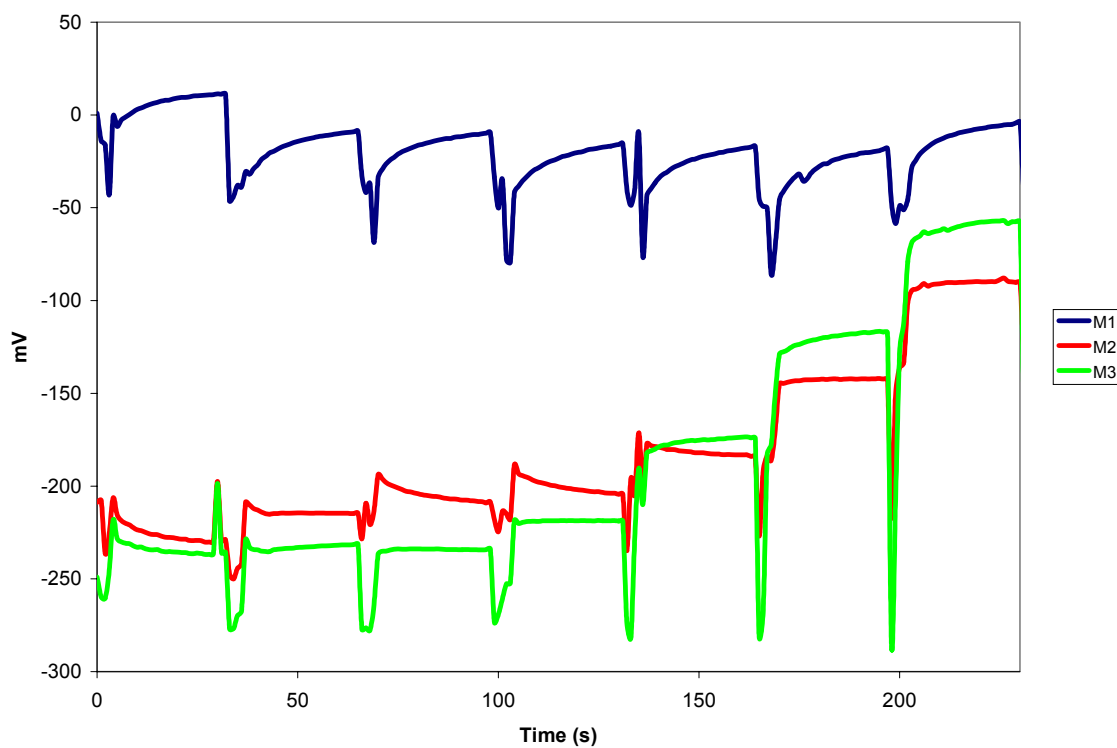


Figure 16: Potentiometric responses of planar ISEs to NH_4^+ ($10^{-4} - 10^{-1}$ M) for membranes 1-3 based on **6d**

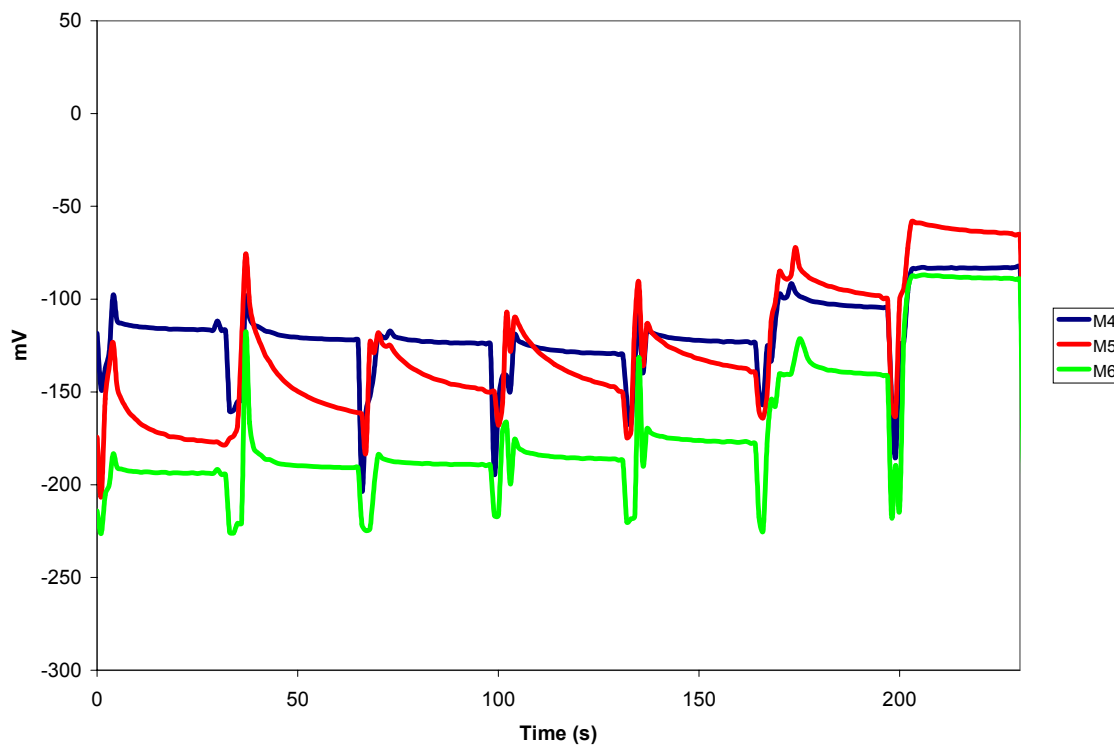


Figure 17: Potentiometric responses of planar ISEs to NH_4^+ (10^{-4} – 10^{-1} M) for membranes 4-6 based on **6d**

In the case of membrane formulations utilizing NPOE (M1-M3), it can be seen that as the mole ratio of lipophilic salt to **6d** increases there is a corresponding increase in the slope of the sensors as a function of ammonium concentration. In particular, it is observed that in the absence of lipophilic salt (i.e. formulation M1) the sensors essentially exhibit no response to ammonium ions. This general trend is also observed in the case of the membrane formulations utilizing DOP (M4-M6). These results suggest that the response of the sensors is not determined by the ionophore (and is therefore independent of the ionophore), but rather is a function of the lipophilic salt concentration.

Table 2 shows the results of selectivity studies that were carried out on the six membrane formulations using the separate solution method. M3, the formulation showing the best response for ammonium cation, was in fact the most selective for potassium, followed by ammonium, sodium, calcium, magnesium, and lithium cations ($K^+ > NH_4^+ > Na^+ > Ca^{2+} > Mg^{2+} > Li^+$). The other membrane formulations (with the exception of M1, which was least selective for ammonium) showed a similar selectivity pattern. This sequence of cation selectivity shows a good correlation to the Hofmeister series ($K^+ > NH_4^+ > Na^+ > Li^+ \sim Ca^{2+} > Mg^{2+}$), which has been observed for ISE membranes incorporating the plasticizers NPOE and DOP without any ionophore component.¹⁸ The sequence of cation selectivities (in the absence of ionophore) is determined by the difference between the standard free energies of solvation for the ions in the aqueous and organic phases respectively. Taken alone, the results of the selectivity studies indicate that **6d** is more selective for potassium ions than for ammonium ions. However, the potentiometric results (as shown in **Figures 16** and **17**) in combination with the selectivity data provide evidence that the potentiometric response of the sensors is independent of the ionophore and is instead dependent only on the lipophilic salt likely acting as a non-specific ion exchanger. In light of these results, we suggest that the ionophore is not soluble in the membrane phase and is therefore incapable of forming complexes with ions. This suggestion is supported by the low solubility of **6d** observed in nonpolar solvents such as THF and $CHCl_3$. These solvents have dielectric constants ($\epsilon = 7.6$ and 4.8 respectively) on the same order of NPOE and DOP plasticized PVC membranes ($\epsilon_{mem} = 14$ and 4.8 respectively)¹⁸ and thus model the polymeric matrix of the membrane phase. In addition,

¹H-NMR spectra of **6d** in CDCl₃ and THF-*d*₈ show broad structureless resonances for all peaks, indicative of poor solubility.

Table 2: Selectivity of **6d** for Ammonium over Other Cations

Membrane ^a	Selectivity coefficients, log $K_{NH_4^+,j}^{POT}$					Slope ^b
	Li ⁺	Na ⁺	K ⁺	Ca ²⁺	Mg ²⁺	
M1	0.5	0.7	1.2	0.6	0.4	6.8
M2	-1.8	-1.2	-0.3	-1.6	-1.7	48.6
M3	-2.3	-1.0	0.1	-1.5	-1.8	60.7
M4	-1.0	-0.7	0.0	-0.9	-1.1	20.7
M5	-0.7	-0.3	0.3	-0.8	-1.0	37.5
M6	-1.4	-0.8	0.0	-2.6	-2.6	45.8
Nonactin ^d	-3.5 ⁴	-2.4 ⁴	-1.0 ⁴	-3.8 ⁷	-4.0 ⁷	59.3 ^c

^a M1, 69/30/1 wt % of NPOE/PVC/**6d**; M2, same as M1 with 10 mol % of KtpClPB to **6d**; M3, same as M1 with 50 mol % of KtpClPB to **6d**; M4, 69/30/1 wt % of DOP/PVC/**6d**; M5, same as M4 with 10 mol % of KtpClPB to **6d**; M6, same as M4 with 50 mol % of KtpClPB to **6d**. ^bDetermined between 10⁻³ and 10⁻¹ M cation at 37°C. ^cAt 25°C. ^dData for nonactin taken from references indicated.

3.4 ¹³C-NMR Study of Valinomycin binding Potassium Cations

Due to the apparent lack of solubility of **6d** in the ISE membranes, the decision was made to employ solution NMR methods in an attempt to evaluate the selectivity of **6d** for ammonium over other interfering cations. Selectivities of ionophores in solution are calculated from the ratios of the equilibrium dissociation constants for the metal-ligand complexes of the various cations. The dissociation constant (K_d) of a ligand with a given metal cation may be calculated by fitting a sigmoidal plot of experimental data to **Equation 2** to give K_d:

$$y = \frac{B_{\max}x}{K_d + x} \quad (2)$$

Here, x is the concentration of free ligand, y is the complex fraction, and B_{\max} is the maximum number of binding sites. Based on molecular modeling, it appears that the carbonyl groups of **6d** are primarily responsible for forming the hydrogen bonds to ammonium cations (or ion-dipole interactions with interfering cations), although some amide nitrogen atoms also seem to contribute. The carbonyl groups should give the best measure of complexation because they should undergo the greatest change in electronic environment upon cation binding. Carbonyl participation in hydrogen bonding (or ion-dipole interactions) causes an increase in electron density toward the oxygen atom with a concurrent decrease in electron density away from the carbon atom. For this reason, the deshielded carbon atoms of the carbonyls of **6d** should show a downfield shift in the ^{13}C -NMR spectra upon complexation. Comparison of the integration of the free versus complexed carbonyl signals in the ^{13}C -NMR spectra of **6d** should allow determination of the extent of complexation occurring in a given solution.

In order to establish test conditions and validate the method, a control study of valinomycin was performed. Valinomycin (shown in **Figure 7a**) is the standard potassium ionophore used commercially in biosensors. A cyclic depsipeptide consisting of alternating amide and ester linkages (12 total), valinomycin preorganizes through hydrogen bonding of its amide carbonyl groups to form a pocket with its six ester carbonyl oxygens available for electrostatic stabilization of potassium ions through octahedral-type complexation. Due to the symmetry of the molecule, free (uncomplexed)

valinomycin only shows four carbonyl signals, two ester and two amide, in its ^{13}C -NMR spectrum. The ion-dipole interaction which takes place upon binding of potassium by valinomycin induces a shift of electron density on the carbonyl bonds towards the oxygen atoms resulting in an observed downfield shift of these signals.¹⁹

The decision was made to employ a 1:1 CDCl_3 :MeOD solvent system in the NMR study since cation complexation is most favorable in nonpolar solvents, but the polar solvent MeOD is necessary for solubility of **6d**. 20 mg of valinomycin was dissolved in 0.50 mL of 1:1 CDCl_3 :MeOD (3.6 mM solution) and the initial spectrum was attained. Spectra were performed on the same solution after every 10 μL addition of stock solutions of KSCN in 1:1 CHCl_3 :MeOH (with an increasing number of scans as the solvent peaks grew in intensity). The downfield (complexed) carbonyl signals began to appear at a 1:1.6 mole ratio of valinomycin to KSCN and gradually increased in comparison to the free valinomycin signals (see **Figure 18**) until the free signals were indistinguishable from the noise (complexation $\sim 100\%$) at a 1:5.75 mole ratio of valinomycin to KSCN.

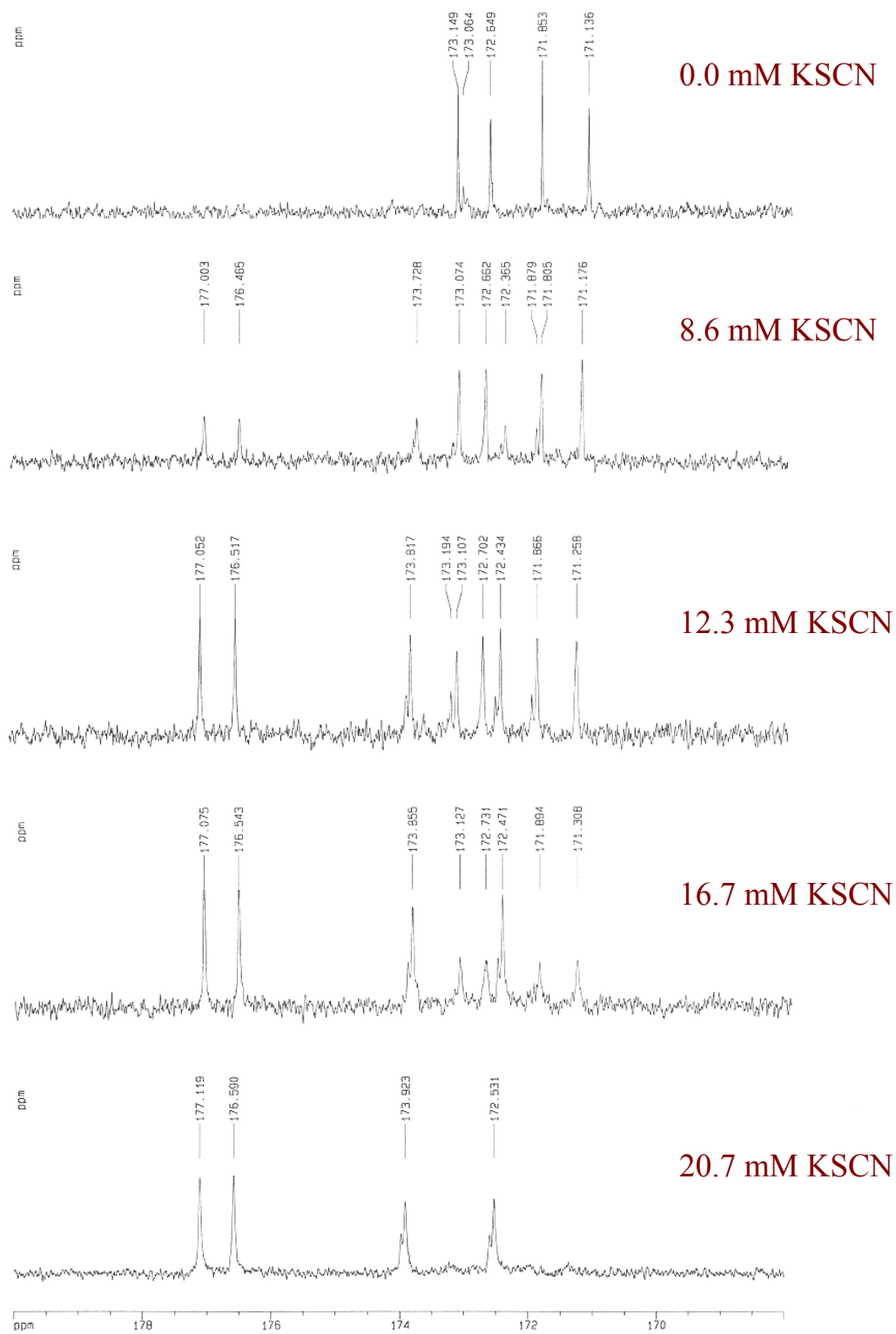


Figure 18: ^{13}C -NMR carbonyl signals of valinomycin as a function of [KSCN]

The extent of complexation of each solution was estimated from comparison of the integration (by peak height) of the farthest upfield (~171 ppm) and farthest downfield (~177 ppm) signals, which were selected because no splitting of these peaks was observed. The slight signal splitting observed is probably due to the loss of symmetry (and therefore signal equivalence) caused by the change in conformation upon binding the potassium cation. The plot of complexation versus KSCN concentration is shown in **Figure 19**. This data was imported into SigmaPlot 8.02 and the program settings for simple ligand binding for one site saturation were used to fit the curve to Equation 2, resulting in $K_d = 10^{-2}$ M. This is two orders of magnitude higher than the known value for the binding of potassium by valinomycin in MeOH ($K_d = 10^{-4}$ M).¹⁸ However, the difference could be due to water contamination of the sample ($K_d = 0.4$ M in H₂O)¹⁸, which could increase the dissociation constant significantly.

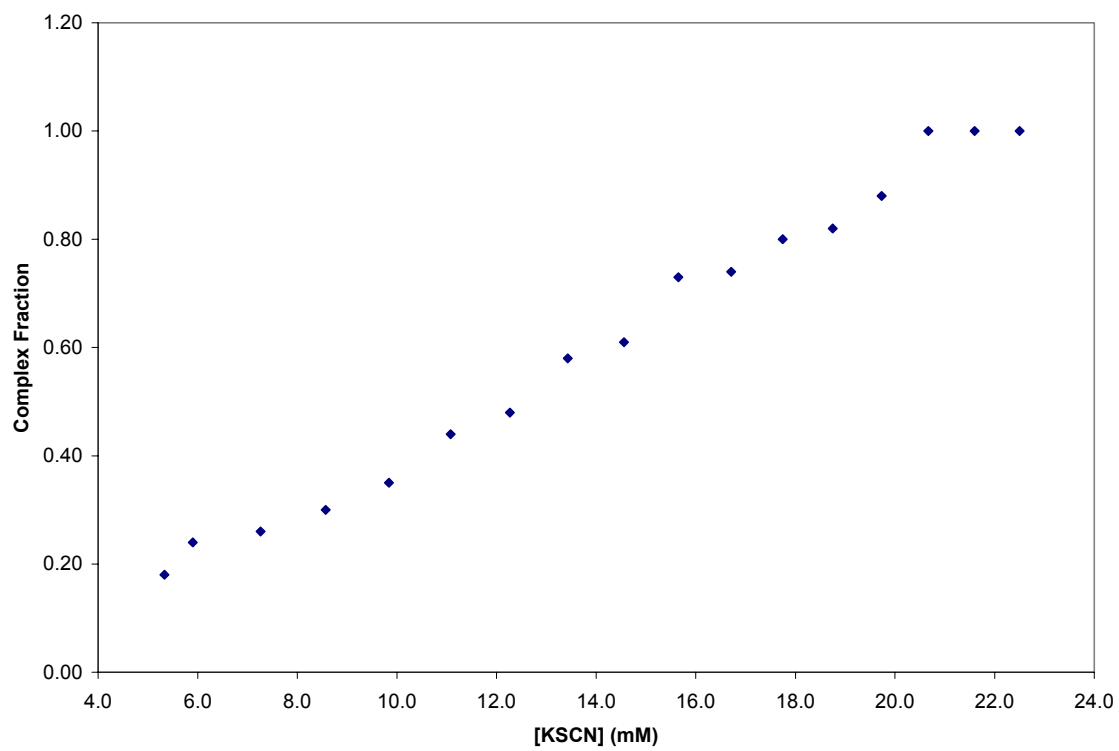


Figure 19: Valinomycin-potassium complex as a function of potassium concentration

4 Conclusions

A series of bicyclic peptides have been designed for complexation of ammonium cations through hydrogen bonding. Molecular modeling suggested these compounds could exhibit better ammonium over potassium cation selectivity than nonactin, the industry standard ammonium ionophore, in an ISE sensor format by exhibiting the tetrahedral coordination geometry required for ammonium binding, but not the octahedral coordination geometry required for potassium binding.

Bicyclic peptide **2d** was synthesized, but lacked the solubility necessary for characterization or evaluation in an ISE sensor. We were successful in enhancing solubility of the peptide intermediates of **5d** in organic solvents through the incorporation of two aminoisobutyric acid residues. However, the second cyclization reaction was unsuccessful, presumably due to an unfavorable steric interaction between one of the aminoisobutyric acid residues and the carbonyl group of the neighboring alanine residue. Replacement of this aminoisobutyric acid residue in **5d** with a leucine residue led to the successful synthesis and characterization of bicyclic peptide **6d**. **6d** was incorporated into an ISE sensor and tested as an ammonium ionophore, but lacked solubility in the ISE membrane.

Future work will involve a solution ^{13}C -NMR study of ammonium, potassium, and sodium ion binding with **6d**. Preliminary results of a control ^{13}C -NMR potassium-binding study of valinomycin suggest this method should be successful in evaluating selectivity of **6d** for ammonium over interfering cations.

References

- ¹ Shih, Y.; Huang, H.J. *Anal. Chim. Acta.* **1999**, *392*, 143.
- ² Chin, J.; Walsdorff, C.; Stranix, B.; Oh, J.; Chung, H.J.; Park, S.M.; Kim, K. *Angew. Chem. Int. Ed.* **1999**, *38*, 2756.
- ³ Benco, J.S.; Nienaber, H.A.; McGimpsey, W.G. *The Spectrum*, **2001**, *14*, 3.
- ⁴ Bühlmann, P.; Pretsch, E.; Bakker, E. *Chem. Rev.* **1998**, *98*, 1593.
- ⁵ Graf, E.; Kintzinger, J.P.; Lehn, J.M.; LeMoigne, J. *J. Am. Chem. Soc.* **1982**, *104*, 1672.
- ⁶ Jon, S.Y.; Kim, J.; Kim, M.; Park, S.H.; Jeon, W.S.; Heo, J.; Kim, K. *Angew. Chem. Int. Ed.* **2001**, *40*, 2116.
- ⁷ Suzuki, K.; Siswanta, D.; Otsuka, T.; Amano, T.; Ikeda, T.; Hisamoto, H.; Yoshihara, R.; Ohba, S. *Anal. Chem.* **2000**, *72*, 2200.
- ⁸ Benco, J.S.; Nienaber, H.A.; McGimpsey, W.G. *Anal. Chem.* **2003**, *75*, 152.
- ⁹ Kim, H.S.; Park, H.J.; Oh, H.J.; Koh, Y.K.; Choi, J.H.; Lee, D.H.; Cha, G.S.; Nam, H. *Anal. Chem.* **2000**, *72*, 4683.
- ¹⁰ *Clinical Diagnosis by Laboratory Methods*; Davidsohn, I., Henry, J.B.; W.B. Saunders Co.: Philadelphia, 1978.
- ¹¹ Pullman, A. *Chem. Rev.* **1991**, *91*, 793.
- ¹² Cusack, R.M.; Grondahl, L; Abbenante, G.; Fairlie, D.P.; Gahan, L.R.; Hanson, G.R.; Hambley, T.W. *J. Chem. Soc., Perkin Trans. 2* **2000**, 323.
- ¹³ Crusi, E.; Giralt, E.; Andreu, D. *Peptide Res.* **1995**, *8*, 62.
- ¹⁴ Kubik, S.; Goddard, R. *J. Org. Chem.* **1999**, *64*, 9475.
- ¹⁵ Zanotti, G.C.; Campbell, B.E.; Easwaran, K.R.K.; Blout, E.R. *Int. J. Peptide Protein Res.* **1988**, *32*, 527.

- ¹⁶ Oliva, R.; Falcigno, L.; D'Auria, G.; Zanotti, G.; Paolillo, L. *Biopolymers* **2001**, *56*, 27.
- ¹⁷ NovaBiochem Catalog and Handbook, **2001**.
- ¹⁸ Bakker, E.; Bühlmann, P.; Pretsch, E. *Chem. Rev.* **1997**, *97*, 3083.
- ¹⁹ Bystrov, V.F.; Ivanov, V.T.; Koz'min, S.A.; Mikhaleva, I.I.; Khalilulina, K.KH.; Ovchinnikov, YU.A. *Febs Letters* **1972**, *21*, 34.
- ²⁰ Gennari, C.; Mielgo, A.; Potenza, D.; Scolastico, C.; Piarulli, U., Manzoni, L. *Eur. J. Org. Chem.* **1999**, 379.
- ²¹ Swinnen, D.; Hilvert, D. *Org. Lett.* **2000**, *2*, 2439.
- ²² Taralp, A.; Türkseven, C.H.; Çakmak, A.Ö.; Çengel, Ö. *J. Chem. Ed.* **2002**, *79*, 87.
- ²³ Virta, P.; Sinkkonen, J.; Lönnberg, H. *Eur. J. Org. Chem.* **2002**, 3616.
- ²⁴ Khasanov, A.; Ghadiri, M.R. Private Communication.
- ²⁵ Carpino, L.A.; Beyermann, M.; Wenschuh, H.; Bienert, M. *Acc. Chem. Res.* **1996**, *29*, 268.
- ²⁶ Lloyd-Williams, P.; Albericio, F.; Giralt, E. *Tetrahedron* **1993**, *49*, 11065.
- ²⁷ Kapurniotu, A.; Taylor, J.W. *Tetrahedron Lett.* **1993**, *34*, 7031.
- ²⁸ Gennari, C.; Mielgo, A.; Potenza, D.; Scolastico, C.; Piarulli, U.; Manzoni, L. *Eur. J. Org. Chem.* **1999**, 379.
- ²⁹ Ösapay, G.; Taylor, J.W. *J. Am. Chem. Soc.* **1990**, *112*, 6046.
- ³⁰ Zhang, W.; Taylor, J.W. *Tetrahedron Lett.* **1996**, *37*, 2173.
- ³¹ Polaskova, M.E.; Ede, N.J.; Lambert, J.N. *Aust. J. Chem.* **1998**, *51*, 535.
- ³² Rovero, P.; Quartara, L.; Fabbri, G. *Tetrahedron Lett.* **1991**, *32*, 2639.
- ³³ Trzeciak, A.; Bannwarth, W. *Tetrahedron Lett.* **1992**, *33*, 4557.
- ³⁴ Cudic, M.; Wade, J.D.; Otvos Jr., L. *Tetrahedron Lett.* **2000**, *41*, 4527.

- ³⁵ Mihara, H.; Yamabe, S.; Niidome, T.; Aoyagi, H. *Tetrahedron Lett.* **1995**, *36*, 4837.
- ³⁶ Yang, L.; Morriello, G. *Tetrahedron Lett.* **1999**, *40*, 8197.
- ³⁷ Kates, S.A.; Daniels, S.B.; Albericio, F. *Anal. Biochem.* **1993**, *212*, 303.
- ³⁸ Erickson, B.W.; Merrifield, R.B. *J. Am. Chem. Soc.* **1973**, *95*, 3757.

Additional References

Allyl Protecting Groups:

Kates, S.A.; de la Torre, B.G.; Eritja, R.; Albericio, F. *Tetrahedron Lett.* **1994**, *35*, 1033.

Yu, B.; Li, B.; Zhang, J.; Hui, Y. *Tetrahedron Lett.* **1998**, *39*, 4871.

Amino Acid Solubility:

Fauchere, J.L.; Pliska, V. *Eur. J. Med. Chem.* **1983**, *18*, 369.

Narita, M.; Chen, J.Y.; Sato, H.; Kim, Y. *Bull. Chem. Soc. Japan* **1985**, *58*, 2494.

Ammonium Ionophores and Cryptands:

Dietrich, B.; Kintzinger, J.P.; Lehn, J.M.; Metz, B.; Zahidi, A. *J. Phys. Chem.* **1987**, *91*,
6600.

Moriuchi-Kawakami, T.; Nakazawa, S.; Ota, M.; Nishihira, M.; Hayashi, H.; Shibutani,
Y.; Shono, T. *Anal. Sci.* **1998**, *14*, 1065.

Siswanta, D.; Hisamoto, H.; Tohma, H.; Yamamoto, N.; Suzuki, K. *Chem. Lett.* **1994**,
945.

Coupling Reagents, General and for Hindered Amino Acids:

- Akaji, K.; Kuriyama, N.; Kiso, Y. *Tetrahedron Lett.* **1994**, *35*, 3315.
- Albericio, F.; Bofill, J.M.; El-Faham, A.; Kates, S.A. *J. Org. Chem.* **1998**, *63*, 9678.
- Angell, Y.M.; García-Echeverría, C.; Rich, D.H. *Tetrahedron Lett.* **1994**, *35*, 5981.
- Carpino, L.A. *J. Am. Chem. Soc.* **1993**, *115*, 4397.
- Carpino, L.A.; El-Faham, A.; Minor, C.A.; Albericio, F. *J. Chem. Soc. Chem. Commun.* **1994**, 201.
- Coste, J.; Dufour, M.N.; Pantaloni, A.; Castro, B. *Tetrahedron Lett.* **1990**, *31*, 669.
- Coste, J.; Frérot, E.; Jouin, P. *Tetrahedron Lett.* **1991**, *32*, 1967.
- Coste, J.; Frérot, E.; Jouin, P. *J. Org. Chem.* **1994**, *59*, 2437.
- Frérot, E.; Coste, J.; Pantaloni, A.; Dufour, M.N.; Jouin, P. *Tetrahedron* **1991**, *47*, 259.
- Li, P.; Xu, J.C. *Tetrahedron* **2000**, *56*, 8119.
- Wijkmans, J.C.H.M.; Blok, F.A.A.; van der Marel, G.A.; van Boom, J.H.; Bloemhoff, W. *Tetrahedron Lett.* **1995**, *36*, 4643.

Cyclic/Bicyclic Peptides and Synthesis of:

- Bonomo, R.P.; Impellizzeri, G.; Pappalardo, G.; Purrello, R.; Rizzarelli, E.; Tabbi, G. *J. Chem. Soc., Dalton Trans.* **1998**, 3851.
- Isied, S.S.; Kuehn, C.G.; Lyon, J.M. *J. Am. Chem. Soc.* **1982**, *104*, 2632.
- Gisin, B.F.; Merrifield, R.B.; Tosteson, D.C. *J. Am. Chem. Soc.* **1969**, *91*, 2691.
- Kubik, S. *J. Am. Chem. Soc.* **1999**, *121*, 5846.
- Kurome, T.; Inami, K.; Inoue, T.; Ikai, K.; Takesako, K.; Kato, I.; Shiba, T. *Tetrahedron*

1996, 52, 4327.

Oliva, R.; Falcigno, L.; D'Auria, G.; Saviano, M.; Paolillo, L.; Ansanelli, G.; Zanotti, G.

Biopolymers **2000**, 53, 581.

Ösapay, G.; Profit, A.; Taylor, J.W. *Tetrahedron Lett.* **1990**, 31, 6121.

Tolle, J.C.; Staples, M.A.; Blout, E.R. *J. Am. Chem. Soc.* **1982**, 104, 6883.

Zanotti, G.; Birr, C.; Wieland, T. *Int. J. Peptide Protein Res.* **1978**, 12, 204.

Ion Selective Electrodes:

Oesch, U.; Ammann, D.; Simon, W. *Clin. Chem.* **1986**, 32, 1448.

NMR Study of Complexation:

Connors, K.A. *Binding Constants: The Measurement of Molecular Complex Stability*;

John Wiley & Sons: New York, 1987.

Gill, V.M.S.; Oliveria, N.C. *J. Chem. Ed.* **1990**, 67, 473.

Macomber, R.S. *J. Chem. Ed.* **1992**, 69, 375.

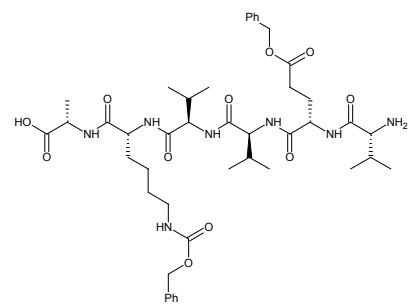
Solid Phase Colorimetric Tests:

Attardi, M.E.; Porcu, G.; Taddei, M. *Tetrahedron Lett.* **2000**, 41, 7391.

Kaiser, E.; Colescott, R.L.; Bossinger, C.D.; Cook, P.I. *Anal. Biochem.* **1970**, 34, 595.

Appendix: ^1H , ^{13}C , and DEPT135 NMR Spectra and ESI MS

1a



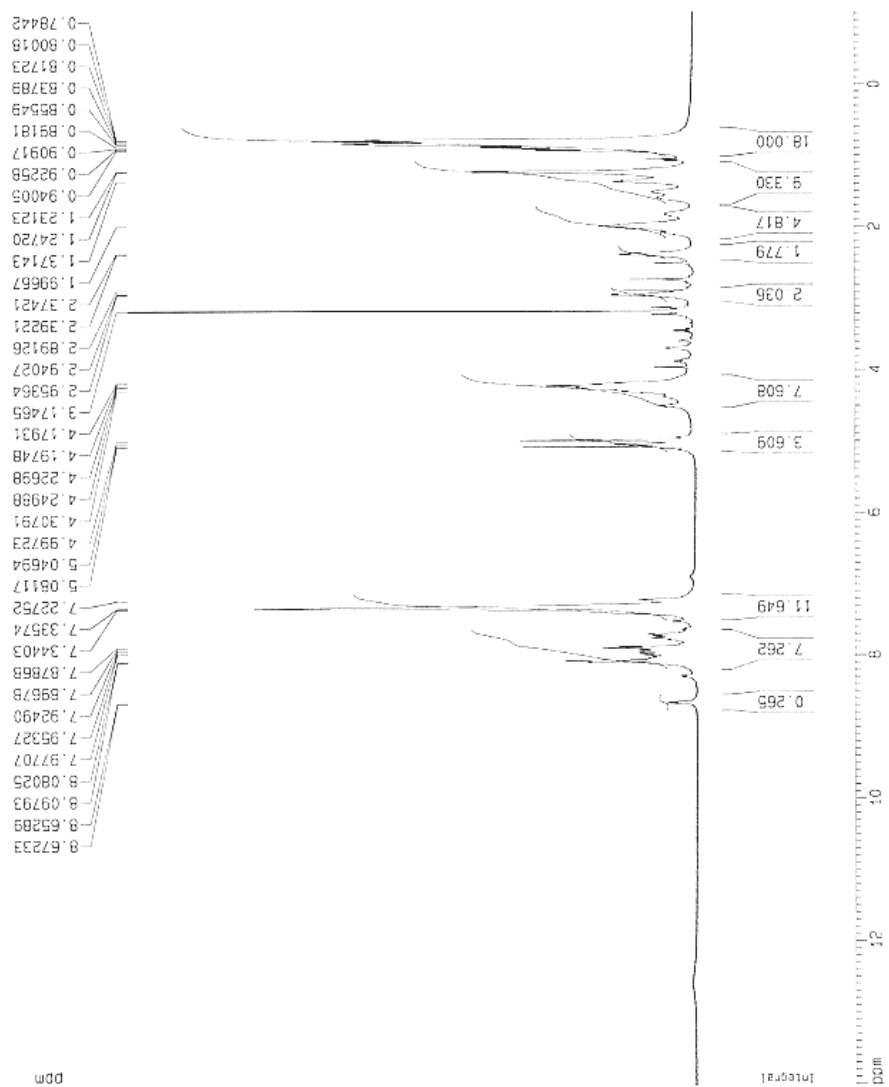
Current Data Parameters
 NAME Oct26-2001-Cha
 EXPNO 10
 PROCNO 1

F2 - Acquisition Parameters
 Date_ 20010226
 Time 19:20
 INSTRUM spect
 PROCNO 5 -n Multifin
 PULPROG zgpg
 TO 32768
 SOLVENT DMSO
 NS 16
 DS 2
 SWH 8278.146 Hz
 FIDRES 0.262628 Hz
 AQ 1.978272 sec
 RG 343.7
 CW 60.400 usec
 DE 6.00 usec
 TE 300.0 K
 D1 1.0000000 sec

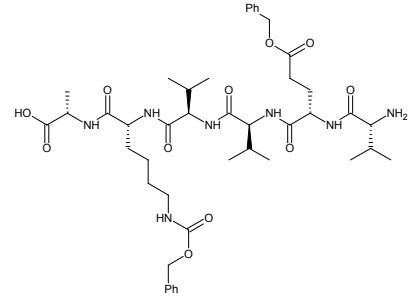
----- CHANNEL f1 -----
 NUC1 1H
 P1 10.00 usec
 PL 0.00 dB
 SFO1 400.1364710 MHz

F2 - Processing parameters
 SI 32768
 SF 400.1364710 MHz
 N 16
 DD 0
 LB 0.00 Hz
 GB 0
 PC 1.00

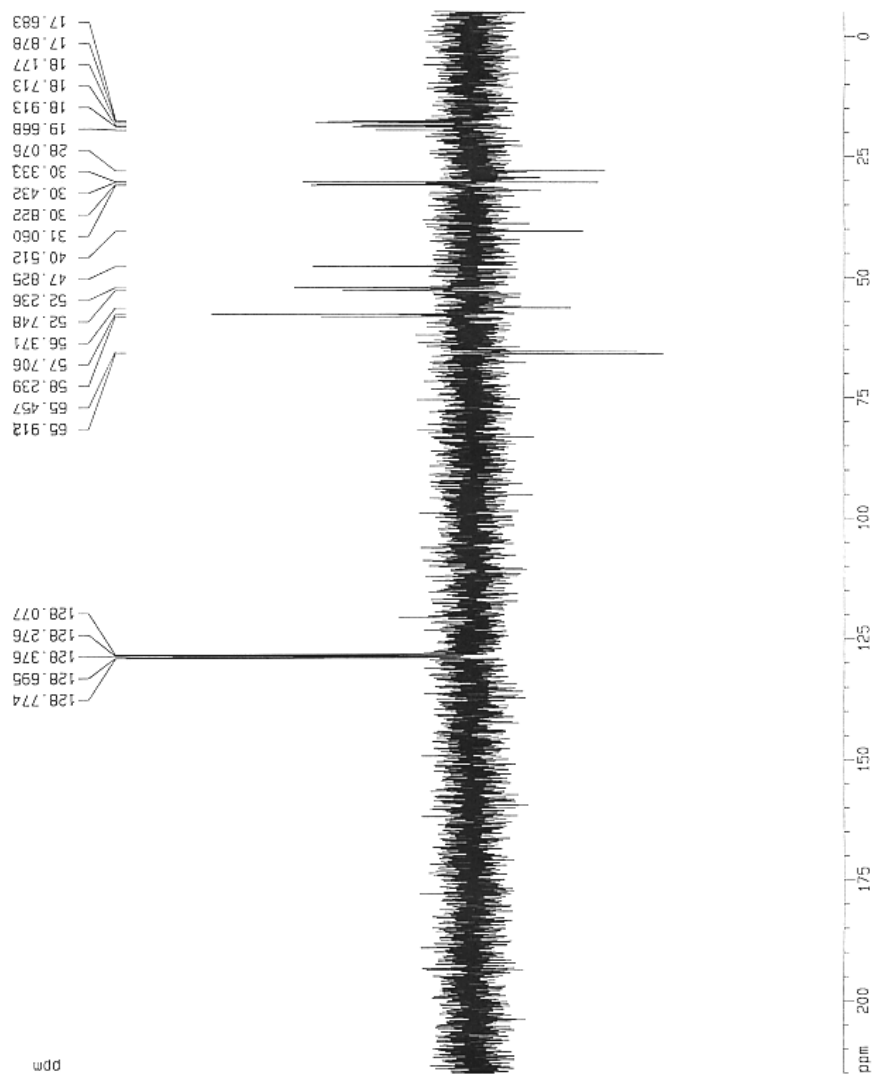
1D NMR plot parameters
 CX 20.00 cm
 F1P 14.825 ppm
 F2 5611.82 Hz
 F2P -1.619 ppm
 F2 4607.73 Hz
 F2AQM 0.75220 ppm/cm
 F2ZCN 360.57766 Hz/cm



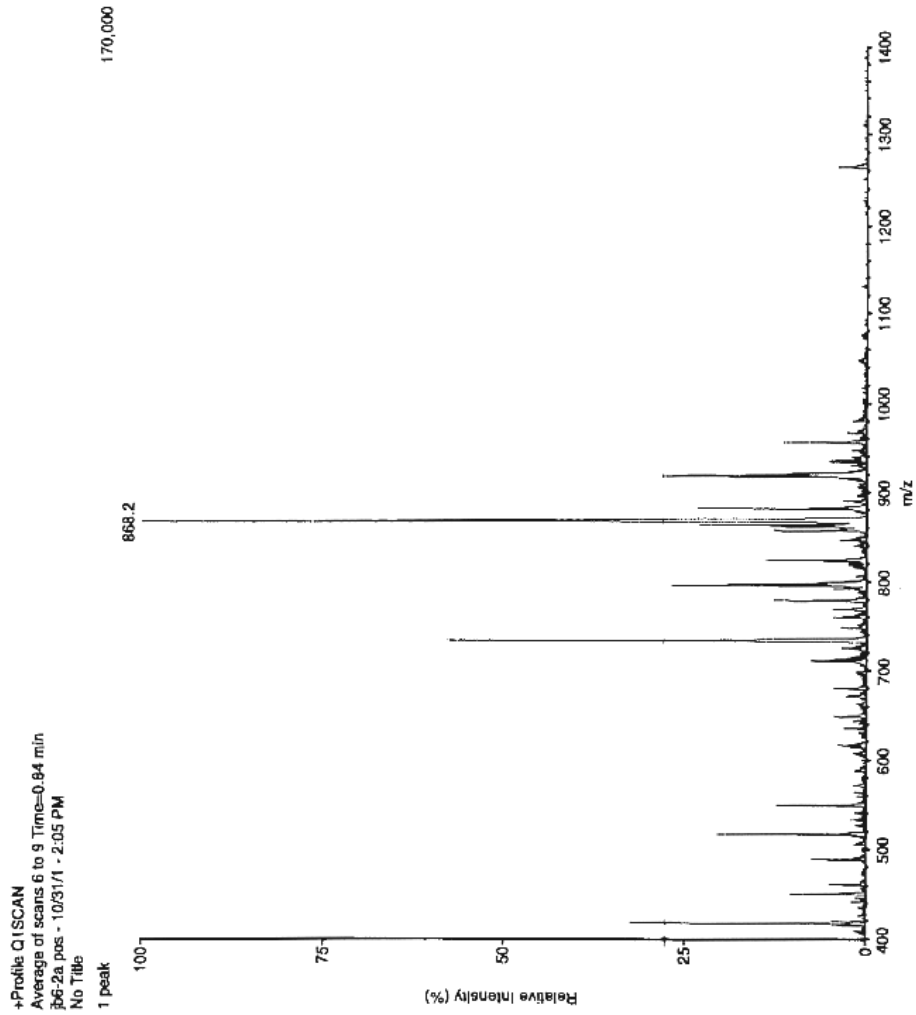
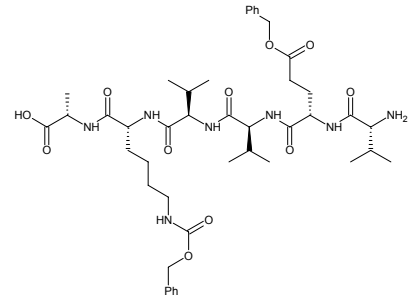
1a



Current Data Parameters
NAME 00101-2001-2Re
EXPNO 1
PROCNO 1
F2 - Acquisition Parameters
Date_ 20080202
Time 17.04
INSTRUM spect
PULPROG 5 nm multirp
AQ 0.01155
TD 65536
SFO1 500.1314000 MHz
NS 512
DS 4
SWH 23600.814 Hz
FIDRES 0.265918 Hz
AQ 1.5684709 sec
RG 400
ZG 28.863 usec
ZM 6.03 usec
TE 300.0 K
CNS1? 145.000000 sec
D1 2.00000000 sec
d2 0.00344628 sec
d3 0.00000000 sec
d4 0.00000000 sec
DELTA 6388.16261719 sec
***** CHANNEL f1 *****
NUC1 13C
P1 0.120 usec
PL1 17.43 usec
PC1 0.00 dB
SFO1 100.6227899 MHz
***** CHANNEL f2 *****
CPDPRG2 waltz16
NUC2 1H
P2 8.70 usec
PL2 17.40 usec
PC2 0.00 dB
PL3 0.00 dB
PL4 23.00 dB
SFO2 400.1314000 MHz
F2 - Processing parameters
SI 32768
SF 100.6227893 MHz
WDW EM
SSB 0
LB 1.00 Hz
GB 0
PC 1.40
IC - NMR plot parameters
CX 20.00 cm
F1P 215.000 Hz
F1 21531.75 Hz
F2P -5.000 Hz
F2 -503.06 Hz
SOLCK 1: 00000 Hz/Hz
H2CN 1: 18.74656 Hz/cm



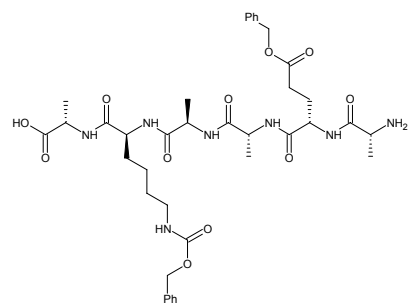
1a



+Profile: Q1SCAN
Average of scans 6 to 9 Time=0.84 min
36-2a_pos - 10/31/1 - 2:05 PM
No Title
1 peak

DI 50
ISV 5000
IN 650
OR 120
R0 30
M1 1000
RE1 118.3
DM1 0.040
R1 25.5
L9 -100
FP 50
MU -5000
CC 1
DI μA 2.3
IS v 5188.08
UV -1338.5

2a



```

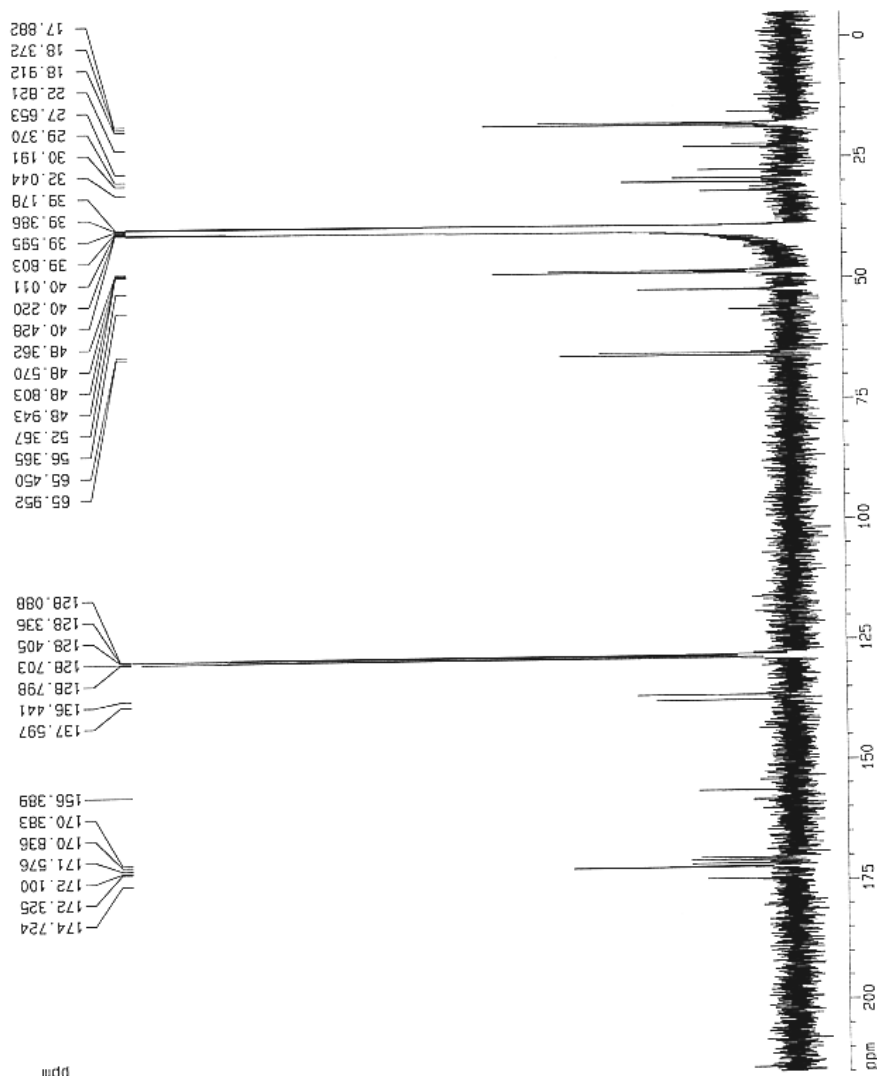
Current Data Parameters
Name: F016-2021-c1e
EXPNO: 12
PROCNO: 1
F2 - Acquisition Parameters
Date_ : 20020219
Time: 3.05
INSTRUM: spect
PROBHD: 5 mm MLL1VM
PULPROG: zgpg30
TD: 65536
SOLVENT: DMSO
NS: 3000
DS: 4
SWH: 25125.629 Hz
FIDRES: 0.383367 Hz
AQ: 1.3042164 sec
RG: 2580.3
Dr: 19.900 uSBC
DE: 6.00 uSBC
TE: 300.0 K
D1: 2.00000000 sec
d11: 0.03000000 sec
d12: 0.06000000 sec

***** CHANNEL f1 *****
NUC1: 13C
PL: 8.70 uSBC
PL1: 0.00 dB
SFO1: 100.6237359 MHz

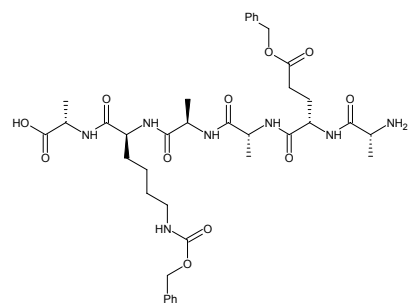
***** CHANNEL f2 *****
CPDPRG2: waltz16
NUC2: 13C
PL2: 107.00 uSBC
PL3: 0.00 dB
PL4: 23.00 dB
PL5: 23.00 dB
SFO2: 400.1316000 MHz

F2 - Processing parameters
SI: 32768
SF: 100.6127263 MHz
WDW: EN
SSB: 0
LB: 1.00 Hz
GB: 0
PC: 1.40

ID: NMR plot parameters
CX: 20.00 cm
F1P: 215.000 ppm
F1: 21.63175 Hz
F2P: -5.000 ppm
F2: -503.06 Hz
P1P1CN: 11.00000 ppm/cm
P2CM: 1106.74660 Hz/cm
  
```



2a



Current Data Parameters
 NAME: Feb18-2012-ene
 EXPNO: 14
 PROCNO: 1

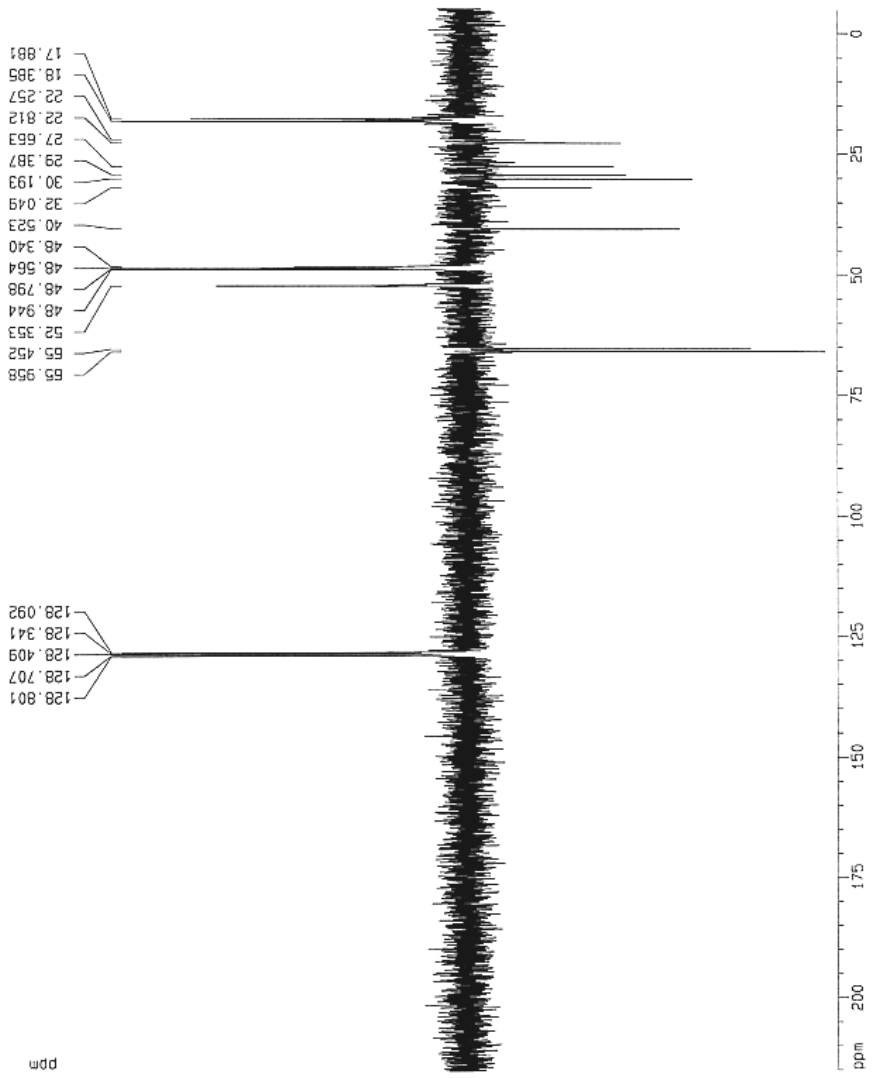
F2 - Acquisition Parameters
 Date_: 20020219
 Time: 9:24
 INSTRUM: spect
 PULPROG: zgpg30
 TO: 65335
 SOLVENT: DMSO
 NS: 1200
 DS: 4
 SWH: 23160.814 Hz
 FIDRES: 0.365916 Hz
 AQ: 1.3664796 sec
 RG: 3281
 DW: 20.050 usec
 DE: 0.0000000 usec
 TE: 300.2 K
 CNV12: 145.0000000
 D1: 2.0000000 sec
 dP: 0.0034460 sec
 C12: 0.0000000 sec
 DELTA: 6366.1666715 sec

***** CHANNEL f1 *****
 NUC1: 13C
 P1: 8.70 usec
 PL1: 0.00 dB
 SFO1: 100.627893 MHz

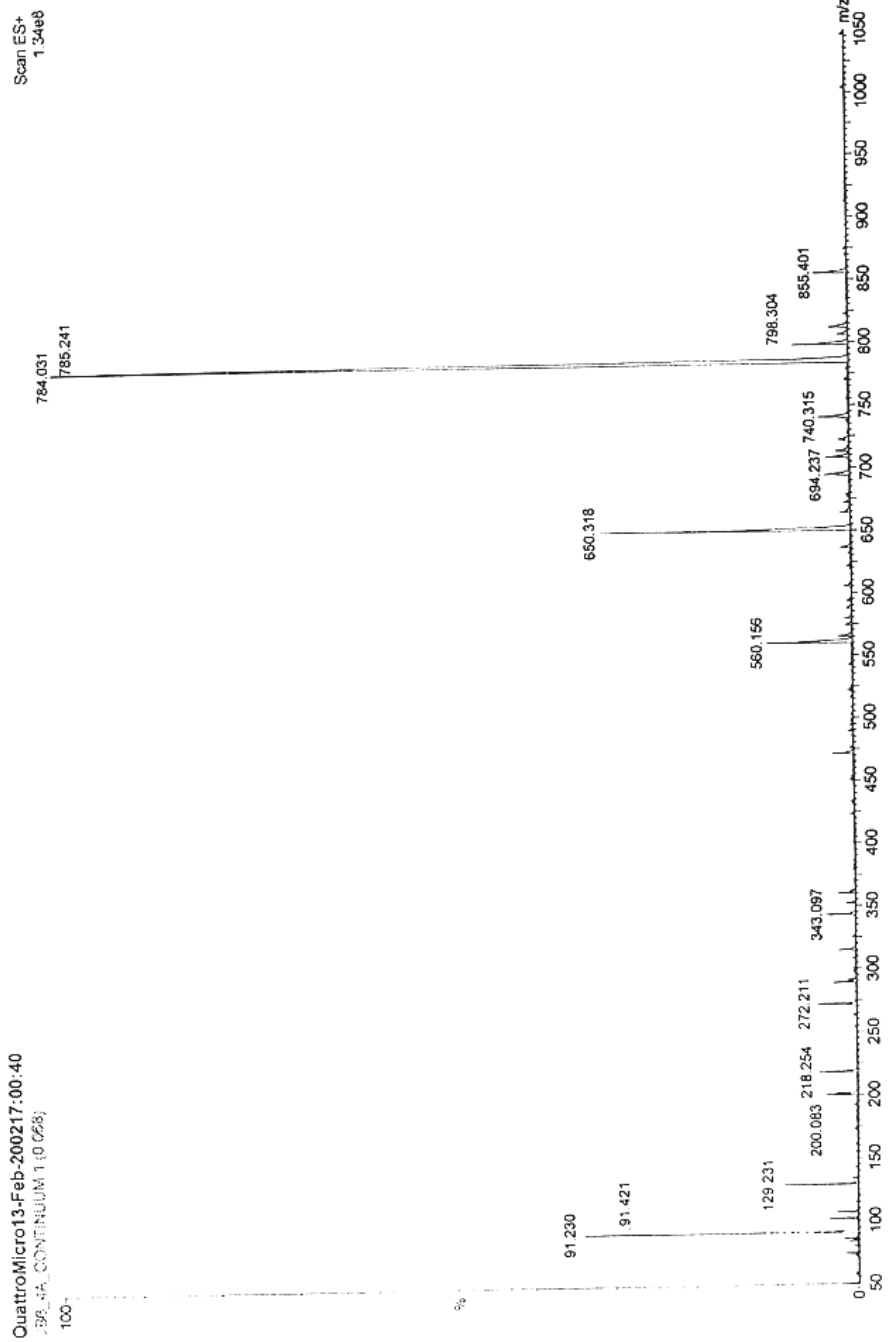
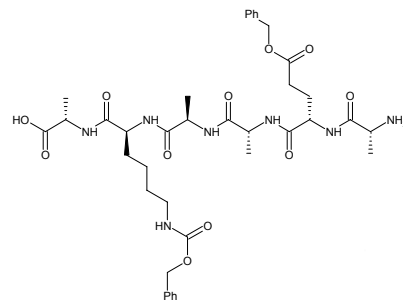
***** CHANNEL f2 *****
 CPDPRG2: waltz16
 NUC2: 1H
 P2: 8.70 usec
 PL2: 0.00 dB
 SFO2: 400.116605 MHz

F2 - Processing parameters
 S1: 32768
 SFO: 100.612793 MHz
 MDK: EN
 SSB: 0
 LB: 1.00 Hz
 GB: 0
 PC: 1.40

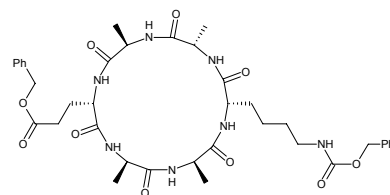
ID NMR D1/L parameters
 CX: 20.00 cm
 F1: 215.000 cmh
 F2: 21631.75 Hz
 F3: -5.000 cmh
 F4: -503.00 Hz
 PRMCM: 11.00000 cmh/cm
 HZCM: 1.0074000 Hz/cm



2a



2b



```

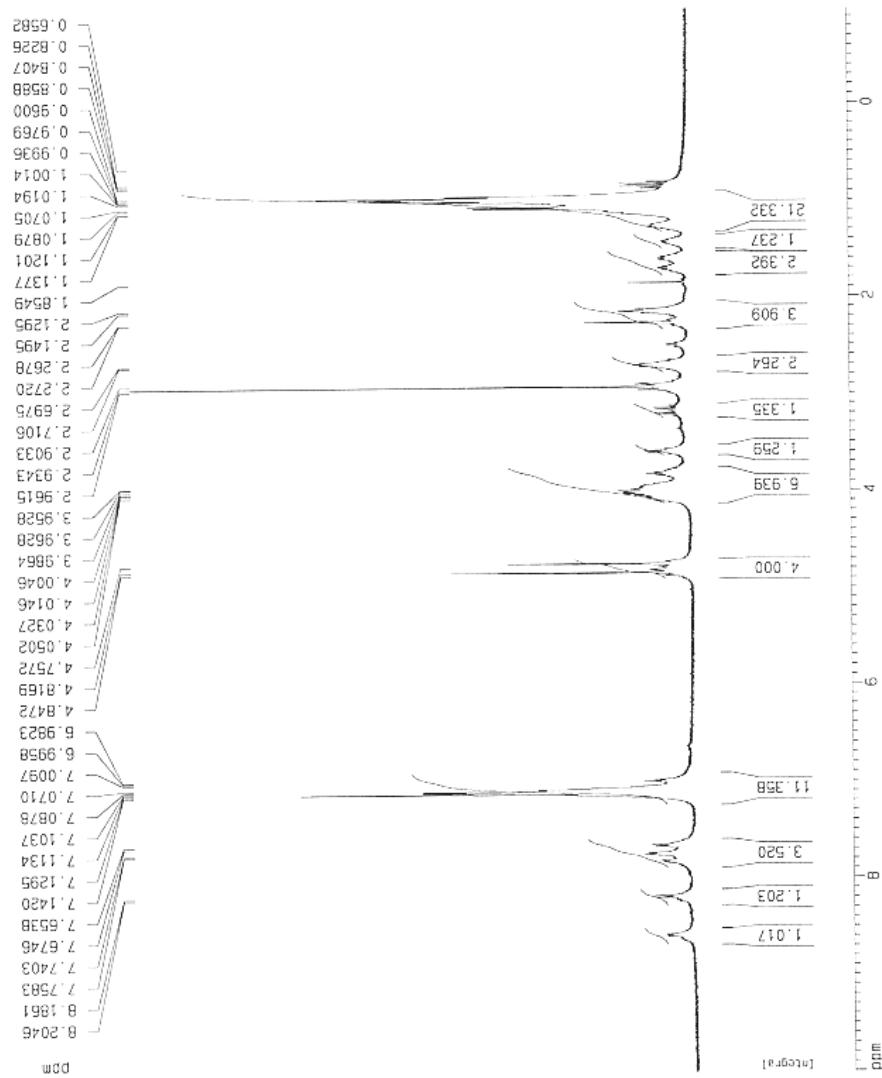
Current Data Parameters
NAME      reb18-2002-018
EXPNO    10
PROCNO   1

F2 - Acquisition Parameters
Date_    2020218
Time     19 23
INSTRUM spect
PROBHD   5 mm WALTIM
PULPROG zg30
TO       32768
SOLVENT DMSO
NS       16
DS       2
SWH      8278.146 Hz
FIDRES   0.252629 Hz
AQ       1.9753372 sec
RG       455.1
CW       60.400 usec
CF       5.00 usec
TE       300.0 K
D1       1.00000000 sec

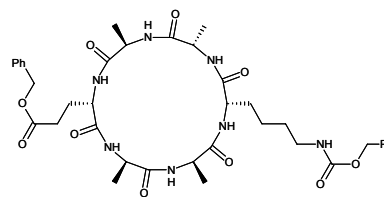
***** CHANNEL f1 *****
NUC1     1H
P1       6.75 usec
PL1      0.00 dB
SFO1     400.1324710 MHz

F2 - Processing parameters
SI       32768
SF       400.1300546 MHz
WDW      tu
SSB      0
LB       0.00 Hz
GB       0
PC       1.00

1D NMR plot parameters
CX       20.00 cm
F1P      10.0000 ppm
F1       4004.74 Hz
F2P      -0.0200 ppm
F2       -261.45 Hz
PPOW     0.56835 dBW/cm
HZDN     219.62948 Hz/cm
  
```



2b



```

Current Data Parameters
NAME      MrB-2002-cha
EXPNO    10
PROCNO   1

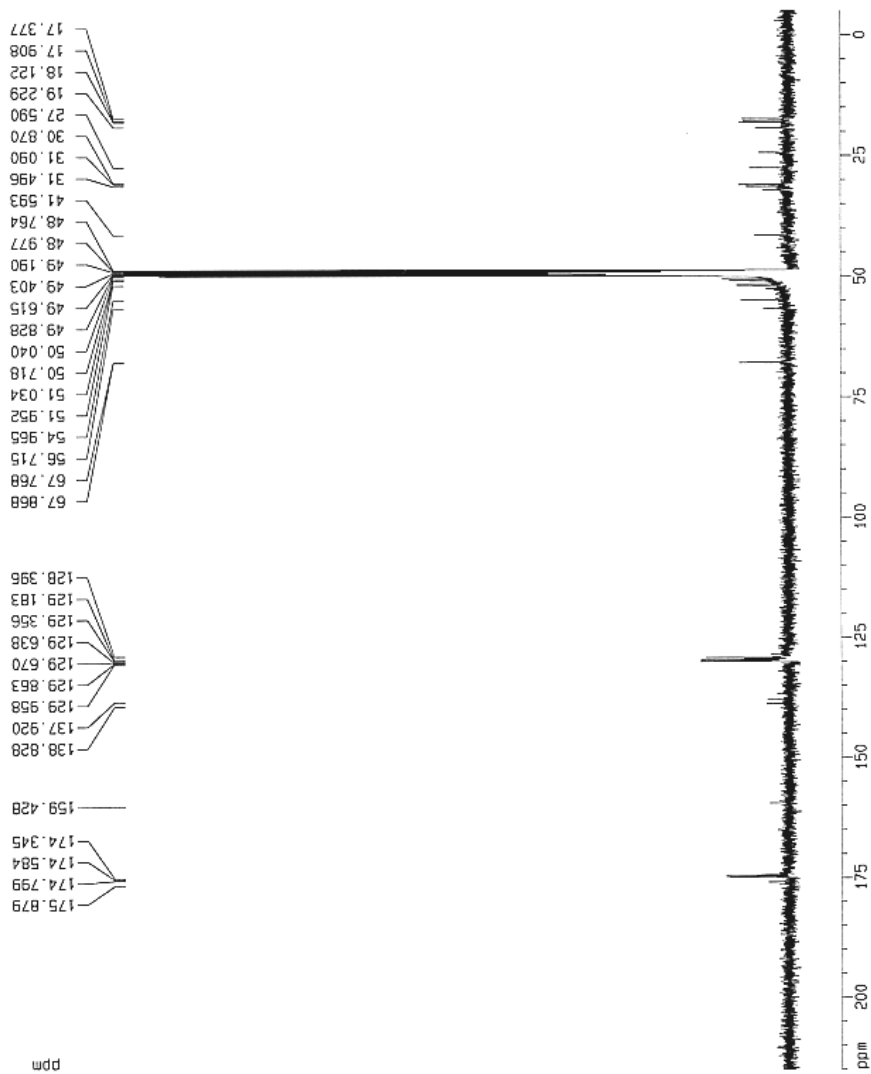
F2 - Acquisition Parameters
DATE_    20050326
TIME     5.00
INSTRUM  spect
PROBHD   5 mm Nucleo
PULPROG  zgpg30
TD        65536
SOLVENT  H2O
NS        2000
DS         4
SWH       25125.629 Hz
FIDRES    0.383387 Hz
AQ        1.3942164 sec
RG         8192
DM         19.500 usec
DE         6.00 usec
TE        300.0 K
D1        2.00000000 sec
d11       0.03000000 sec
d12       0.00002000 sec

***** CHANNEL f1 *****
NUC1      13C
P1        8.70 usec
PL1       0.00 dB
SFO1     100.627855 MHz

***** CHANNEL f2 *****
CPDPRG2  waltz16
NUC2      1H
PCPD2    107.00 usec
PL2       0.00 dB
PL12     23.00 dB
PL13     23.00 dB
SFO2     400.1510005 MHz

F2 - Processing parameters
SI        32768
SF        100.6126851 MHz
WDW       EM
SSB       0
LB        1.00 Hz
GB        0
PC        1.40

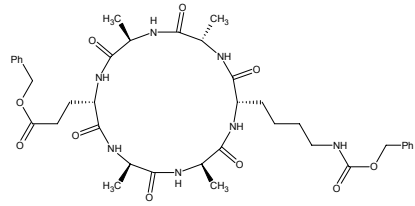
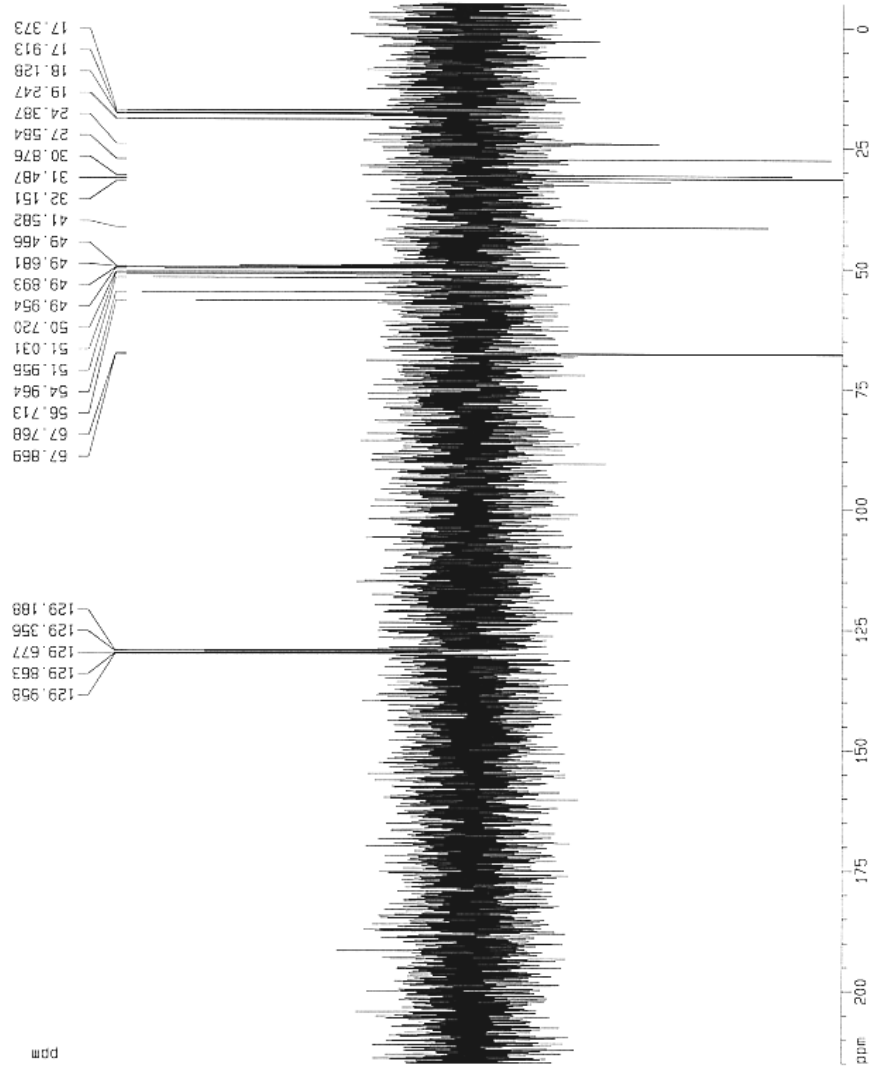
1D NMR data parameters
CX        20.00 cm
F1P       215.000 ppm
F1        21631.71 Hz
F2P       -5.000 ppm
F2        -503.06 Hz
PRWCM     11.00000 ppm/cm
HZCN      1105.73840 Hz/cm
  
```



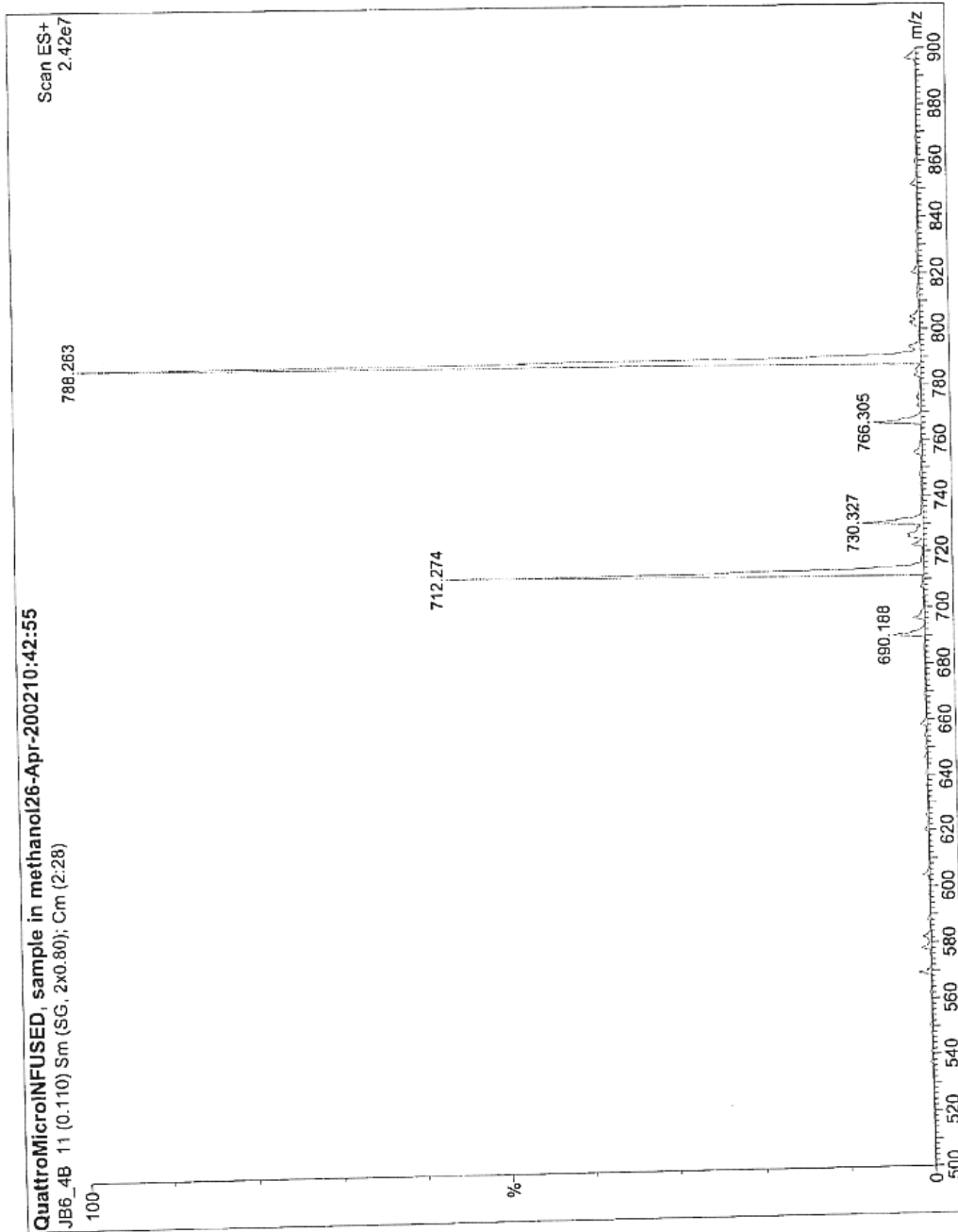
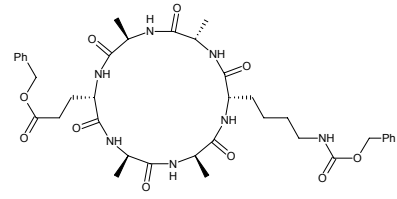
2b

```

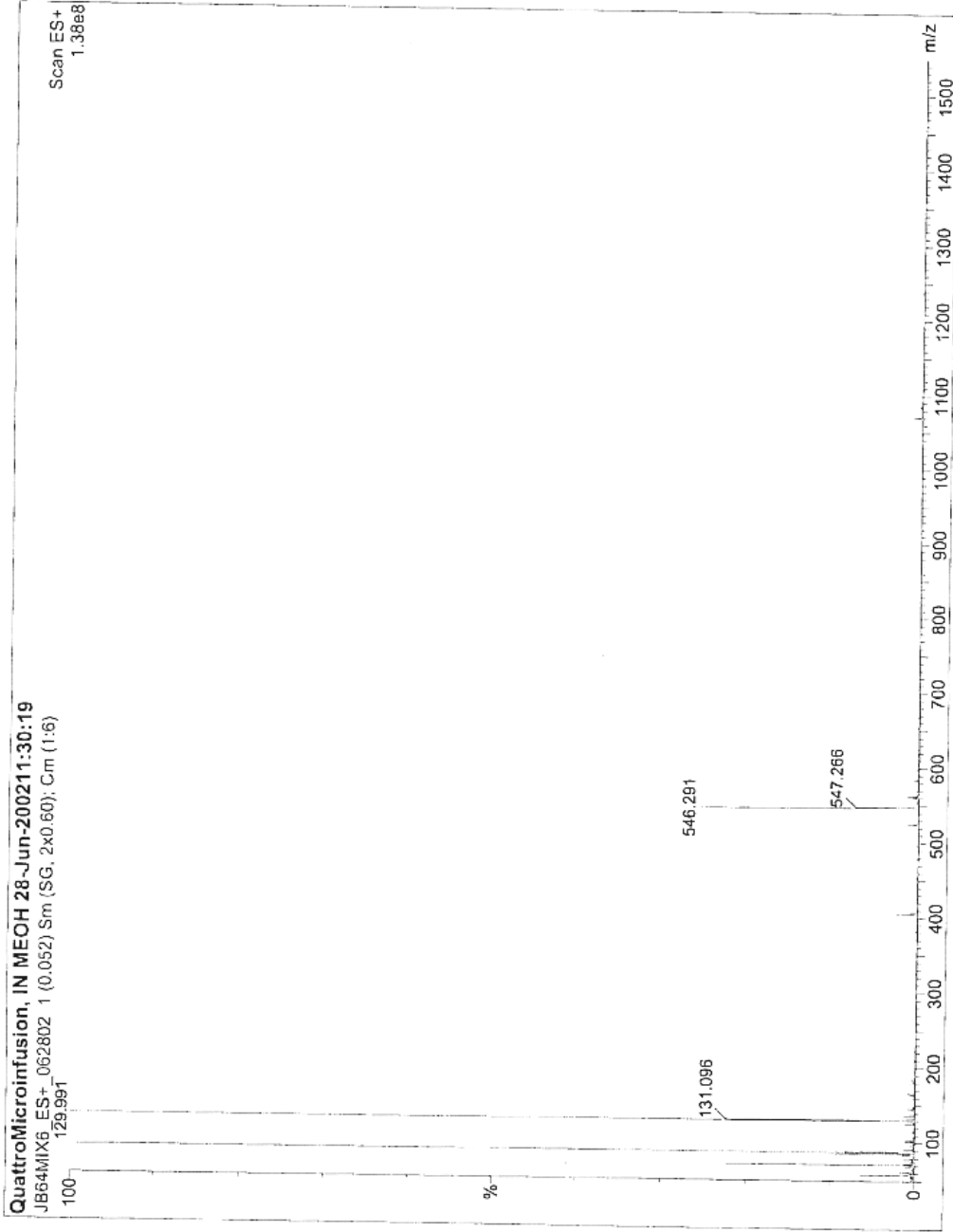
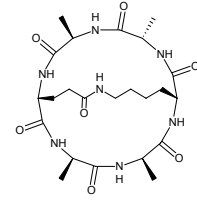
Current Data Parameters
NAME      May11-2002-che
EXPNO    13
PROCNO   1
----- Acquisition Parameters -----
Date_    20020512
Time     3.44
INSTRUM  spect
PROBHD   5 mm Multiv
PULPROG  zgpg30
TD        65536
SOVENT   H2O
NS        4000
DS        4
SWH       23900.624 Hz
FIDRES    0.0009588 Hz
AQ         1.3565248 SEC
RG         328
OR        20.8521880C
DE        6.001686C
TE        300.0 K
CSTRT     1.45:00:00.00
D1        2.0000000 SEC
D2        0.00344928 SEC
D3        0.0000000 SEC
DELTA    6.9981531719 SEC
----- CHANNEL f1 -----
NUC1      13C
P1        8.701686C
G1        17.403372C
RG1       0.0045
SFO1     100.6278936 MHz
----- CHANNEL f2 -----
DEPRGR   waltz16
NUC2      1H
P2        8.701686C
G2        17.403372C
RG2       0.0045
SFO2     400.1316005 MHz
----- Processing parameters -----
SI        32768
AQ        1.3565248 SEC
RG         328
WDW       EM
SSB       0
GB        1.001/2
PC        1.40
ID        NMR data: parameters
CX        20.00 cm
F1P       215.000 MHz
F2        215.3171 Hz
F2P       -5.000 MHz
PC        1.00000 Hz
SFO1MHz  100.6278936
SFO2MHz  400.1316005
  
```



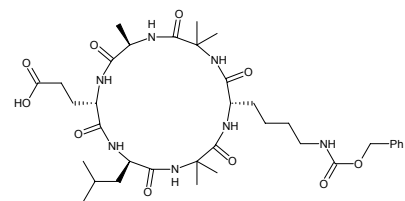
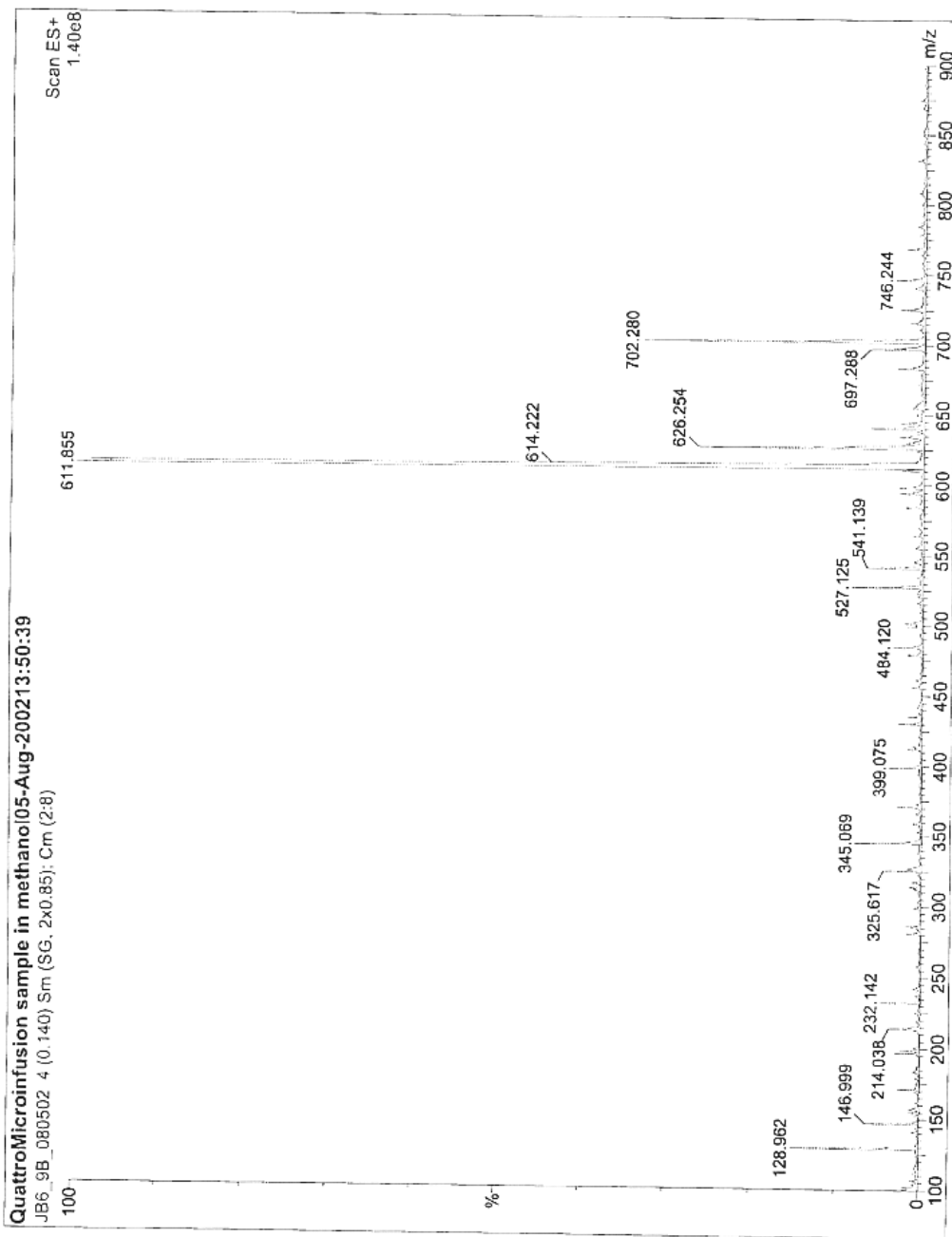
2b



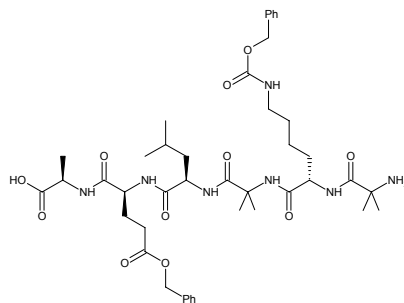
2d



4b



5a



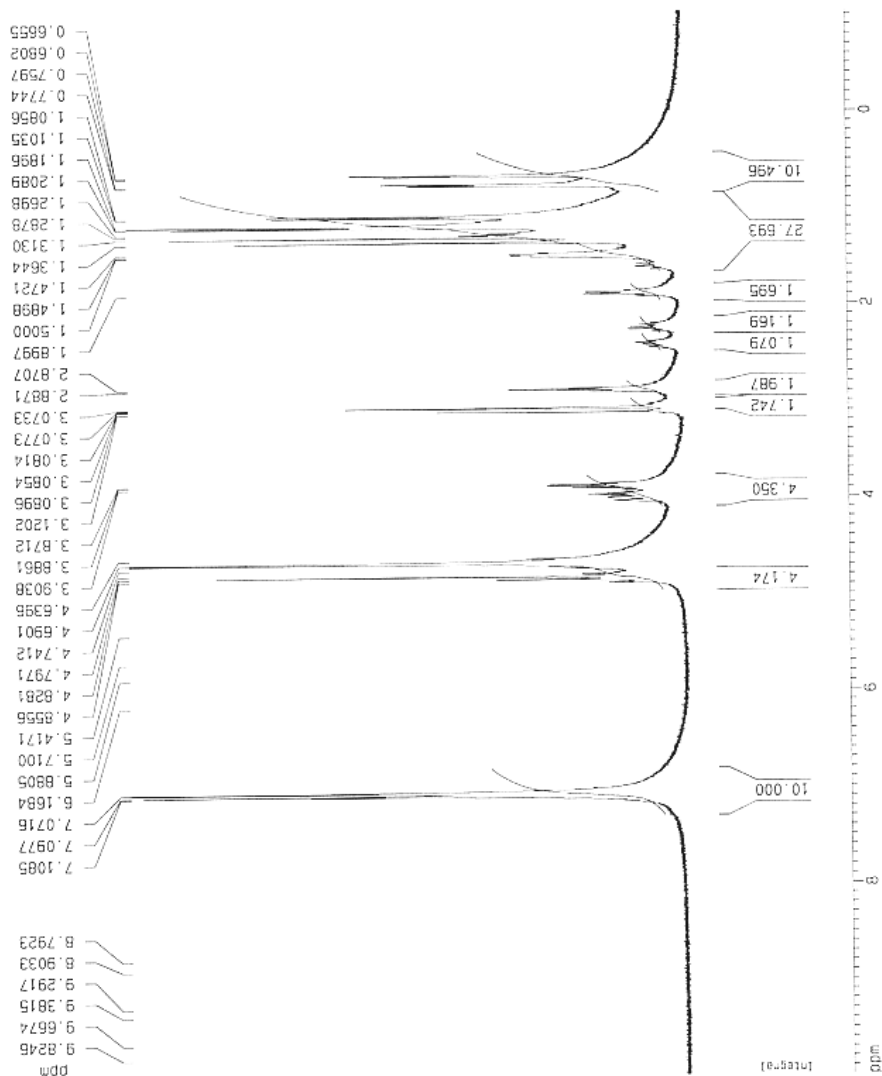
Current Data Parameters
 NAME Oct16-2002.cns
 EXPNO 12
 PROCNO 1

F2 - Acquisition Parameters
 Date_ 20021016
 Time 19.50
 INSTRUM spect
 PROBHD 5 mm Multisfu
 PULPROG zgpg30
 TD 32768
 SOLVENT NSCLH
 NS 15
 CS 2
 SMH 8278.146 Hz
 FIDRES 0.258469 Hz
 AQ 1.5752372 sec
 RG 287.4
 DK 60.400 usec
 DE 6.00 usec
 TE 300.2 K
 O1 1.00000000 sec

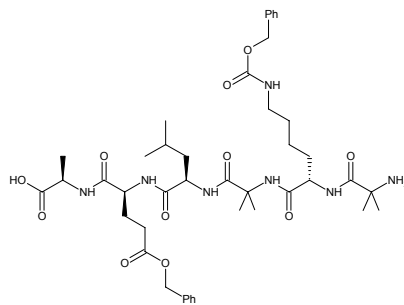
***** CHANNEL f1 *****
 NUC1 H
 P1 8.60 usec
 PL 0.00 dB
 SFO1 400.132410 MHz

F2 - Processing parameters
 SI 32768
 SF 400.132410 MHz
 NDK no
 SSB 0
 LB 0.00 Hz
 GB 0
 PC 1.00

10 NMR list parameters
 CX 20.00 cm
 F1 6.848 mm
 F2 400.54 Hz
 F3 1.005 ppm
 F4 -733.61 Hz
 PRNC 0.00165 rpm/cm
 HZCM 250.81776 Hz/cm

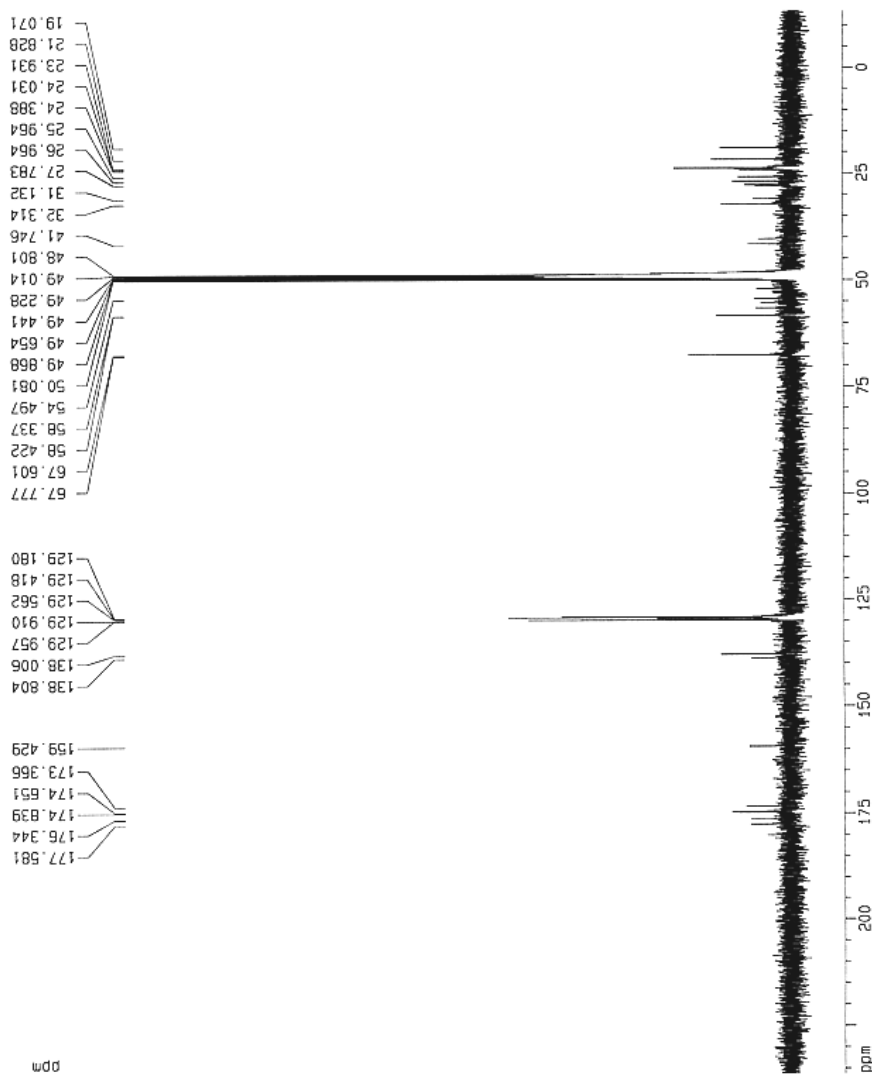


5a

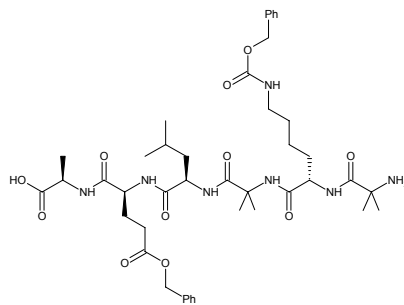


```

Current Data Parameters
NAME      Oct14-2002.cis
EXPNO    10
PROCNO   1
F2 - Acquisition Parameters
Date_    20021013
Time     2.24
INSTRUM spect
PROBHD   5 mm Maltz16
PULPROG zgpg30
TD       65536
AQ       2.5938
RG       4096
SOLVENT  H2O
NS       3000
DS       4
SWH      25125.625 MHz
FIDRES   0.383387 MHz
AQ       1.3042164 sec
RG       4096
DM       19.902 usec
DE       6.00 usec
TE       300.0 K
FID      2.00000000 sec
SI       0.03000000 sec
SF       0.00000000 sec
AQ       0.00000000 sec
***** CHANNEL f1 *****
NUC1     13C
P1       8.70 usec
PL1     0.00 dB
SFO1    100.6237959 MHz
***** CHANNEL f2 *****
CPDPRG2  maltz16
NUC2     1H
P2       107.00 usec
PL2     0.00 dB
PL3     23.00 dB
PL13    23.00 dB
SFO2    400.1316005 MHz
F2 - Processing parameters
SI       32768
SF       100.6237959 MHz
RG       0
DE       0.00 usec
TE       0
LB       0
GB       0
PC       1.40
ID NAME parameters
CY      20.00 cm
F1P     235.275 ppm
F1      23772.60 Hz
F2P     -13.448 ppm
F2      -1353.03 Hz
PPMCM   12.48533 ppm/cm
HZCM    1255.828149 Hz/cm
  
```



5a



```

Current Data Parameters
NAME      DC119-2002-enc
EXPNO    17
PROCNO   1
F2 - Acquisition Parameters
Date_    20021020
Time     4.37
INSTRUM spect
PROBHD   5 mm MSL100
PULPROG  zgpg30
TD        65536
SOLVENT  H2O
NS        500
DS        4
SFO1      125.760 MHz
FIDRES    0.365940 Hz
AQ         1.2664756 SEC
RG         4096
DM         20.850 uSEC
DE         6.00 uSEC
TE        300.0 K
CA1ST2   145.000000
D1         2.0000000 SEC
CP         0.00344289 SEC
C1P2      0.0000000 SEC
DELTA     656.1626179 SEC

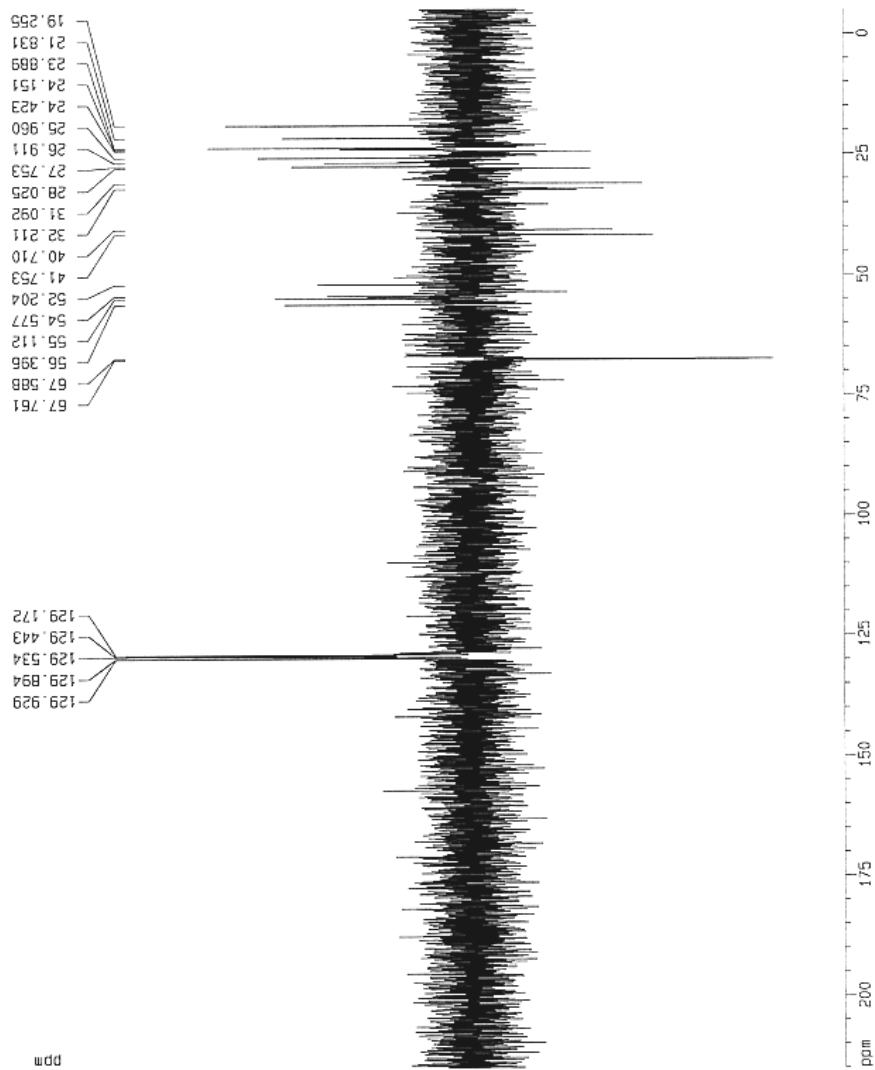
***** CHANNEL f1 *****
NUC1      13C
P1         8.70 uSEC
PR         17.40 uSEC
PL1       0.00 dB
SFO1      100.622769 MHz

***** CHANNEL f2 *****
CPDPRG2  waltz16
NUC2      1H
P2         8.00 uSEC
PR         17.40 uSEC
PL2       0.00 dB
PL3       0.00 dB
PL4       23.00 dB
SFO2      400.1316005 MHz

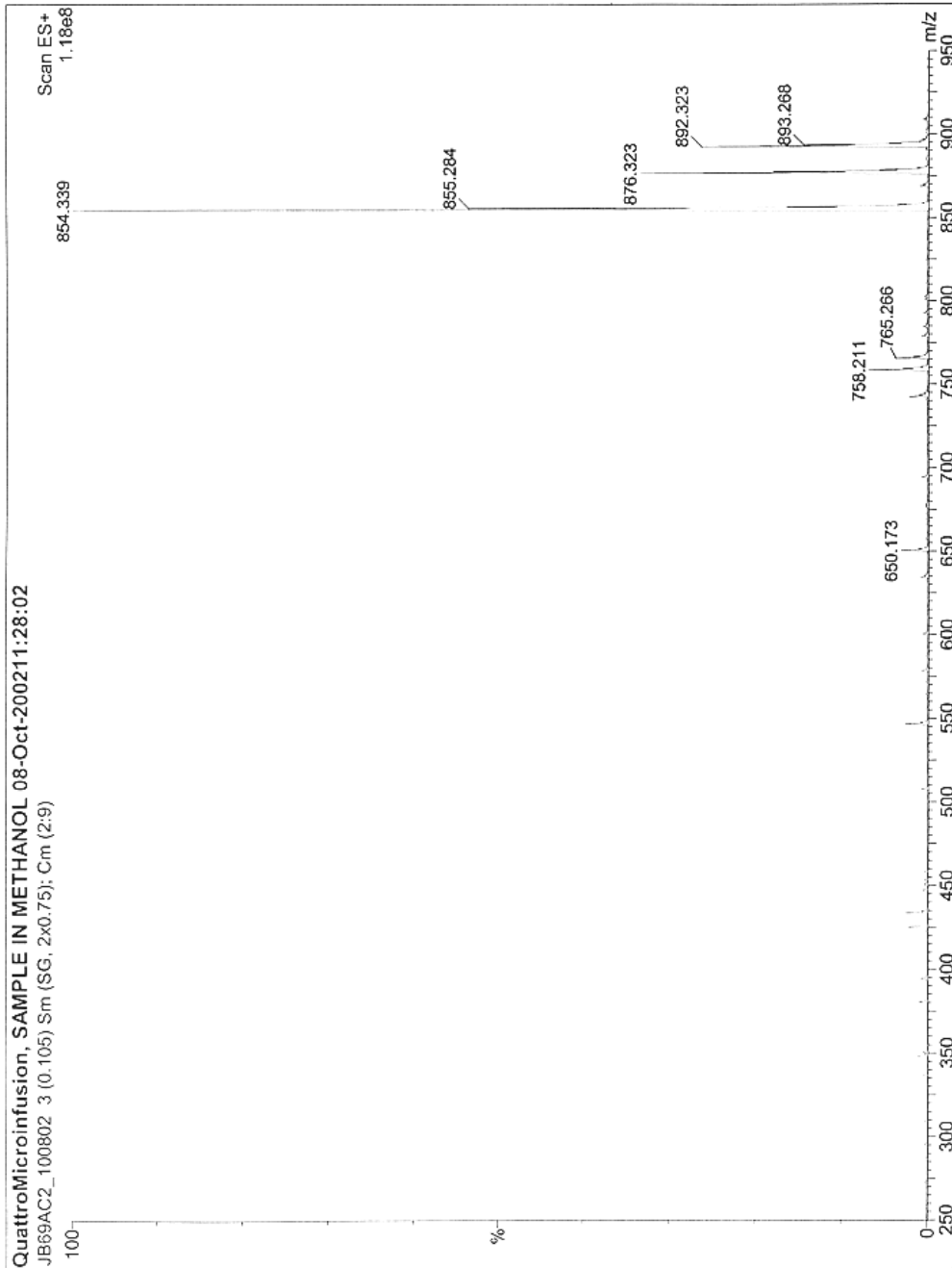
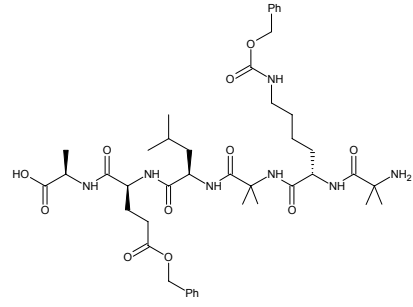
F2 - Processing parameters
SI         32768
SF         100.6129651 MHz
NUC1      13C
NUC2      1H
GB         0
PC         1.40

10 NMR plot parameters
CX         20.00 cm
F1P        215.000 dB
F1         21631.71 Hz
F2P        -5.000 dB
F2         -503.00 Hz
SFO1      100.622769 MHz
SFO2      400.1316005 MHz

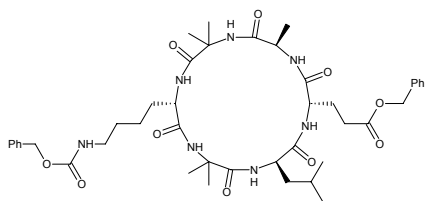
```



5a



5b



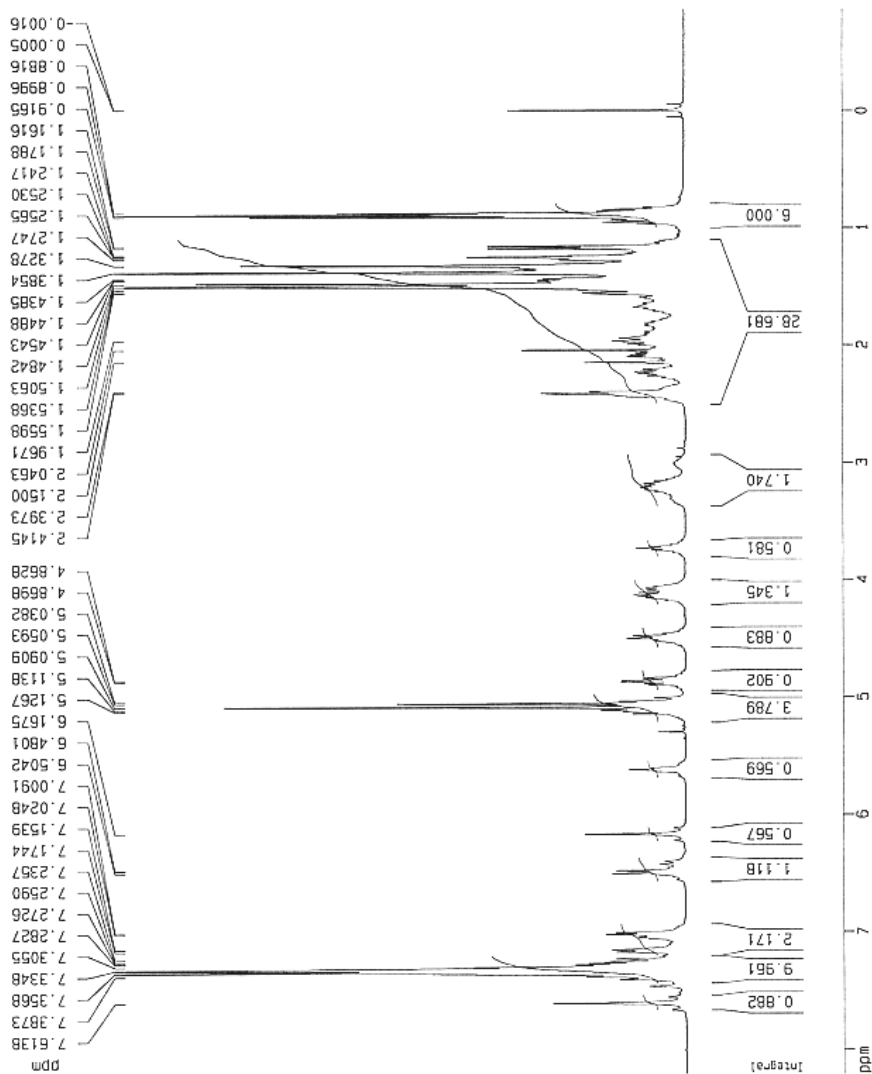
Current Data Parameters
 NAME Oct28-2002-che
 EXPNO 10
 PROCNO 1

F2 - Acquisition Parameters
 Date_ 20021028
 Time 15.26
 INSTRUM spect
 PROBHD 5 mm Multibow
 PULPROG zgpg30
 TD 32768
 SOLVENT CCl₄
 NS 16
 DS 2
 SWH 8278.146 Hz
 FIDRES 0.252629 Hz
 AQ 1.9752372 sec
 RG 80.6
 DH 60.400 usec
 DE 6.00 usec
 TE 300.0 K
 D1 1.0000000 sec

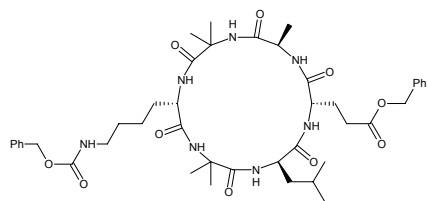
***** CHANNEL f1 *****
 NUC1 ¹H
 P1 8.60 usec
 PL1 0.00 dB
 SFO1 400.1324710 MHz

F2 - Processing parameters
 SI 32768
 SF 400.1300040 MHz
 HW na
 SSB 0
 LB 0.00 Hz
 GB 0
 PC 1.00

1D NMR plot parameters
 CX 20.00 cm
 F1P 8.212 ppm
 F1 3265.77 Hz
 F2 -348.42 Hz
 PPVCH 0.45425 ppm/cm
 HZCM 181.75531 Hz/Hz



5b



```

Current Data Parameters
NAME      Cc12b-2002-c1b
EXPNO    11
PROCNO   1

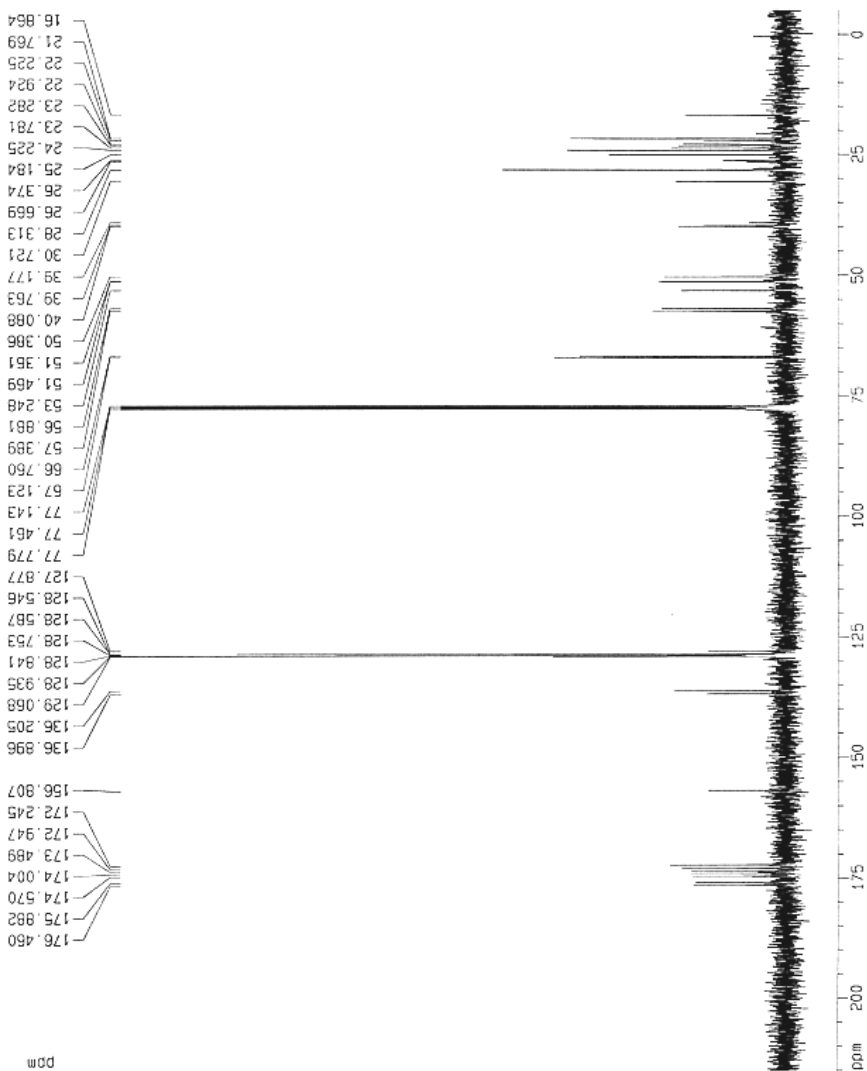
F2 - Acquisition Parameters
Date_    20021028
Time     15.55
INSTRUM  spect
PROBHD   5 mm Multifit
PULPROG  zgpg30
TD       65536
SOLVENT  CDCl3
NS       512
DS       4
SWH      2525.629 Hz
FIDRES   0.383307 Hz
AQ       1.3042164 sec
RG        8192
DA       19.500 usec
DE       6.00 usec
TE       303.2 K
D1       2.0000000 sec
d11      0.0500000 sec
d12      0.0500000 sec

***** CHANNEL f1 *****
NUC1     13C
P1       6.70 usec
PL1     0.00 dB
SFO1    100.6263655 MHz

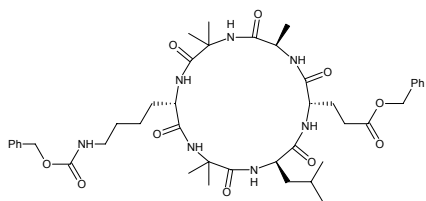
***** CHANNEL f2 *****
CPDPRG2  waltz16
NUC2     1H
PCPD2   107.00 usec
PL2     0.00 dB
PL12    23.00 dB
PL13    23.00 dB
SFO2    400.1318005 MHz

F2 - Processing parameters
SI       32768
SF      100.6127250 MHz
WDW      EM
SSB      0
LB       1.00 Hz
GB       0
PC       1.40

1D NMR plot parameters
CX      20.00 cm
FID     215.003 ppm
F1      21631.74 Hz
F2      -5.003 ppm
F3      303.65 Hz
PNUC1   11.00003 ppm/cm
PNUC2   15.0673955 Hz/cm
  
```

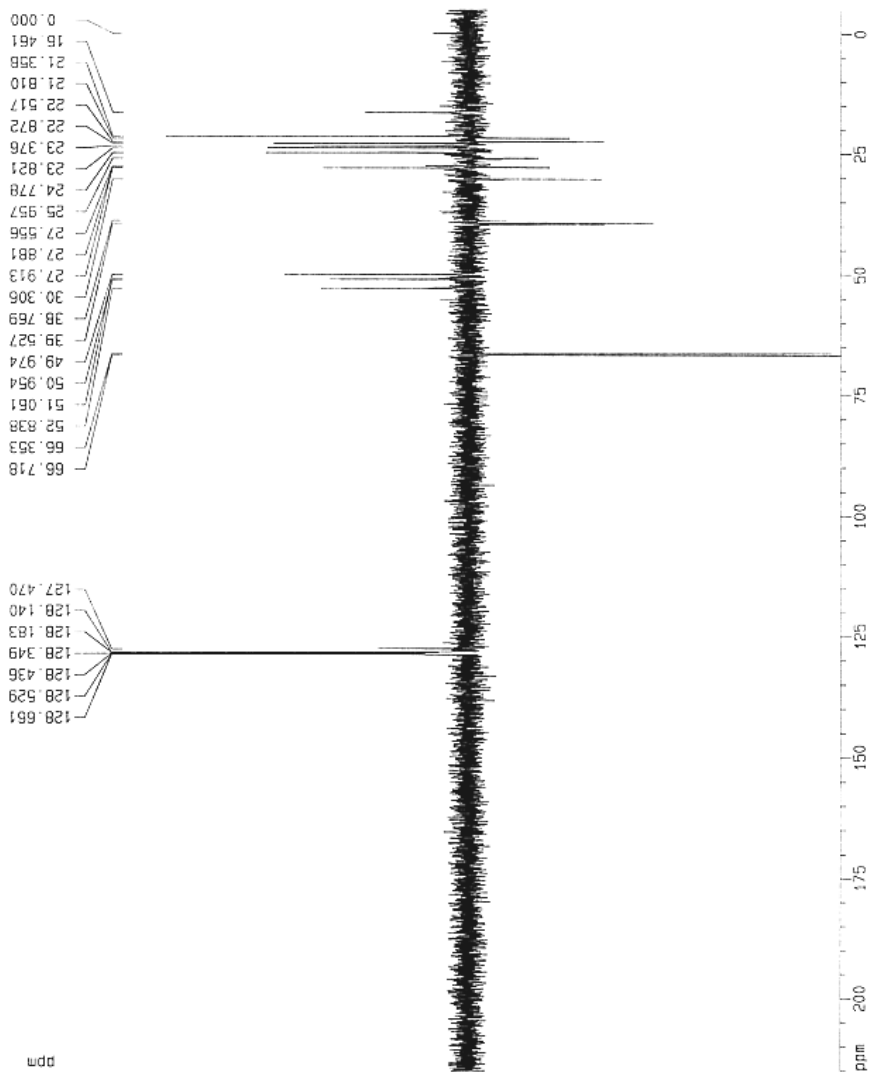


5b

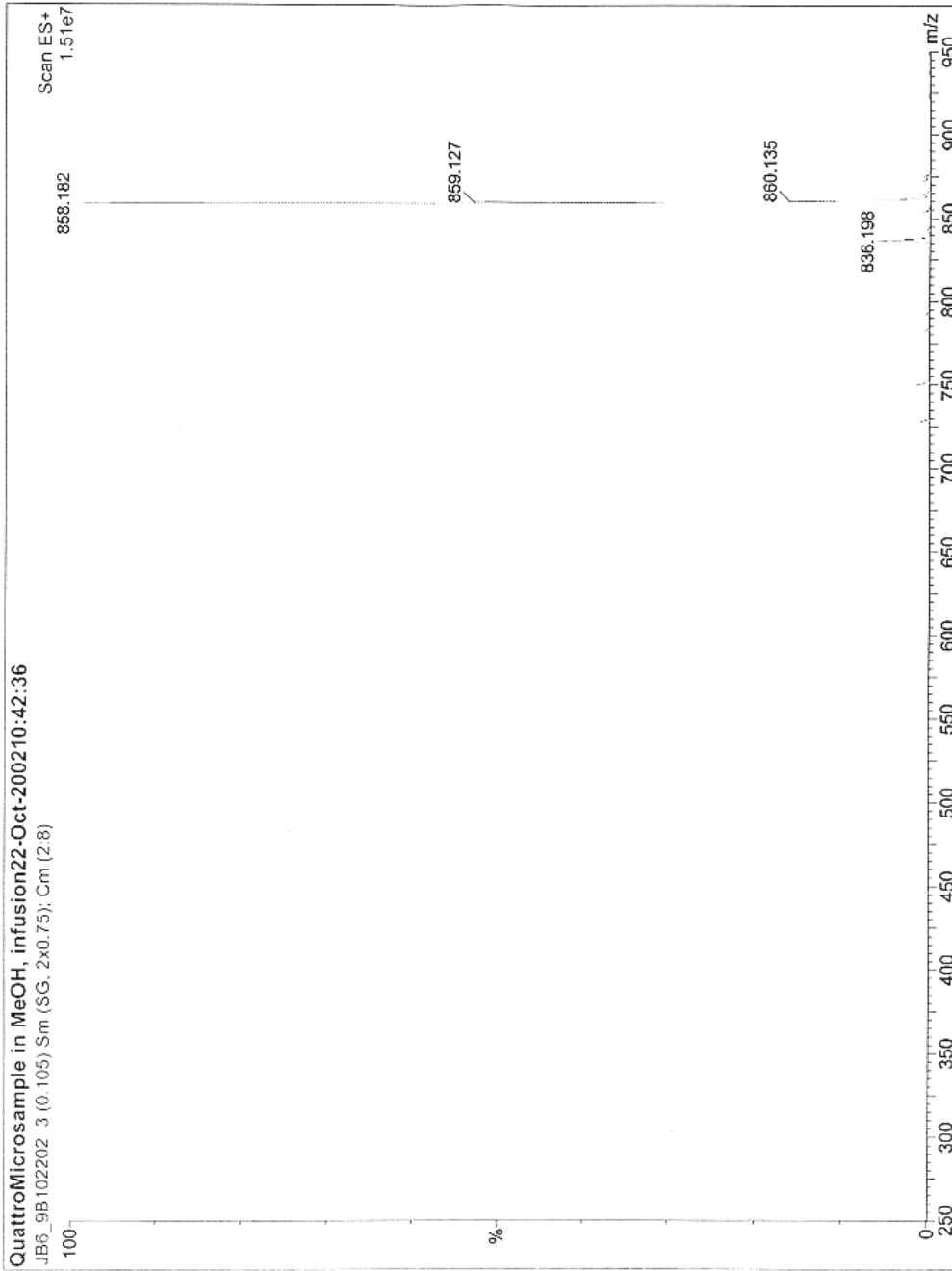
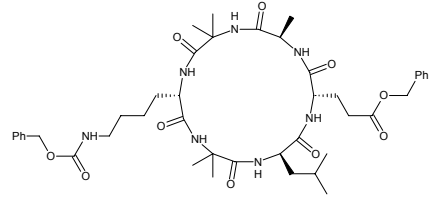


```

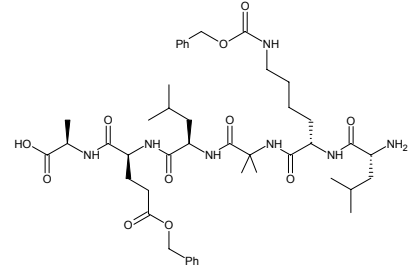
Current Data Parameters
NAME          04246-2002-116
EXPNO         13
PROCNO        1
-----
F2 - Acquisition Parameters
Date_         20021028
Time          16.52
INSTRUM       spect
PROBHD        5 mm Multif1
PULPROG       zgpg30
TD            65536
SOLVENT       DMS
NS            512
DS            4
SWH            23800.000
FIDRES        0.47180596
AQ            1.35647584
RG            256
DE            6.00 uSSEC
TE            300.0 K
-----
===== CHANNEL f1 =====
NUC1          13C
P1            6.70 uSSEC
PL1           1.740 uSSEC
SFO1          100.6270950 MHz
===== CHANNEL f2 =====
NUC2          1H
P2            6.70 uSSEC
PL2           1.740 uSSEC
SFO2          400.1316005 MHz
-----
F2 - Processing parameters
SI            32768
SF            300.6300000 MHz
WDW           EM
SSB           0
LB            1.00 Hz
GB            0
PC            1.40
-----
1D NMR aqst parameters
AQ            20.00 s
FIDRES        245.000 Hz
F1            25681.75 Hz
F2            50.000 Hz
PRGCM         11
MTCM          1100
MTCX          30248 Hz/cm
  
```



5b



6a



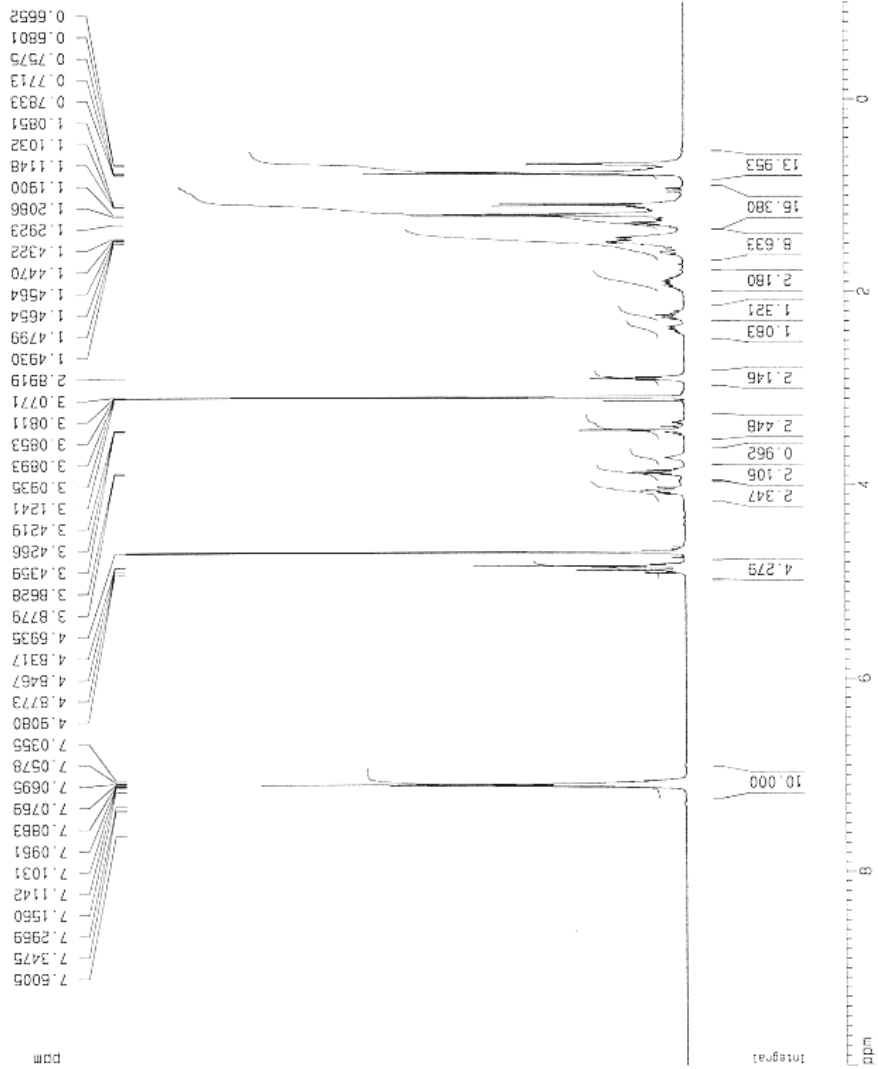
Current Data Parameters
 NAME JandB-2003-w-n
 EXPNO 15
 PROCNO 1

F2 - Acquisition Parameters
 Date_ 20030105
 Time_ 0.27
 INSTRUM spect
 PROSD 5 mm Multino
 PULPROG zgpg30
 TD 32768
 SOLVENT MeOH
 NS 15
 DS 2
 SWH 8278.145 Hz
 SFO 400.13209172 MHz
 FIDRES 0.214829 Hz
 AQ 1.9192372 sec
 RG 322.5
 DK 60.400 usec
 DE 6.00 usec
 TE 300.0 K
 D1 1.00000000 sec

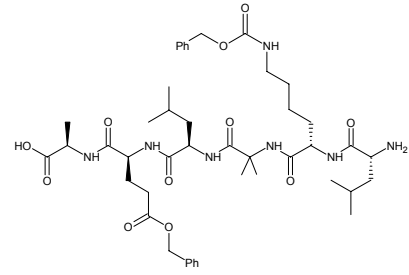
----- CHANNEL f1 -----
 NUC1 1H
 P1 8.60 usec
 PL1 0.00 dB
 SFO1 400.13209172 MHz

F2 - Processing parameters
 SI 32768
 SF 400.13209172 MHz
 WDK EM
 SSS 0
 LB 0.30 Hz
 GB 0
 PC 1.00

1D NMR plot parameters
 CX 20.00 cm
 FIP 10.002 ppm
 F1 4002.10 Hz
 F2P -1.010 ppm
 F2 -404.17 Hz
 PRGM 0.56560 ppm/cm
 HZCM 220.31363 Hz/cm

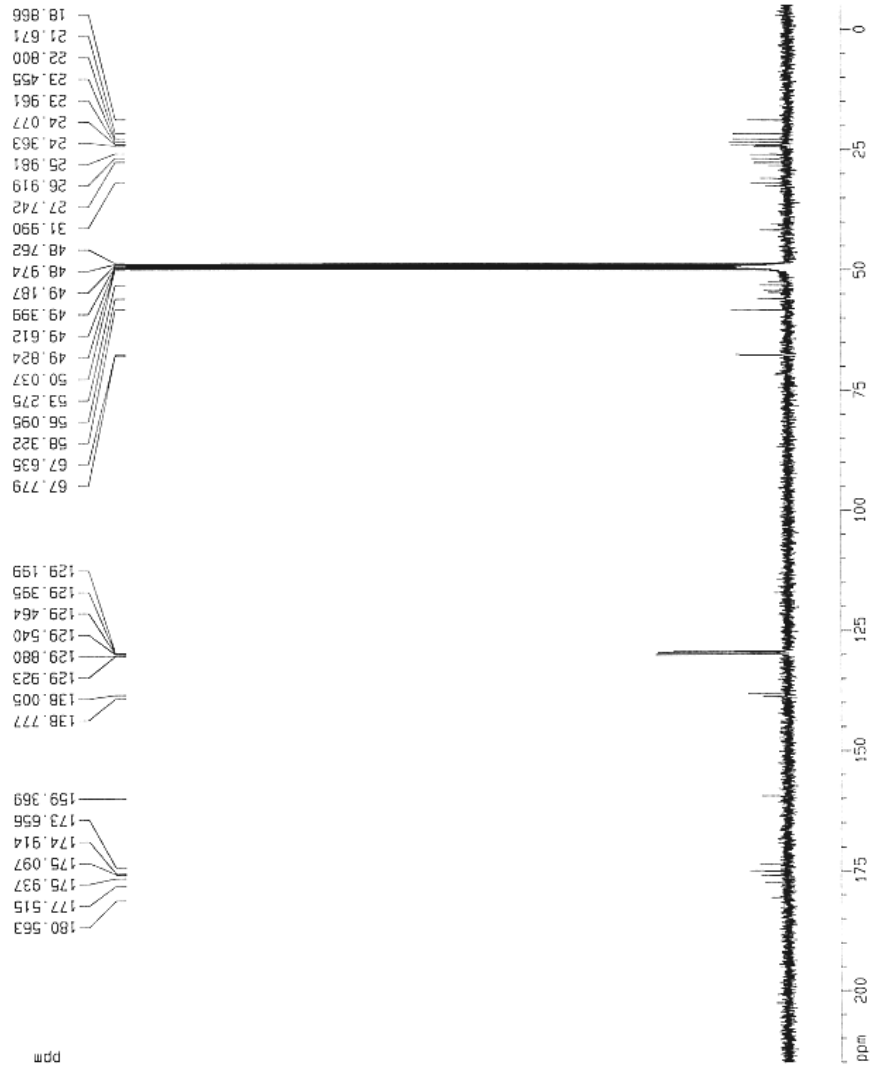


6a

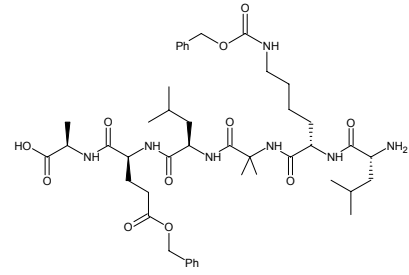


```

Current Data Parameters
NAME      Jan10-2003-che
EXPNO    10
PROCNO   1
F2 - Acquisition Parameters
Date_    20030111
Time     4.15
INSTRUM spect
PROBHD   5 mm Multinu
PULPROG zgpg30
TD        65536
SOLVENT  MeD4
NS        6000
DS         4
SWH       25125.623 Hz
FIDRES   0.383387 Hz
AQ        1.3042164 sec
RG        16384
DW        19.500 USEC
DE        6.00 USEC
TE        300.0 K
D1        2.00000000 sec
d11       0.03000000 sec
d12       0.00000000 sec
***** CHANNEL f1 *****
NUC1      13C
P1C1      8.70 USEC
PL1       0.00 dB
SFO1     100.6257659 Mhz
***** CHANNEL f2 *****
CPDPRG2  waltz16
NUC2      1H
P1C2      167.00 USEC
PL2       0.00 dB
PL12     23.00 dB
PL13     23.00 dB
SFO2     400.1316005 Mhz
F2 - Processing parameters
SI        32768
WDW       EM
SSB       0
LB        1.00 Hz
GB        0
PC        1.40
ID NMR list parameters
CX        20.00 cm
F1P       215.003 ppm
F2P       27631.71 Hz
F2P2      5.000 ppm
F2P3      50.00 Hz
P1PCK     11.000 ppm/Hz
H1C1W     1100.72040 Hz/cm
  
```



6a



```

Current Data Parameters
NAME          Jan09-2003-c1e
EXPNO        11
PROCNO       1

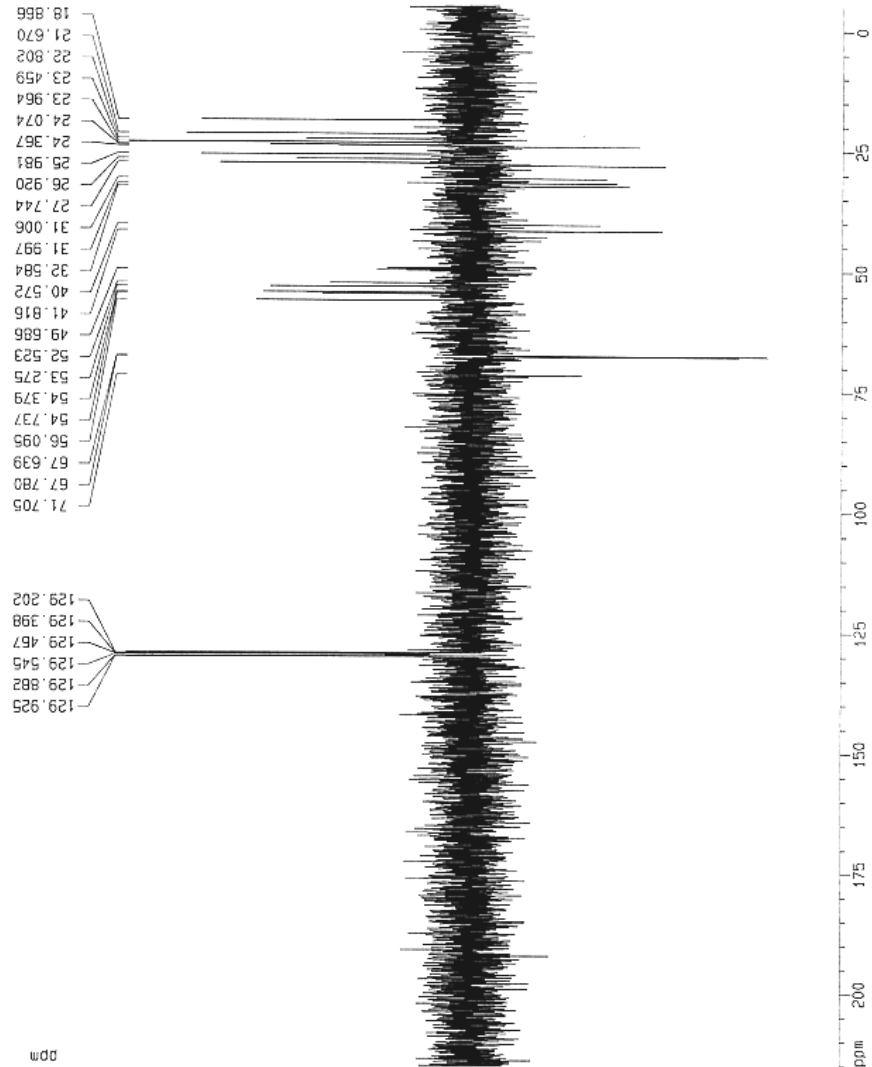
F2 - Acquisition Parameters
Date_         20030110
Time          2:40
INSTRUM      zgpg30
PROBHD       5 mm MSL100
PULPROG      zgpg135
TD            65536
SOLVENT      MeOH
NS            1500
DS            4
SWH           23980.614 Hz
FIDRES       0.365918 Hz
AQ           1.3864058 SEC
RG            6132
DE            28.00 uSEC
TE            300.0 K
CNS12        145 0000000
D1            2 0000000 SEC
d2            0 00344828 SEC
d3            0 0000000 SEC
d12           0 0000000 SEC
DELTA        6.386 18651719 SEC

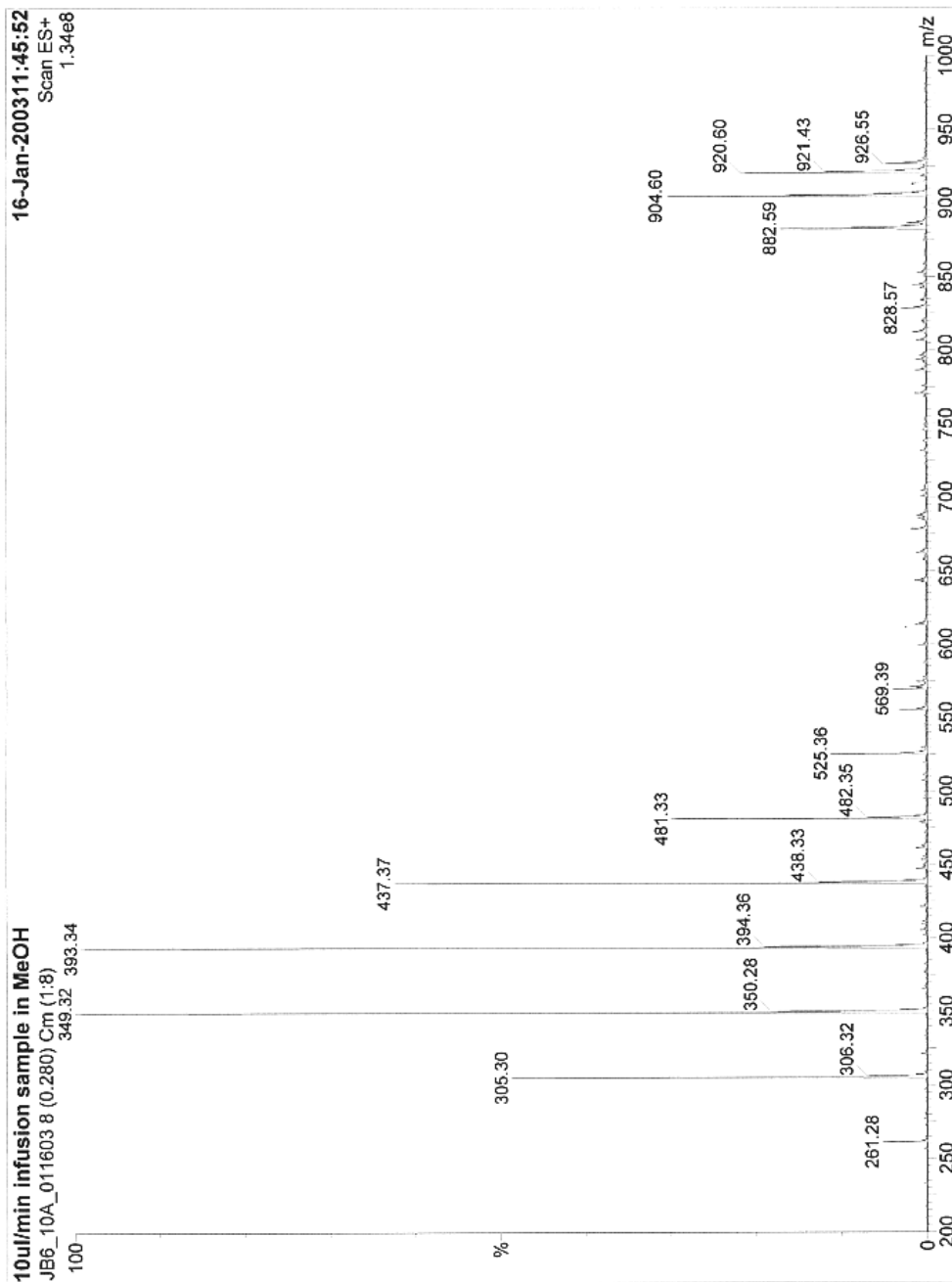
***** CHANNEL f1 *****
NUC1          13C
P1            81.70 uSEC
PR            17.40 uSEC
PL1           0.00 dB
SFO1         100.6227858 MHz

***** CHANNEL f2 *****
EXPOR2       waltz16
NUC2          1H
P2            8.70 uSEC
PR            107.00 uSEC
PL2           0.00 dB
PL12         23.00 dB
SFO2         400.1166055 MHz

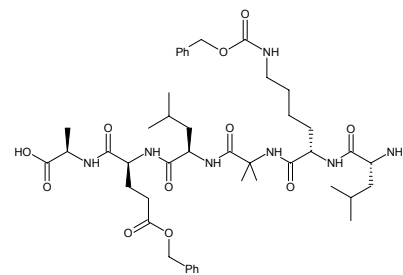
F2 - Processing parameters
SI            32768
WDW           EM
SSB           0
LB            1.00 Hz
GB            0
PC            1.40

1D NMR plot parameters
CX            20.00 cm
F1P           215.000 Cpm
F1            21631.71 Hz
F2P           -5.000 PPM
F2            -533.00 Hz
RG            11 00000 000/24
WDW           HANN
SSB           0
PC            1165 73646 117/24
  
```

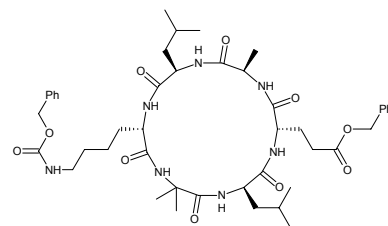




6a

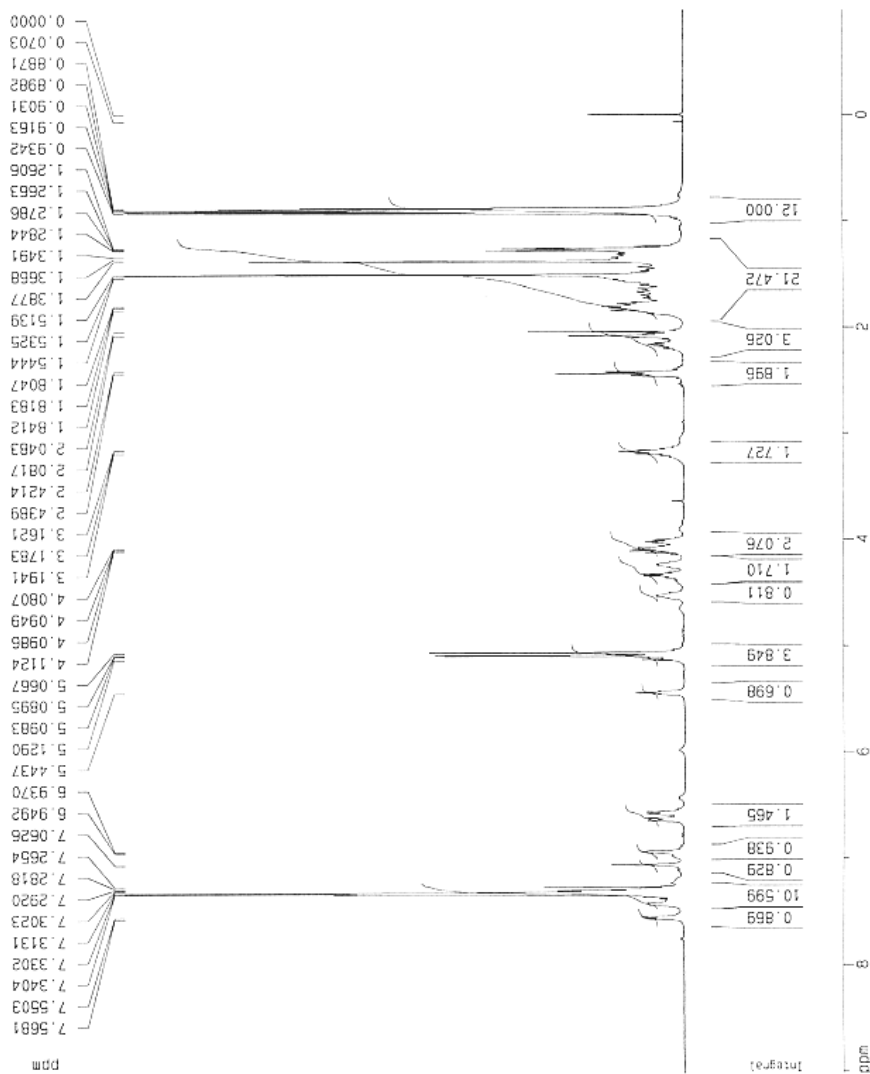


6b

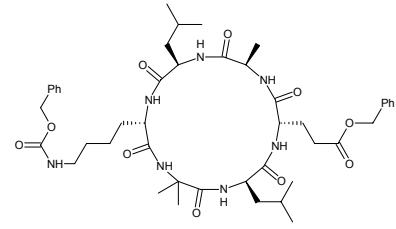


```

Current Data Parameters
NAME          Jun13-2003-che
EXPNO        10
PROCNO       1
----- Acquisition Parameters -----
Date_        20030113
Time         22:52
INSTRUM      spect
PROBHD       5 mm Multino
PULPROG      zgpg
TD           5950
SOLVENT      CDCl3
NS           16
DS           2
SOLVENT      CDCl3
FIDRES       0.252629 Hz
AQ           1.9792372 sec
RG           181
DK           60.400 usec
DE           6.00 usec
TE           300.0 K
D1           1.00000000 sec
----- CHANNEL f1 -----
NUC1         13C
P1           8.60 usec
PL1          0.00 dB
SFO1         400.1324710 MHz
----- Processing parameters -----
SI           32768
SF           400.1300099 MHz
RG           0
KON          0
SSB          0
LB           0.30 Hz
GB           0
PC           1.00
----- 1D NMR plot parameters -----
CX           20.00 cm
F1P          8.029 ppm
F2P          3611.29 Hz
F3P          -0.998 ppm
F2         -389.34 Hz
PRMCK       0.5016 ppm/cm
HZCM        200.52536 Hz/cm
  
```



6b



```

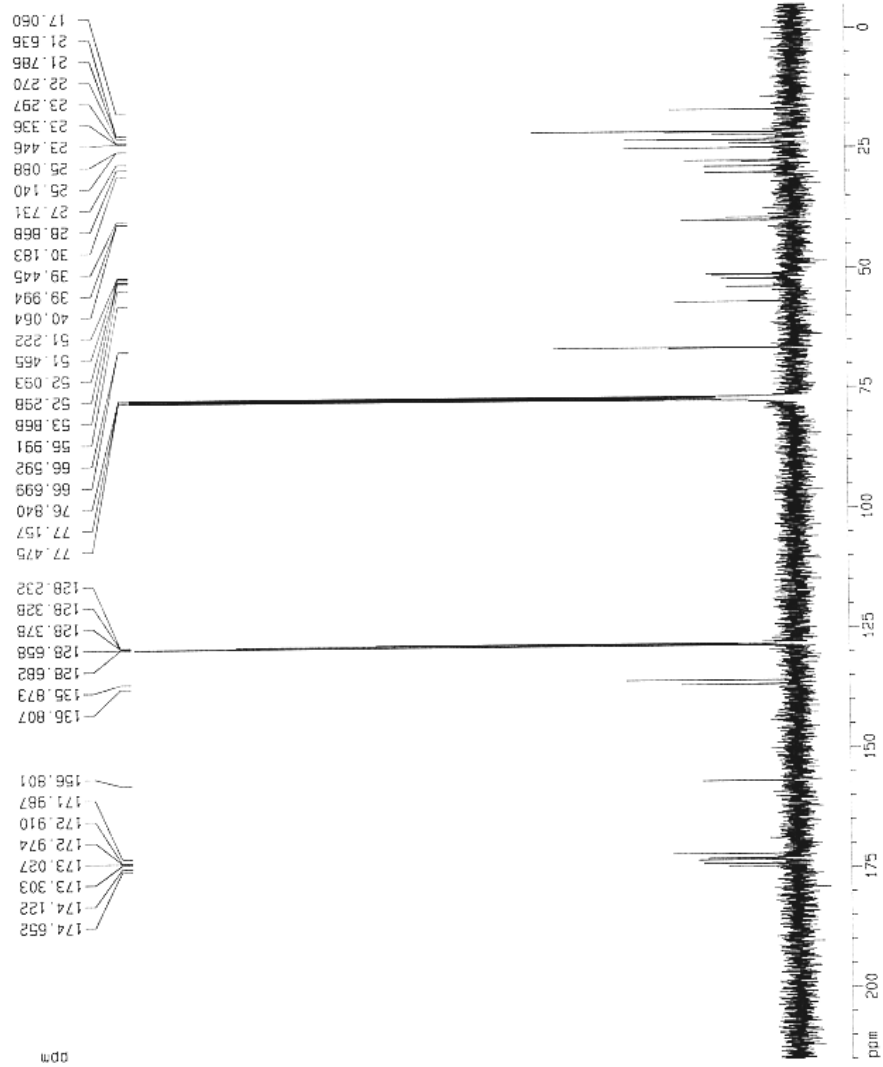
Current Data Parameters
NAME      Jan15-2023-che
EXPNO    14
PROCNO   1

F2 - Acquisition Parameters
Date_    20030115
Time     7.58
INSTRUM  spect
PROBHD   5 mm WJ319a
PULPROG  zgpg30
TD        65536
SOLVENT  CDCl3
NS        2500
DS        4
SWH       25126.652 Hz
FIDRES    0.303361 Hz
AQ        1.302164 SEC
RG         3648
DQ         18.800 uSEC
CA         6.000 uSEC
TC         300.0 K
TE         6.000 uSEC
D1         2.00000000 SEC
d11        0.03000000 SEC
d12        0.00000000 SEC
----- CHANNEL f1 -----
NUC1      13C
P1         6.70 uSEC
PL1        0.00 dB
SFO1      100.627559 MHz

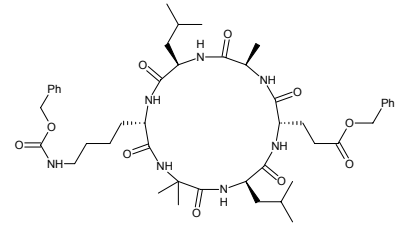
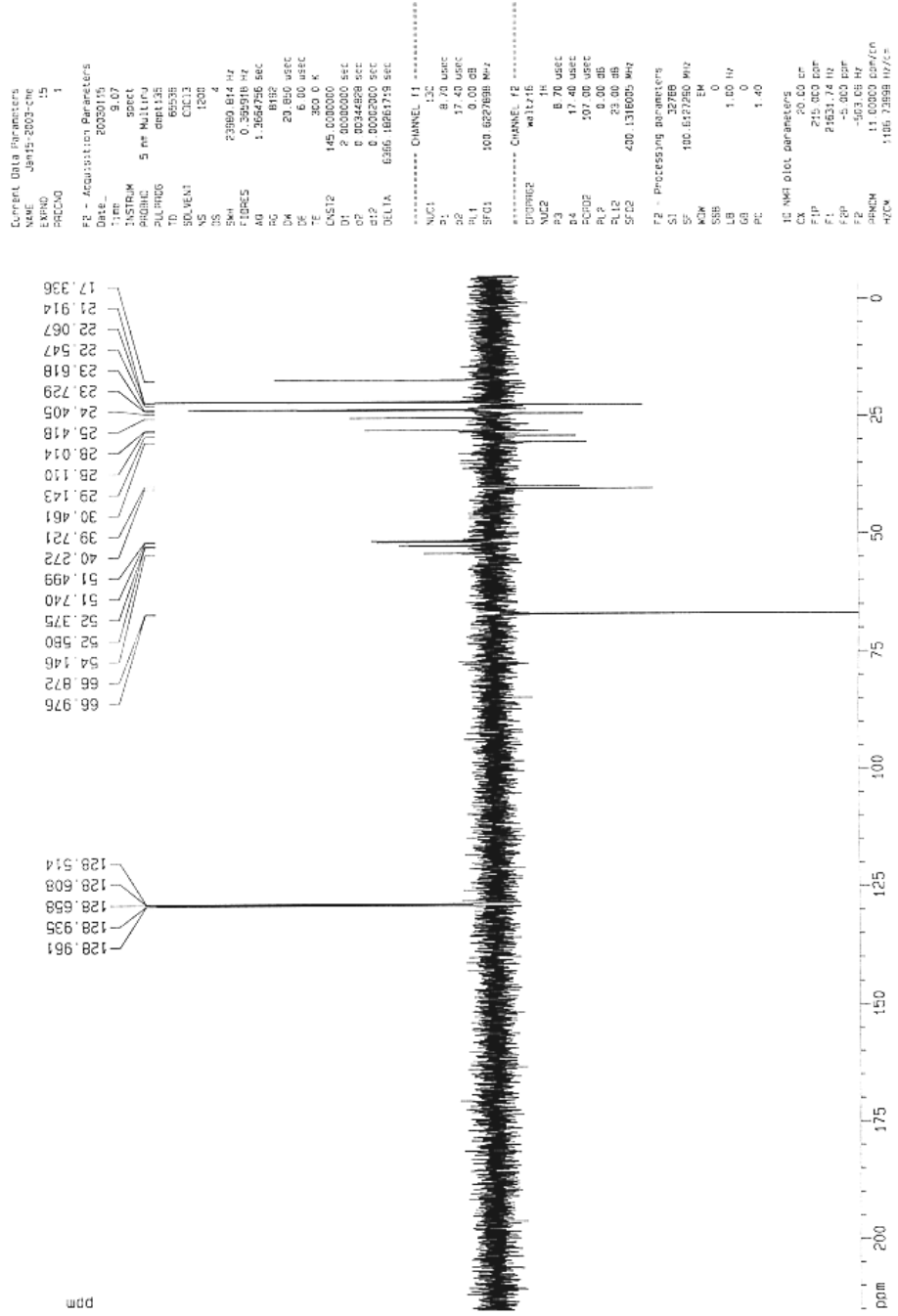
----- CHANNEL f2 -----
COPROG2  waltz16
NUC2       1H
PCPD2     167.80 uSEC
PL2        0.00 dB
PL12      23.00 dB
PL13      23.00 dB
SFO2      400.1316000 MHz

F2 - Processing parameters
S1         32768
SF         100.627559 MHz
RG         0
WDW         EM
SSB         0
LB         1.00 Hz
GB         0
PC         1.42

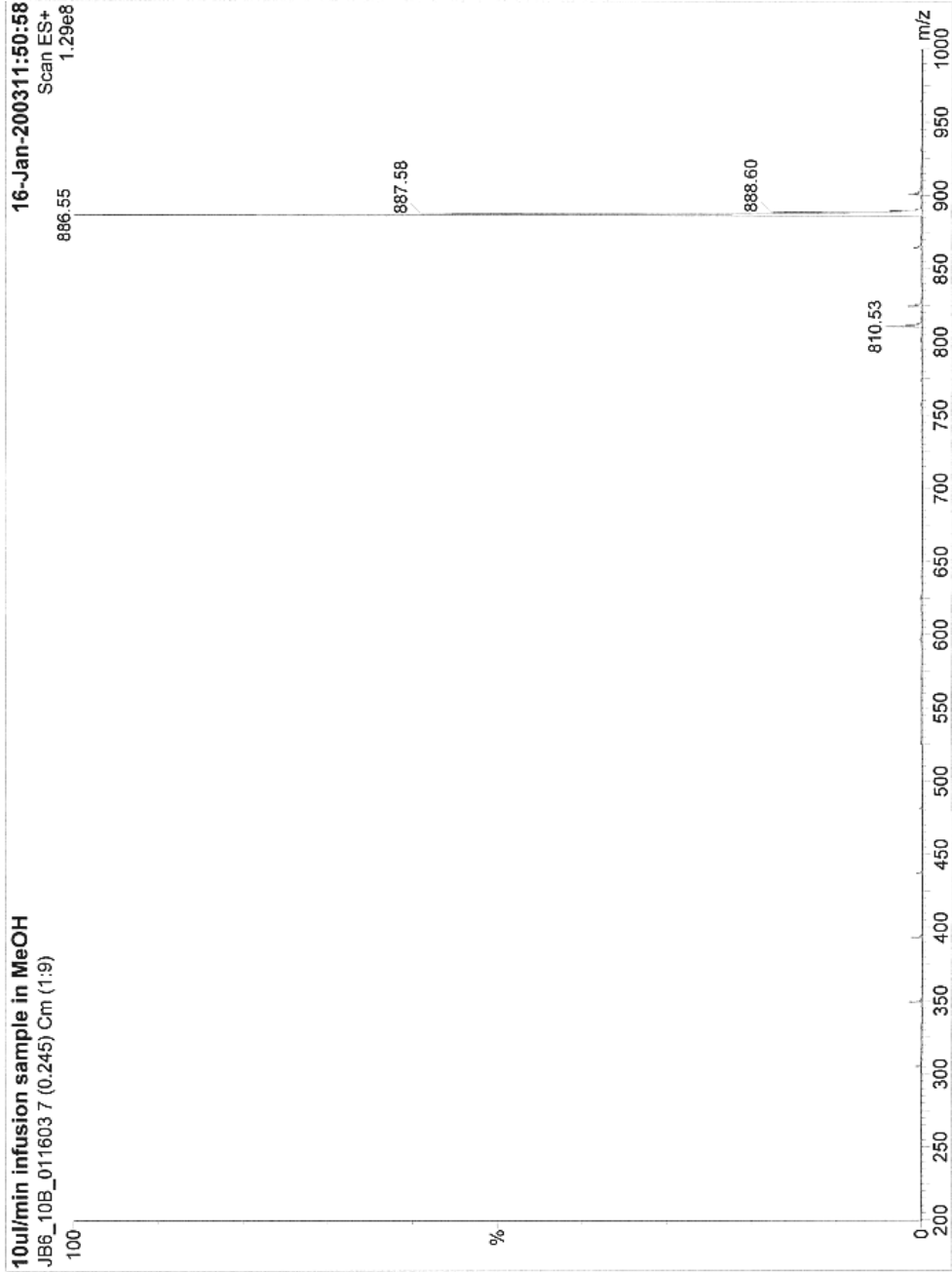
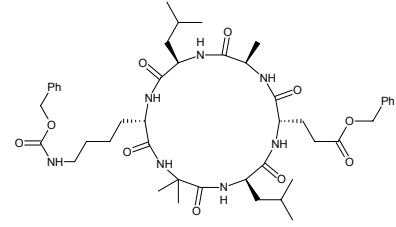
ID NH1 a1c1 parameters
CX         20.00 CH
F1P        216000 Hz
F2P        21531.72 Hz
F3P        5.000000 Hz
F4P        503.06 Hz
PCSKW     11.0000000000
AQ2CH     1155.74025 Hz/CH
  
```



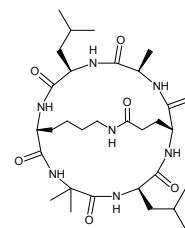
6b



6b



6d



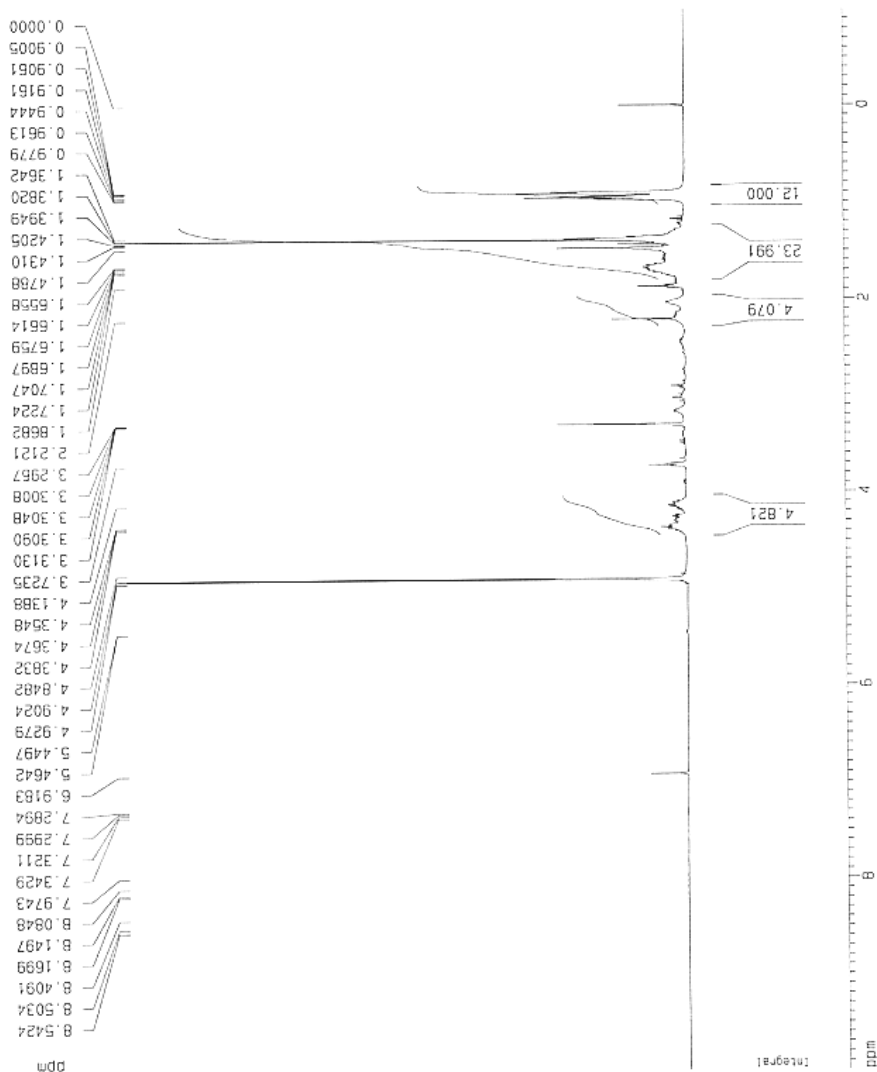
Current Data Parameters
 NAME Jan28-2003-c1c
 EXPNO 12
 PROCNO 1

F2 - Acquisition Parameters
 Date_ 20030128
 Time 1:37
 INSTRUM spect
 PROBNM 5 mm Multicore
 PULPROG zg30
 TD 32768
 SOLVENT MeOH
 NS 16
 DS 2
 SWH 8278.146 Hz
 SFO1 0.256259 Hz
 FIDRES 1.9796372 SFC
 AQ 203.12
 RG 60.400 usec
 DE 6.00 usec
 TE 300.0 K
 D1 1.00000000 sec

***** CHANNEL f1 *****
 NUC1 1H
 P1 0.60 usec
 PL1 0.00 dB
 SFO1 400.1324710 MHz

F2 - Processing parameters
 SI 32768
 SF 400.1330093 MHz
 KW 64
 EN 0
 LB 0.30 Hz
 GB 0
 PC 1.00

1D NMR plot parameters
 CX 20.00 cm
 F1 8.985.00um
 F2 2989.30 Hz
 F3 -0.592 ppm
 F4 -385.88 Hz
 PRGM 0: s4935 pch/cm
 HZCM 219: 80946 Hz/cm



6d

```

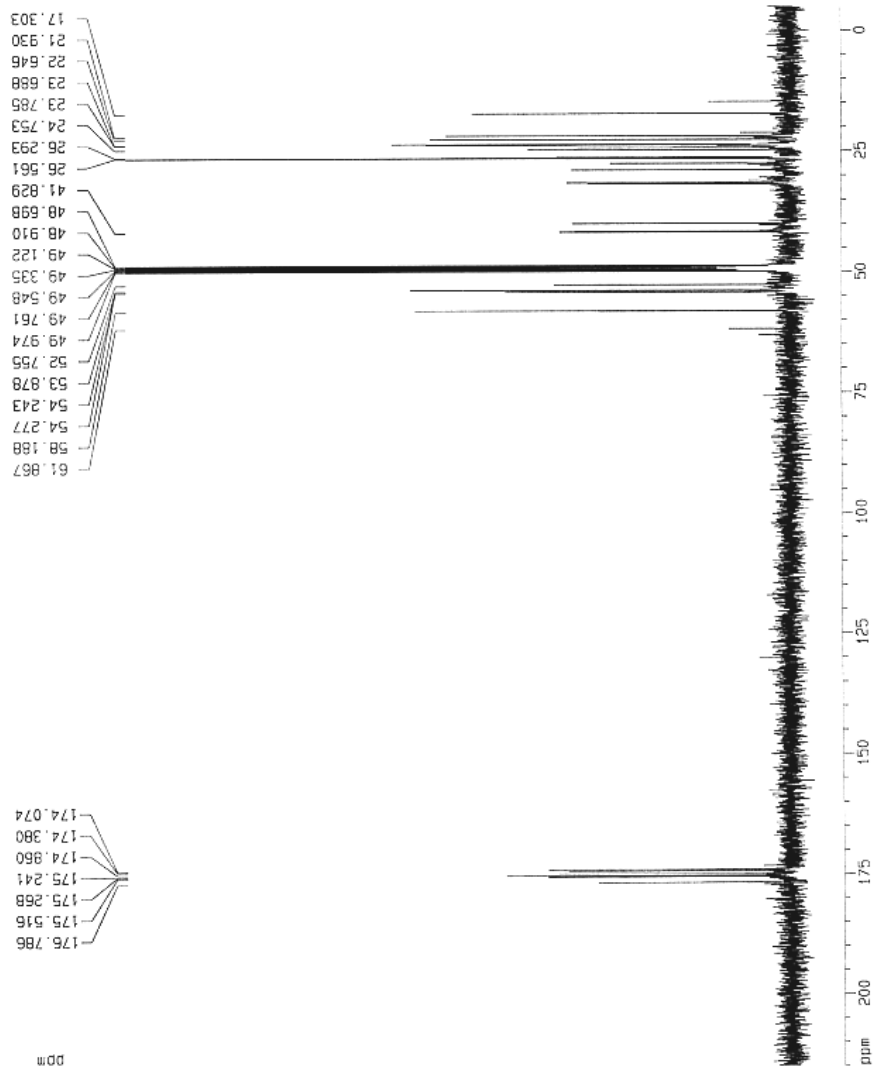
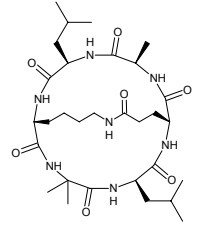
Current Data Parameters
NAME      Jan24-2003-one
EXNO     11
PROCNO   1
F2 - Acquisition Parameters
Date_    20030123
Time     1:37
INSTRUM spect
PROBHD   5 mm NUC13C
PULPROG zgpg30
AQ       0.39036715
RG       4096
SOLVENT  H2O
NS       4000
DS       4
SWH      25125.630 Hz
FIDRES   0.39036715 Hz
AQ       1.3042164 SEC
RG       4096
DM       19.500 USEC
DE       6.00 USEC
TE       300.0 K
D1       2.00000000 SEC
d11      0.03000000 SEC
d12      0.00020000 SEC

***** CHANNEL f1 *****
NUC1     13C
P1       8.70 USEC
PL1      0.00 DB
SF01     100.623559 MHz

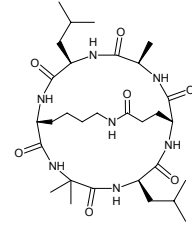
***** CHANNEL f2 *****
CPDPRG2 waltz16
NUC2     1H
PCPD2    107.00 USEC
PL2      0.00 DB
PL12     23.00 DB
PL13     23.00 DB
SF02     400.136005 MHz

F2 - Processing parameters
SI       32768
SF       100.615984 MHz
RG       4096
DSB      0
GB       1.00 Hz
EB       0
PC       1.40

1D NMR Data Parameters
CX       20.00 cm
F1p     215.602 ppm
F1       21531.71 Hz
F2p     -5.602 ppm
F2       -503.65 Hz
PRFCHM  11.00002 ppm/cm
HZCN     1106.73653 Hz/cm
    
```

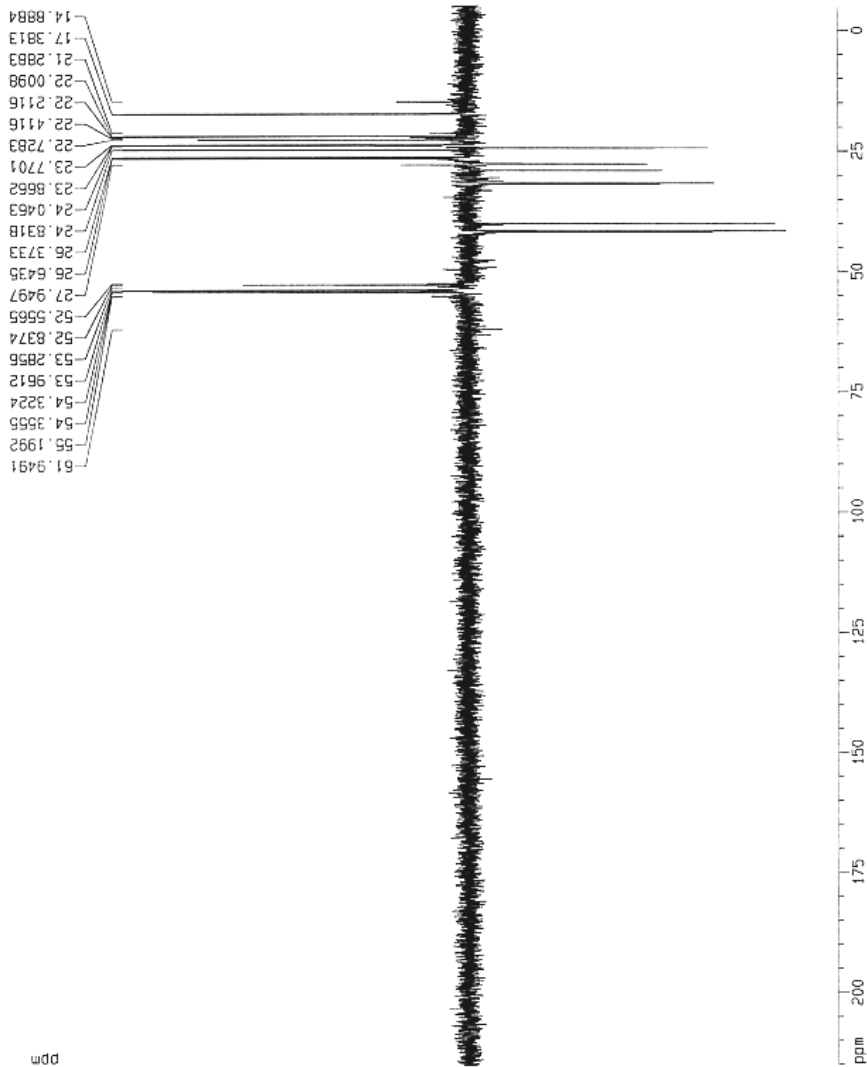


6d



```

Current Data Parameters
NAME      Jan64-2003-one
EXPNO    12
PROCNO   1
F2 - Acquisition Parameters
Date_    20030125
Time     4.19
INSTRUM  SPECT
PROBHD   5 mm NUL1:nu
PULPROG  zgpg13b
TD       65535
SOLVENT  MCDN
NS       2500
DS       4
SWH      20960.814 Hz
FIDRES   0.352581 Hz
AQ       1.3672956 SEC
RG        2048
DQ       20.850 USEC
DE       6.00 USEC
TE       300.0 K
CNV12    145.0000000
D1       2.0000000 SEC
d2       0.0044498 SEC
d12      0.0002908 SEC
DELTA    6.585.16261715 SEC
***** CHANNEL f1 *****
NUC1     13C
P1       8.70 USEC
PL1     17.40 DB
SFO1    100.627698 MHz
***** CHANNEL f2 *****
CPDPRG2  waltz16
NUC2     13C
P2       8.70 USEC
PL2     17.40 USEC
PCPD2    107.00 USEC
PL3      0.00 DB
PL4      23.00 DB
SFO2     400.1316902 MHz
F2 - Processing parameters
SI       32768
SF       100.625861 MHz
WDW      EM
SSB      0
LB       1.00 Hz
GB       0
PC       1.40
10 NMR data parameters
CX       20.00 cm
F1P      215.000 ppm
F1       21633.71 Hz
F2P      -5.000 ppm
F2       -503.05 Hz
F20M     11.73840 Hz/cm
F21M     1198.73840 Hz/cm
  
```



6d

